

Response to Reviewer #1

[Reviewer Comment; RC1] This manuscript presents measurements from a 5 month study of fluorescing biological aerosol particles (FBAP) at an elevated, moderately remote site in southern India. The data quality appears to be very good and the scientific significance is potentially high. The problem is that the paper is probably twice as long as it needs to be and the conclusions drawn are much too speculative with not enough concrete statistics to support the hypotheses put forth regarding either the source of the FBAPs or the physical mechanisms underlying the observed trends. When discussing the results, the objective is to highlight the main points without trying to describe each and every peak and wiggle. Let the Tables list all the statistical details and focus on the most important variations that will then be used to drive the discussion. At the moment there are probably twice as many pages of results and twice as many figures as needed.

[Author Response; AR1] We would like to thank Dr. Baumgartner for his positive evaluation of our results mentioning, “The data quality appears to be very good and the scientific significance is potentially high”. The comments provided by the reviewer and corrections suggested in the manuscript have greatly helped us to improve the quality of the manuscript. The suggestions have been meticulously implemented wherever appropriate and we believe changes will be acceptable. As suggested by the Reviewer manuscript is shortened by cutting short the description on of monthly plots and supplementary figures and also by rearranging the text wherever appropriate. We have also revised the figures by combining few of them and moving one to the supplement. The description on size distribution is also shortened and modified accordingly, to highlight the main points.

What is missing:

[RC2] A topographical map of the research site and surrounding area, preferably something like a Google Earth rendition that would show the surrounding vegetation as well as areas with no vegetation such as is referred to in the text. Given the very low wind speeds, it is likely that most of the trends that are seen can be linked to more local sources.

[AR2] We have now provided a land-use map of the southern India in the supplement clearly indicating the significance of the chosen site. As for the topography, note that Fig. 1 in the main text is scaled by the altitude. Relation between low wind speed and local source is explained in the manuscript (L726 – L730)

[RC3] A more in depth analysis of the periods with rain, taking a much closer look at the properties of the FBAP just before, during and after each event.

[AR3] We have performed the in-depth analysis exploring the relation between rainfall and FBAP number concentration just before, during, and after rainfall and the result indicated no significant effect on FBAP number concentration.

Hence, it was very difficult to make any sound and conclusive statement pertaining to effect of rainfall on FBAP number concentration. One reason, as pointed out by Reviewer#3, could be the persistent and heavy rainfall. However, during the second part of the campaign carried out during winter season, we did observe impact of rainfall on the FBAP number concentrations. These results will be discussed in detail in follow up study. In addition we have given a hypothesis explaining the absence of effect of rainfall on FBAP number concentration at this particular location (L850 – L863).

[RC4] A cross-correlational analysis between the FPAB properties and the meteorological conditions. One would not necessarily expect a one to one correlation between the meteorology and the FPAB concentrations, particularly if the spore production is local. Only for advected aerosols would they be linked one to one.

[AR4] We agree with Reviewer that one cannot expect one to one correlation between meteorology and FBAP concentration, however, it may not be true in all the cases and not necessary be always linked for advected bioaerosols. For example, FBAP concentration, depending up on the type of spore, is known to have varied response/relationship with relative humidity (RH). The emissions of few specific types of spores emitted locally are positively related with relative humidity whereas some have shown decrease in concentration with increasing RH (Oliveira et al., 2010; Herrero et al., 1996; Kurkela, 1997; Oh et al., 1998; Healy et al., 2014., Quintero et al., 2010; Hjelmroos, 1993; Ho et al., 2005., Sabariego et al., 2000., Calderon et al., 1995). This has been clearly mentioned in the manuscript (L764 – L774). The relation of wind speed and direction may be useful to further study the impact of advected bioaerosols, which has been detailed in the manuscript (L731 – L738; Hameed et al., 2012; Almaguer et al., 2013; Lyon et al., 1984; Quintero et al., 2010; Huffman et al., 2012; Jones and Harrison, 2004; Troutt and Levetin, 2001; Kurkela, 1997).

[RC5] It is impossible to compare the shapes of size distributions when they are on different figures. Since the concentrations are quite different, normalize them to a unit area then put only the means or medians on the same figure so that any differences in the shapes can be clearly seen. These differences can then be evaluated quantitatively and linked to the hypothesis.

[AR5] Based on Reviewer's suggestion we attempted to prepare a figure comparing the mean FBAP number and mass size distribution for each focus period in single panel. We have replaced Fig. 10 and 11 (original manuscript) with the new figure (Fig.8, revised manuscript). We have also added the prepared figure below for Reviewer's kind read-through.

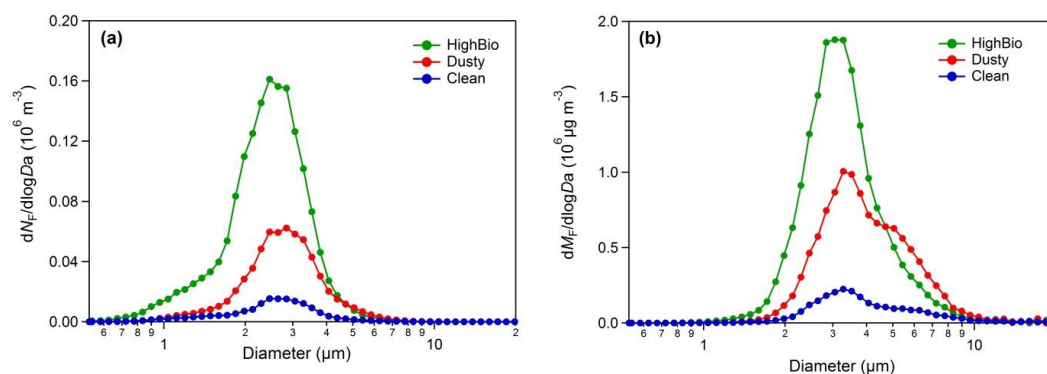


Figure R1.1: FBAP number size distributions ($dN_F/d\log D_a$) and mass size distribution ($dM_F/d\log D_a$) averaged over each distinct focus periods during the measurement campaign carried out at Munnar.

[RC6] The back trajectory analysis is useless as currently given. There needs to be an analysis of not only where the air came from horizontally, but vertically as well. Questions to be asked: a) How long had the air been close to the surface before reaching the site? b) What were the meteorological conditions along the trajectory, i.e. precipitation and humidity and c) How long had the air been close to the site? These all will impact the history of the particle as well as the air and whether particles had been removed after leaving their source.

[AR6] Indeed, the back trajectory plots shown in Figure 1 are color-scaled by pressure (altitude) to highlight the vertical component of the air motion. We chose not to discuss this in great detail in the paper, because it would make the already long manuscript even longer and we felt this analysis would be beyond the scope of the manuscript. We also felt that it would not be helpful in improving the primary scientific conclusion specifically that during the monsoon season over Indian region, and could lead to further confusion. Further, our sole aim with this figure is to show the back trajectory is only to provide an orientation to reader that this site experiences very contrasting winds during contrasting seasons (monsoon vs. winter), and a broader picture of air mass origin with rough estimates about air mass composition (Vinoj and Satheesh, 2003; Li and Ramanathan, 2002; Satheesh and Srinivasan, 2002; Vinoj et al., 2010, 2014; Prospero, 1979; Moorthy et al, 1991.). To investigate the relation of impact of wind direction and speed separate meteorological measurement in high time resolution were performed and were reported. In any case, we believe that Referee has overlooked the fact that back trajectories are already color scaled by pressure.

[RC7] An error analysis of the measurements. What is the expected error in size and concentration based on error propagation that no doubt has already be detailed in earlier publications. Nothing is said about FBAPs that are not complete particles but are fragments. There needs to be an estimate of the size dependent losses in the sampling system. Even with no bends, there will be diffusion and turbulence losses that can easily be calculated with Aerocalc (Baron and Willeke).

[AR7] Reviewer may be aware of the fact that UV-APS cannot differentiate the particle type; instead it only measures the aerodynamic diameter and spectrally integrated fluorescence. Under this scenario, a plant/animal fragment sampled will be treated as a complete particle where instrument will assign the equivalent aerodynamic diameter. We have calculated the equivalent aerodynamic diameter of a non-spherical particle. For example an ellipsoid particle with length of 4 μm long and width of 2 μm will be treated as particle with aerodynamic diameter of 3.6 μm . As suggested by Reviewer a sentence (average penetration efficiency of 99.8% at 290K and 840 hPa) discussing about the size dependent losses in the sampling system is now added based on Aerocalc/previous literature.

I have attached an annotaed version of the paper that includes many more questions and comments, The paper is relatively readable, given that the first author is not a native English; however, I am annoyed whenever I read a paper written by a non-English speaker but who has co-authors that are but who obviously have not read the paper, otherwise the numerous grammatical errors would have been corrected.

The suggestions provided in the annotated version of the manuscript have been implemented wherever appropriate and we thank Reviewer for his valuable edits.

References:

Almaguer, M., Aira, M.-J., Rodríguez-Rajo, F. J., and Rojas, T. I.: Temporal dynamics of airborne fungi in Havana (Cuba) during dry and rainy seasons: influence of meteorological parameters, *International Journal of Biometeorology*, 58, 1459-1470, 10.1007/s00484-013-0748-6, 2013.

Calderon, C., Lacey, J., McCartney, H. A., and Rosas, I.: Seasonal and diurnal-variation of airborne basidiomycete spore concentrations in Mexico-city, *Grana*, 34, 260-268, 1995.

Hameed, A. A. A., Khoder, M. I., Ibrahim, Y. H., Saeed, Y., Osman, M. E., and Ghanem, S.: Study on some factors affecting survivability of airborne fungi, *Science of the Total Environment*, 414, 696-700, 10.1016/j.scitotenv.2011.10.042, 2012.

Healy, D. A., Huffman, J. A., O'Connor, D. J., Poehlker, C., Poeschl, U., and Sodeau, J. R.: Ambient measurements of biological aerosol particles near Killarney, Ireland: a comparison between real-time fluorescence and microscopy techniques, *Atmospheric Chemistry and Physics*, 14, 8055-8069, 10.5194/acp-14-8055-2014, 2014.

Herrero, B., FombellaBlanco, M. A., FernandezGonzalez, D., and ValenciaBarrera, R. M.: The role of meteorological factors in determining the annual variation of *Alternaria* and *Cladosporium* spores in the atmosphere of Palencia, 1990-1992, *International Journal of Biometeorology*, 39, 139-142, 10.1007/bf01211226, 1996.

Hjelmroos, M.: Relationship between airborne fungal spore presence and weather variables - *cladosporium* and *alternaria*, *Grana*, 32, 40-47, 1993.

Ho, H. M., Rao, C. Y., Hsu, H. H., Chiu, Y. H., Liu, C. M., and Chao, H. J.: Characteristics and determinants of ambient fungal spores in Hualien, Taiwan, *Atmospheric Environment*, 39, 5839-5850, 10.1016/j.atmosenv.2005.06.034, 2005.

Huffman, J. A., Sinha, B., Garland, R. M., Snee-Pollmann, A., Gunthe, S. S., Artaxo, P., Martin, S. T., Andreae, M. O., and Pöschl, U.: Size distributions and temporal variations of biological aerosol particles in the Amazon rainforest characterized by microscopy and real-time UV-APS fluorescence techniques during AMAZE-08, *Atmospheric Chemistry and Physics*, 12, 11997-12019, 10.5194/acp-12-11997-2012, 2012.

Jones, A. M., and Harrison, R. M.: The effects of meteorological factors on atmospheric bioaerosol concentrations - a review, *Science of the Total Environment*, 326, 151-180, 10.1016/j.scitotenv.2003.11.021, 2004.

Kurkela, T.: The number of *Cladosporium* conidia in the air in different weather conditions, *Grana*, 36, 54-61, 1997.

Li, F., and Ramanathan, V.: Winter to summer monsoon variation of aerosol optical depth over the tropical Indian Ocean, *Journal of Geophysical Research-Atmospheres*, 107, 10.1029/2001jd000949, 2002.

Lyon, F. L., Kramer, C. L., and Eversmeyer, M. G.: Variation of airspora in the atmosphere due to weather conditions, *Grana*, 23, 177-181, 1984.

Oh, J.-W., Lee, H.-B., Lee, H.-R., Pyun, B.-Y., Ahn, Y.-M., Kim, K.-E., Lee, S.-Y., and Lee, S.-I.: Aerobiological study of pollen and mold in Seoul, Korea, *Allergology International*, 47, 263-270, <http://dx.doi.org/10.2332/allergolint.47.263>, 1998.

Oliveira, M., Amorim, M. I., Ferreira, E., Delgado, L., and Abreu, I.: Main airborne Ascomycota spores: characterization by culture, spore morphology, ribosomal DNA sequences and enzymatic analysis, *Applied Microbiology and Biotechnology*, 86, 1171-1181, 10.1007/s00253-010-2448-z, 2010.

Prospero, J. M.: Mineral and sea salt aerosol concentrations in various ocean regions, *Journal of Geophysical Research-Oceans and Atmospheres*, 84, 725-731, 10.1029/JC084iC02p00725, 1979.

Quintero, E., Rivera-Mariani, F., and Bolanos-Rosero, B.: Analysis of environmental factors and their effects on fungal spores in the atmosphere of a tropical urban area (San Juan, Puerto Rico), *Aerobiologia*, 26, 113-124, 10.1007/s10453-009-9148-0, 2010.

Sabariego, S., de la Guardia, C. D., and Alba, F.: The effect of meteorological factors on the daily variation of airborne fungal spores in Granada (southern Spain), *International Journal of Biometeorology*, 44, 1-5, 10.1007/s004840050131, 2000.

Satheesh, S. K., and Srinivasan, J.: Enhanced aerosol loading over Arabian Sea during the pre-monsoon season: Natural or anthropogenic?, *Geophysical Research Letters*, 29, 10.1029/2002gl015687, 2002.

Troutt, C., and Levetin, E.: Correlation of spring spore concentrations and meteorological conditions in Tulsa, Oklahoma, *International Journal of Biometeorology*, 45, 64-74, 10.1007/s004840100087, 2001.

Vinoj, V., and Satheesh, S. K.: Measurements of aerosol optical depth over Arabian Sea during summer monsoon season, *Geophysical Research Letters*, 30, 10.1029/2002gl016664, 2003.

Vinoj, V., Rasch, P. J., Wang, H., Yoon, J.-H., Ma, P.-L., Landu, K., and Singh, B.: Short-term modulation of Indian summer monsoon rainfall by West Asian dust, *Nature Geoscience*, 7, 308-313, 10.1038/ngeo2107, 2014.

Vinoj, V., Satheesh, S. K., and Moorthy, K. K.: Optical, radiative, and source characteristics of aerosols at Minicoy, a remote island in the southern Arabian Sea, *Journal of Geophysical Research-Atmospheres*, 115, 10.1029/2009jd011810, 2010.

Moorthy, K. K., Nair, P. R., and Murthy, B. V. K.: Size distribution of coastal aerosols - effects of local-sources and sinks, *Journal of Applied Meteorology*, 30, 844-852, 10.1175/1520-0450(1991)030<0844:sdocae>2.0.co;2, 1991.

Response to Reviewer #2

[Reviewer Comment; RC1] The manuscript presents measurements of Fluorescent Biological Aerosol Particles (FBAP) made using an Ultraviolet Aerodynamic Particle Sizer (UV-APS) at a high-altitude tropical site in southern India over a period covering the southwest monsoon season. A thorough background research, set of measurements and description of these has been presented and is potentially worthy of publication. However, I do feel some improvements could be made to the current manuscript as detailed below. Although I'm sure any new field measurements using a UVAPS or similar qualify as valid research, it is difficult to see the real contribution of this work to the field, other than to validate previous similar measurements at a new location. I believe the information is there, but is swamped in meticulous depiction and description of all measurements. Perhaps the manuscript could be streamlined and given more structure to emphasize this. The properties of the new site and results specific to this should be highlighted, with an eye on how it will be useful for future research and how the presented measurements will support that research. The technical content of the paper appears good and accurate. Figures have been chosen well to depict and compare the measurements (haven't seen the supplementary figures, which do not appear to be with the manuscript). Work in the field I was aware of, and much more besides has been appropriately cited.

[AR1] We would like to thank Reviewer for positively evaluating our manuscript stating following important points:

- "A thorough background research, set of measurements and description of these has been presented and is potentially worthy of publication"
- "The technical content of the paper appears good and accurate"
- "Figures have been chosen well to depict and compare the measurements"
- "Work in the field I was aware of, and much more besides has been appropriately cited"

The reviews provided here have been very helpful for us in improving the overall quality of the manuscript. We have also tried to fine-tune the key messages highlighting the findings of this study and how it would be useful in future in conclusion section. In addition to reduce the length of the manuscript we have now moved few figures to supplementary material and merged Fig. 3 and Fig. 5.

Some suggested alterations below.

[RC2] Pg 10: The inlet system is described here. Could the effects of the inlet system be assessed by a comparison of measurements of a range of particle sizes under controlled conditions both with and without the inlet tubing in place?

[AR2] Following the experiment, we performed a test with room air to estimate particle losses in the inlet tube. Observing particle distributions with and without tubing showed that no noticeable difference in the particle number

concentration or size distribution. We also performed theoretical calculations to calculate the diffusion losses during the entire sampling for all the size-ranges sampled and found that average penetration was 99.8% at 290K and 849 hPa.

[RC3] Line 445: Should read "Basically the UV-APS measures the particle number and aerodynamic size; the average mass of size-resolved particles can"
Lines 445-447: Can this statement be backed-up by a reference?

[AR2] We have now added an appropriate reference for this statement.

[RC3] Line 457 and few lines preceding: Were all the compared measurements made using the same density value?

[AR3] As far as we could found out from the literature all the measurements were carried out using same density values (1 g cm^{-3}).

[RC4] Lines 709-716: Description is confusing; maybe a mistake in the period references in the figure has been made? Here and everywhere else the three named focus periods are mentioned, the period names should perhaps be written within inverted commas or in italics to make reading easier.

[AR4] We thank Reviewer for pointing this out. The *focus* periods are now written in italics throughout manuscript.

[RC5] Figure 2: The shadowed blocks representing the focus periods don't seem to be visible on my copy of the manuscript.

[AR5] This mistake has been corrected. We have now added the shadowed blocks in Fig. 2.

[RC6] Finally grammar details. While the document is largely well written, there are numerous grammar mistakes that, at times, make it quite difficult to read. These often consist of a missing 'a' or 'the'. Although too numerous for individual attention, I have indicated some instances below and suggest that one of the authors go through the whole manuscript again and tidy this up.

[AR6] We thank Reviewer for pointing this out. Once we receive the final acceptance from The Editor before the final publication we intend to get our manuscript English edited from a professional service.

[RC6.1] Line 27: Missing 'a' between 'constitute' and 'large'.

[AR6.1] Done

[RC6.2] Line 55: Should read "selected areas. These measurement results confirm the fact that the fraction of PBAP to TAP is".

[AR6.2] Done

[RC6.3] Line 56: Missing 'a' between 'constitute' and 'significant'.

[\[AR6.3\] Done](#)

[RC 6.4] Line 172: Missing 'the' between 'including' and 'Arabian'.

[\[AR6.4\] Done](#)

[RC6.5] Line 173: Should read, "movement of the ITCZ reaching up to the equator is associated with the NE monsoon, which is also marked".

[\[AR6.5\] Done](#)

Response to Reviewer #3

General

[Reviewer Comment; RC1] This paper reports results of a three month measurement campaign of fluorescent biological aerosol particles (FBAP) at a high altitude tropical site in southern India. There are some unique aspects on the data. First, the marine air masses can be compared to local FBAP sources. Secondly, the campaign included long periods of heavy and persistent rain. Consequently, the authors observed a lack of correlation of FBAP with precipitation, contrary to several recent studies from other areas. The data has been presented in diverse ways that are also comparable to earlier studies. The material seems to merit publication. However, there are several issues that should be treated.

[Authors Response; AR1] We would like to thank reviewer for his thoughtful and detailed comments, which have helped us in improving the quality of the manuscript. We also thank reviewer for making following positive observations about our work.

- “There are some unique aspects on the data”
- “First, the marine air masses can be compared to local FBAP sources. Secondly, the campaign included long periods of heavy and persistent rain”
- “The data has been presented in diverse ways that are also comparable to earlier studies”

[RC2] Most importantly, the paper is unnecessarily long. The authors should concentrate on the findings that are unique to this study. Although it is good to treat many facets of the data, I think the paper would benefit of focusing also in this respect. The authors have divided the three month period first into months and later to three focus periods that they call dusty, clean, and high bio. I find the latter division much more useful. I recommend keeping it and getting rid of the monthly results. Because the data is treated from many angles, many of the explaining factors and arguments are presented several times. An example is the effect of the clean SW winds. It would be good to try to collect the findings first and then treat them at once.

[AR2] We thank Reviewer for pointing this out and we have now implemented Reviewer's suggestions. Accordingly, we have reduced the length of manuscript by moving figures related to monthly division of the observed data to the supplement and corresponding description has also been reduced substantially.

Specific

[RC3] In subsection 3.5 on SEM images the authors state that “these images are not being presented here for any quantitative purpose and to draw any specific scientific conclusions”. Indeed, there are only a few particles shown. However, the authors use the images to support their hypotheses on the particle species. I

propose either analyzing a large number of samples and particles to corroborate the hypotheses or moving the subsection to the supplement and being cautious on using them as evidence.

[AR3] We understand the reviewer's concern. What we meant was not to draw any scientific conclusions using the SEM images regarding neither the variabilities in bioaerosol number/mass concentration nor the type of bioaerosols. Our sole intention was to orient the reader to the dominant particle types in an air mass during three distinct focus periods. Note that we have investigated more than 100 individual particles randomly collected on five occasions and have shown few as exemplary images. This has now been clarified in the revised manuscript text (L637 – L639).

[RC4] The measurements have been done with the UV-APS. Regarding the data interpretation, it would be good to acknowledge and point out that the detection efficiency for fluorescent particles of the UV-APS is low especially below approximately 2 microns (e.g. Healy, et al., ACP2014, Saari et al., AST 2014). This mostly affects the reported fluorescent particle size distributions. Further, it would be good to state whether a zero check cycle for the instrument was used.

[AR4] As pointed out by the Reviewer few studies have reported that counting efficiency of UV-APS decreases below 2 μ m. Considering this limitation associated with the instrument we report the number concentrations of FBAPs measured using UV-APS as the lower limit proxy for bioaerosols present in the atmosphere. A line (L200) is now added in the manuscript to point out this limitation in the detection efficiency. We have performed the zero tests using HEPA filter and found no particle was detected during zero test.

[RC5] Line 250 to 273: The authors find that the fluorescent and total particle concentrations do not correlate much, independent of whether the particles are coarse or fine. They then argue that the fluorescent concentration is not affected by non-biological particles. They later hypothesize that particles from combustion or similar activities do not get transported to the measurement site. This might well be the case, but what are the high concentrations of fine non-fluorescent particles (figure S2) then? Maybe a scatter plot of NF (<1 μ m) VS NF (>1 μ m) would be useful. I would expect the submicron biological particles to correlate with the supermicron biological ones somewhat. Maybe use this point for shortening the paper and just state that there seldom are major sources of fluorescent non-biological coarse particles and therefore the numbers reported are relevant. I hypothesize that the lack of correlation for fine particles is at least partly caused by the low fluorescent particle detection efficiency of the UV-APS unit.

[AR5] We understand Reviewers concern. Our intention of carrying out the correlation analysis was to indicate that under certain conditions (mainly clean conditions persisting during monsoon at this site) UV-APS may be used to detect and segregate the particles of biological origin in sub-micron range from non-biological aerosol particles. However, interference from non-biological but fluorescent particles needs to be carefully analyzed. Further, as pointed out by

Reviewer there may be a high number concentration of the particles in sub-micron range, which are non-biological and non-fluorescent (as in our case); these particle do not likely affect the number concentration of fluorescent aerosol particles. In our case we believe, as supported by TAP number size distribution and SEM images, the non-biological and non-fluorescent particles in submicron range were mostly dominated by sea-salt and mineral dust. As suggested by Reviewer we have prepared the scatter plot of N_F for particle size range of $<1\ \mu\text{m}$ and $>1\ \mu\text{m}$ and is shown below. We infer that the particles in submicron size range, which are of not likely of biological origin are not introducing any interference in the fluorescence.

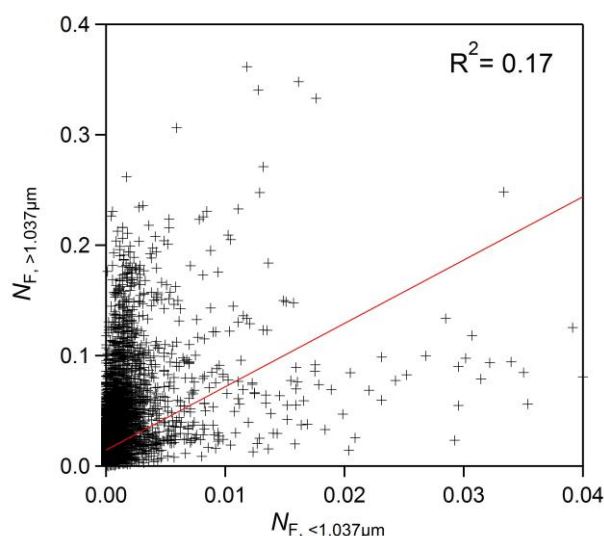


Figure R3.1: Scatter plot between N_F concentration integrated for particle size range of $<1\ \mu\text{m}$ and $>1\ \mu\text{m}$.

[RC6] Line 357-360: The high extreme values of N_F/N_T actually do result from high variations of N_F , as evident from fig S2. The presented figures do not support the argued inverse correlation between N_T and N_F/N_T . The argument should be backed with a figure or a calculation or removed.

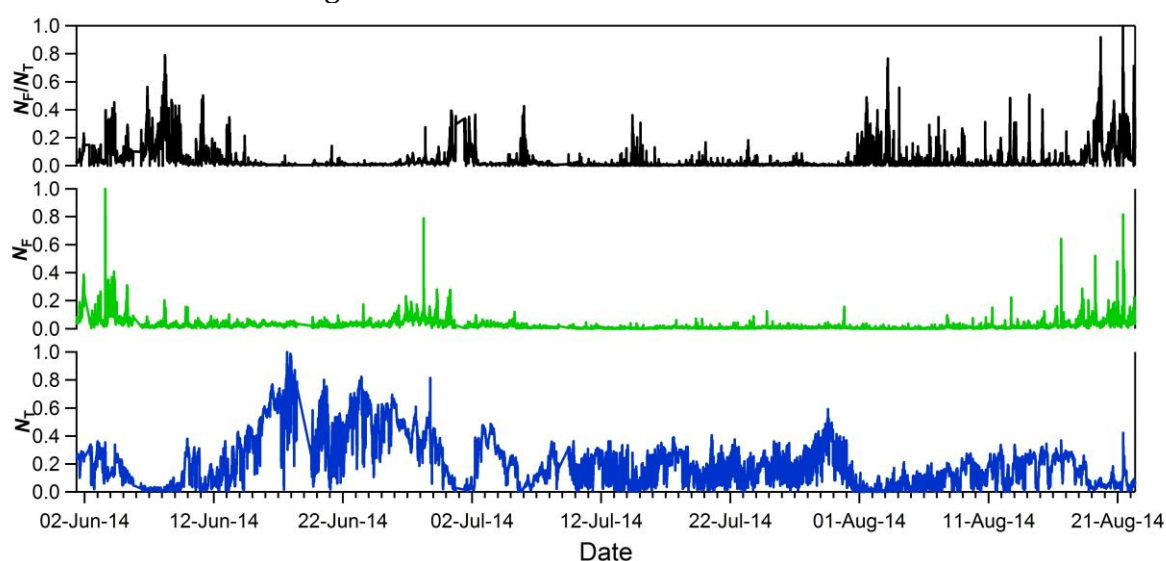


Figure R3.2: Variability in N_T , N_F and N_F/N_T averaged over the course of entire campaign.

[AR6] We are unable to understand what Reviewer means to point out. Note that we have mentioned that “The time series of relative contribution of FBAP to TAP number during the campaign overall exhibited the similar temporal variability to N_F . However, pronounced extreme values of N_F / N_T , on the other hand, resulted from strong variability in the concentration of N_T . Please refer to Figure R3.2 above, where it clearly shows the high variability in N_T (lowest panel) is much pronounced and higher during the entire measurement period. However, the corresponding variability in N_F much less pronounced and episodic. Hence, resulting variability in N_F / N_T is to an extent shows similar temporal variability as like N_F but clearly shows the inverse relation with N_T . We have mentioned the equation to derive the variability in the manuscript [L768 - L770]

[RC7] Line 703-729: The N_F axis in fig 13 is such that it is very difficult to spot small changes in concentration. However, the slightly higher concentration starts at 17.00, not at 20.00. Apparently this data does not support the nocturnal sporulation argument. The argument on humidity is later supported by the scatter plot, but it might be good to show the diurnal pattern of RH here also.

[AR7] We thank Reviewer for pointing this out, which resulted from wrong choice of scaling. This error has now been corrected in the revised version. We have also removed the sentence mentioning the nocturnal sporulation of spores to avoid confusions. As suggested by Reviewer we have now added the diurnal variations in RH, temperature, and wind speed in the revised figures. We hope that changes will be acceptable to the Reviewer.

Technical

[RC8] Line 75: The first paragraph of introduction is rather long. It would be good to separate the latter part into a new paragraph, starting on line 75 from “It is likely that the surface”. This latter part should also be reformulated, as it is very difficult to follow the line of thought now:

[AR8] Done.

[RC9] “surface structure, ice nucleating proteins, and other characteristics” – characteristics of what? Of PBAP, bacteria, bacterial spores?

[AR9] We meant to mention that surface structure, ice nucleating proteins, and other characteristics of bioaerosols can influence heterogeneous ice formation. The sentence has been modified accordingly.

[RC10] “Other bioaerosols like pollen” Other than what?
 “..Other bioaerosols like pollen and fungal spores are often using air as the transport medium.”. By definition, all atmospheric aerosol particles use air as the transport medium. Maybe: Plants and fungi use the air as a transport medium for their pollen and spores

[AR10] We agree to the Reviewer and have modified the sentence as per his/her suggestion.

[RC11] “Play an important role in public health..” It would be good to convey the idea that the role is negative.

[AR11] As per Reviewers suggestion the sentence has been modified accordingly.

[RC12] Line 123: The authors should either explain the relevance of the present study to Indian agriculture (or vice versa) or remove the sentence.

[AR12] The sentence has been modified to emphasis the importance of present study to Indian agriculture.

[RC13] Lines 192: The description of the drop of the detection efficiency is tautological with the text starting on line222.

[AR13] We thank Reviewer for indicating this. To avoid repeatability we have removed this statement from line L192.

[RC14] Line 195 on: For particles in the size range of 15-20 microns, the aspiration and transport efficiency of the sampling system probably is a more important issue than the calibration of the APS.

[AR14] This has been removed to avoid further confusion.

[RC15] Line 225: It would be good to state that the 1 micron as the fine particle size limit is adhoc.

[AR15] The sentence has been modified accordingly.

[RC16] Line 316-318: This is plausible, but should be written so that it is clear that there is no direct evidence within the present study.

[AR16] The sentence has been modified accordingly.

[RC17] Line 476-478: This is not due to the calculation. The mode mass will peak at higher diameter than number for any atmospheric particles one could find.

[AR17] To avoid any confusion, we have now removed this sentence.

[RC18] Line 484-486: Although the size limit is the same, the authors should warn the readers that the mode largely absent in NT as submicron is present in MT as supermicron.

[AR18] The reason behind such a shift from a mode in N_T in submicron range to a mode in M_T in supermicron range is clearly explained in revised manuscript (L422 – L423).

[RC19] Lines 496, 659: Note that the downwards slope of the APS detection efficiency might cause a peak to appear at around 0.9 μm even when the mode would actually peak at much lower particle diameter.

[AR19] The actual peak in the size distribution of TAP would generally occur at lower diameters ($<0.5 \mu\text{m}$). However in case of marine aerosols a secondary peak at diameter $<1 \mu\text{m}$ was also reported which was mostly contributed by the sea salt particles. In the present study since the air masses were of marine origin we believe it's important to report this peak.

[RC20] Line 536: Should this be figure 14?

[AR20] This description was with reference to the figures reported in the paper Valsan et al., 2015.

[RC21] Line 591 and elsewhere: The date format should be homogenized between the text and figures

[AR21] The date format has been homogenized.

[RC22] Line 625: "As expected, the NF was highest during the high bio period.."! This should be reformulated as the period was specifically chosen to be high bio.

[AR22] The sentence has been modified accordingly.

[RC23] Line 669 on: The medians in distributions do not make much sense for channels that exhibit a high number of zero values.

[AR23] For the completeness and consistency of the proper representation of figures we Request reviewer to retain us the same format of the figure.

[RC24] Line 770 on: The pollution/concentration rose figures are hard to read and difficult to use in backing up quantitative arguments. The interpretation instruction text in the caption of fig 15 is not helpful and the numbers seem to be wrong. Overall, it would be helpful if someone came up with a better way of displaying the correlation of measured quantities and wind. Why not start with this MS?

[AR24] We thank Reviewer for pointing this out. The caption of Fig. 15 (now Fig. 12) has been corrected accordingly and the scales shown in the wind rose diagrams were also revised for better understanding.

[RC25] Figures 10-12: If the median values are shown, it would be good to continue to show the mean/median legends on the figures.

[AR25] As indicated by the Reviewer, the mean/median legends were added on the appropriate figures.

References:

Healy, D. A., Huffman, J. A., O'Connor, D. J., Poehlker, C., Poeschl, U., and Sodeau, J. R.: Ambient measurements of biological aerosol particles near Killarney, Ireland: a comparison between real-time fluorescence and microscopy techniques, *Atmospheric Chemistry and Physics*, 14, 8055-8069, 10.5194/acp-14-8055-2014, 2014.

Saari, S., Reponen, T., and Keskinen, J.: Performance of two fluorescence-based real-time bioaerosol detectors: BioScout vs. UVAPS, *Aerosol Science and Technology*, 48, 371-378, 10.1080/02786826.2013.877579, 2014.

Valsan, A. E., Priyamvada, H., Ravikrishna, R., Després, V. R., Biju, C. V., Sahu, L. K., Kumar, A., Verma, R. S., Philip, L., and Gunthe, S. S.: Morphological characteristics of bioaerosols from contrasting locations in southern tropical India – A case study, *Atmospheric Environment*, 122, 321-331, <http://dx.doi.org/10.1016/j.atmosenv.2015.09.071>, 2015.

1 **Fluorescent Biological Aerosol Particle Measurements at a Tropical High Altitude Site in**
2 **Southern India during Southwest Monsoon Season**

3 A. E. Valsan^{1,*}, R. Ravikrishna², C. V. Biju³, C. Pöhlker⁴, V. R. Després⁵, J. A. Huffman⁶, U.
4 Pöschl⁷, and S. S. Gunthe^{1,**}

5
6 ¹EWRE Division, Department of Civil Engineering, Indian Institute of Technology Madras,
7 Chennai – 600 036, India.

8 ²Department of Chemical Engineering, Indian Institute of Technology Madras, Chennai – 600
9 036, India.

10 ³Department of Civil Engineering, College of Engineering Munnar, PB.No:45, County Hills,
11 Munnar – 685612, India.

12 ⁴Biogeochemistry Department, Max Planck Institute for Chemistry, P. O. Box Number 3060,
13 Mainz, Germany.

14 ⁵Institute of General Botany, Johannes Gutenberg University, Mainz, Germany.

15 ⁶Department of Chemistry and Biochemistry, University of Denver, 2190 E. Iliff Ave., Denver,
16 CO, 80208, USA.

17 ⁷Multiphase Chemistry Department, Max Planck Institute for Chemistry, P. O. Box 3060, Mainz,
18 Germany

19

20

21 To whom correspondence should be addressed:

22 * Aswathy E. Valsan (aswathyerat@gmail.com)

23 ** Sachin S. Gunthe (s.gunthe@iitm.ac.in)

24

25 Abstract

26 ~~Primary Biological Aerosol Particles (PBAPs) like fungal spores, bacteria, pollen, etc. are~~
27 ~~reported to constitute large fraction of the atmospheric aerosols. They are responsible for the~~
28 ~~spread of organisms and diseases throughout the biosphere and may impact atmospheric~~
29 ~~processes and the hydrological cycle by acting as ice nuclei (IN) and giant cloud condensation~~
30 ~~nuclei (CCN). Despite their importance in the biosphere and climate, continuous measurements~~
31 ~~of PBAPs in high time and size resolutions are not available for the Indian subcontinent. Here we~~
32 ~~report the first measurements of fluorescent biological aerosol particles (FBAPs) in India. The~~
33 ~~measurements were carried out using an ultraviolet aerodynamic particle sizer (UV-APS) in~~
34 ~~Munnar, a high altitude tropical site in southern India. The study was conducted for three~~
35 ~~consecutive months during the Southwest monsoon season (1.June.2014 — 21.August.2014),~~
36 ~~which is marked by heavy and persistent rainfall and strong Westerly/Southwesterly clean winds.~~
37 ~~Averaged over the entire campaign arithmetic mean number and mass concentrations of coarse-~~
38 ~~mode FBAP ($> 1 \mu\text{m}$) were 0.02 cm^{-3} and $0.24 \mu\text{g m}^{-3}$, respectively, which corresponded to ~2~~
39 ~~and 6 % of total aerosol loading, respectively. An ultraviolet aerodynamic particle sizer (UV-~~
40 APS) was continuously operated for the first time during two seasons to sample the contrasting
41 winds during monsoon and winter to characterize the properties of fluorescent biological aerosol
42 particles (FBAPs), at a high altitude site in India. Averaged over the entire monsoon campaign
43 (June 1, 2014 – August 21, 2014) the arithmetic mean number and mass concentrations of
44 coarse-mode ($>1 \mu\text{m}$) FBAP were 0.02 cm^{-3} and $0.24 \mu\text{g m}^{-3}$, respectively, which corresponded
45 to ~2 and 6 % of total aerosol loading, respectively. Average FBAP number size distribution
46 exhibited a peak at $\sim 3 \mu\text{m}$, which ~~was most likely contributed by~~ is attributed to the fungal
47 spores, as supported by scanning electron microscope (SEM) images, and these results are

Formatted: Justified

48 consistent with previous studies made for FBAP. During eleven weeks of measurements the
49 variability of the ~~-corresponding-~~total coarse mode particle number (TAP) ~~coarse mode particle~~
50 ~~number~~ concentration was high compared to that ~~highly variable in contrast to the variability~~
51 observed in FBAP number concentration. ~~Averaged over the entire campaign the TAP number~~
52 ~~and mass concentrations were 1.8 cm^{-3} and $7.0 \text{ }\mu\text{g m}^{-3}$.~~ The TAP and FBAP number
53 concentrations measured at this site were strongly dependent on changes in wind direction and
54 rainfall. During ~~the periods~~ of westerly/southwesterly winds with heavy ~~continuous and~~ persistent
55 rainfall, ~~s~~ the TAP and FBAP concentration exhibited very low ~~concentration levels~~ values (1.3
56 cm^{-3} and 0.005 cm^{-3} , respectively) with no ~~observed~~ significant diurnal variations. Whereas
57 during periods of Northerly winds with scattered rainfall FBAP exhibited relatively high
58 concentration values (0.05 cm^{-3}) with pronounced diurnal variations, which were strongly
59 coupled with diurnal variations in meteorological parameters. ~~Averaged over the entire~~
60 ~~campaign FBAP exhibited a moderately diurnal variation with highest concentration during early~~
61 ~~morning hours (~06:00–08:00 hrs).~~ The campaign averaged FBAP number concentrations were
62 shown to correlate with daily patterns of meteorological parameters and were positively
63 correlated with relative humidity (RH; $R^2=0.58$), and negatively with temperature ($R^2=0.60$) and
64 wind speed ($R^2=0.60$). We did not observe any significant positive correlation with precipitation
65 as reported by previous researchers from selected areas. These measurement results confirms the
66 fact that ~~fraction~~ the ratio of PBAPs to TAP is strongly dependent on particle size and location
67 and thus may constitute a significant proportion of total aerosol particles.

1 Introduction

Aerosols are generally defined as a colloidal system of solid or liquid particles suspended in a gaseous medium (Fuzzi et al., 1997; Pöschl, 2005) and are ubiquitous in the Earth's atmosphere. The term "Primary Biological Aerosol Particles" (PBAPs; sometimes also referred as bioaerosols or biological aerosols), describes a subset of ~~aerosol particles, i.e. the~~ solid airborne particles originating from biological organisms, including viruses, pollen, microorganisms (bacteria, fungal spores, etc.) and, protozoa or algae, etc., together with fragments of biological materials such as animal dander, plant debris etc. (Artaxo and Hansson, 1995; Coz et al., 2010; Després et al., 2007, 2012; Elbert et al., 2007). Bioaerosols can range in size from a few nanometers to few hundred micrometers in aerodynamic diameter, D_a , (Coz et al., 2010; Després et al., 2012; Jones and Harrison, 2004; Matthias-Maser and Jaenicke, 1994). ~~with viruses being the smallest in size amongst the PBAPs followed by bacterial and fungal spores, while pollen, and plant and animal fragments represent the largest in size. Depending upon size and ecosystem~~ PBAPs can have been shown to constitute 14 – 70% of total number of coarse mode particles and around 20 – 24 % of total mass of PM_{10} (particulate matter with size $\leq 10 \mu m$; Elbert et al., 2007; Després et al., 2012; Pöschl et al., 2010; Huffman et al., 2012). ~~Bioaerosols are present in the ambient atmosphere either as a single particle, or as agglomerates (Valsan et al., 2015) and exhibit a variety of shapes and morphological characteristics.~~ Further, it is likely that the surface structure, ice nucleating proteins, and other characteristics of bioaerosols can influence substantially the heterogeneous ice nuclei formation at ~~various~~relatively high temperature levels (Morris et al., 2004, 2014) and they can also act as giant cloud condensation nuclei (GCCN), thus affecting the hydrological cycle (Andreae and Rosenfeld, 2008; Möhler et al., 2007). ~~Other bioaerosols like pollen or fungal spores are often using air as the transport medium for distribution and transfer of~~

91 ~~genetic material and thus can travel and get transported over large distances.~~ It is also known that
92 plants and fungi use air as a medium for transport of their pollens and spores, respectively, thus
93 resulting in distribution and transfer of genetic material over large distances. (Huffman et al.,
94 2010; Elbert et al., 2007; Hallar et al., 2011; Burrows et al., 2009). A side effect of such a
95 transport and distribution, however, is that they are produced and spread in large quantities and
96 can play an important a negative role in public health. ~~as they can cause allergies.~~ Pathogenic
97 fungi have long been recognized as major threats to animal health and plants including crops
98 severely jeopardizing the food security (Fisher et al., 2012 and references therein).

99 ~~Since the last century numerous studies have been conducted in different parts of the world to~~
100 ~~understand the abundance and diversity of bioaerosols using various sampling and measurement~~
101 ~~techniques, however confining to traditional methods.~~ The last decade has experienced a
102 substantial development and application of advanced online and offline techniques for studying
103 the characteristic properties of bioaerosols in both ~~the~~ field and laboratory (Fröhlich-Nowoisky,
104 et al., 2009; DeLeon-Rodriguez et al., 2013; Prenni et al., 2009; Huffman et al., 2010, 2012,
105 2013; Schumacher et al., 2013; Pöhlker et al., 2012, 2013).

106 Instruments utilizing laser-induced fluorescence (LIF) have been frequently deployed to the
107 field, enabling real-time characterization of the number size distribution of PBAPs in high time
108 and size resolution. However, instruments based on LIF do not provide detailed information
109 directly about PBAPs or particle origin, but rather provide broadly categorized information due
110 to a mixture of biological fluorophores, each detected with varying efficiency (Pöhlker et al.,
111 2012, 2013). Most FBAP measurements have shown that the dominant size range for PBAPs
112 number size distribution is 1 – 4 µm with concentration varying within the factor of 10 (Gabey et
113 al., 2011, 2013; Healy et al., 2014; Huffman et al., 2010, 2012, 2013; Saari et al., 2015;

114 Schumacher et al., 2013; Toprak and Schnaiter, 2013; Yu et al., 2016). As studied and described
 115 by Huffman et al., (2010), based on ~~long-term four-months of PBAP~~ measurements in central
 116 Europe, the signal detected by UV-APS (Ultraviolet Aerodynamic Particle Sizer) ~~in ambient~~
 117 ~~settings~~ was defined as Fluorescent Biological Aerosol Particles (FBAP). ~~and the resulting~~
 118 ~~quantification of FBAP was further discussed and it was concluded that FBAP represents an~~
 119 ~~approximate lower limit of actual abundance of PBAPs present in the ambient air sampled by the~~
 120 ~~UV APS. Thus, for the consistency and simplicity we use the similar terminology as suggested~~
 121 ~~by Huffman et al., (2010).~~ Hence, the term FBAP is used as a lower limit proxy for primary
 122 biological aerosol particles (PBAPs), biological aerosols, biological aerosol particles, bioaerosols
 123 and similar terms mentioned in this study.

124 Despite such instrumental advancements described above, ~~the~~ studies related to the
 125 quantification of bioaerosols and their role in climate and human health have been extremely
 126 limited in space and time. ~~This is P~~ particularly ~~true~~, for the Indian subcontinent, which constitute
 127 ~~around~~ ~18% of the world's total population, ~~where~~ studies related to the bioaerosols are
 128 relatively few ~~and~~ with ~~spotty~~ analysis performed only by traditional techniques (Bhati and Gaur,
 129 1979; Chakraborty et al., 1998; Gangamma, 2014; Srivastava et al., 2012; Sharma and Rai, 2008;
 130 Pachauri et al., 2013; Valsan et al., 2015; Ansari et al., 2015; Adhikari et al., 2004). ~~Thus,~~
 131 ~~sources, abundance, and properties of bioaerosols,~~ The abundance of bioaerosols, which ~~are is~~
 132 strongly dependent on location and season, remains poorly characterized over the Indian
 133 subcontinent and need to be addressed systematically.

134 Additionally, ~~I~~ investigating and quantifying the role of bioaerosols over the Indian continent is
 135 ~~not only~~ important ~~because of the scarcity in the literature but also~~ due to its diverse land-use
 136 pattern and the unique climatic condition experienced ~~by the~~ in terms of two ~~M~~ monsoon seasons

137 associated with two distinct synoptic scale wind patterns. ~~Indian agriculture is strongly~~
138 ~~dependent on the Southwest Monsoon, and is the largest livelihood provider in India and~~
139 ~~contributes a significant figure to the Gross Domestic Product (GDP).~~ The concentration of
140 fluorescent aerosol particles in a semi-arid forest in the Western US was shown to increase
141 during and after rainfall (Huffman et al., 2013). Rainfall-triggered increase in bioaerosol
142 concentration can potentially enhance further precipitation by convective upward movement of
143 bioaerosols into clouds where they can serve either as IN or giant CCN (Shcumacher et al., 2013;
144 Huffman et al., 2013). Thus, the bioaerosols emitted during monsoon rainfall could potentially
145 play an important role in cloud and precipitation formation over India (Ansari et al., 2015).

146 Therefore, it is very important to better understand and quantify the role of bioaerosols in cloud
147 and precipitation formation during ~~M~~monsoon and convective rainfall. ~~The concentrations of~~
148 ~~fluorescent aerosol was shown to increase during and after rainfall in a semi arid forest in the~~
149 ~~Western US (Huffman et al., 2013), but the same pattern was not observed in a similar study in~~
150 ~~the Amazon basin (Huffman et al, 2012). Thus, the bioaerosols emitted during monsoon season~~
151 ~~could potentially play an important role in cloud and precipitation formation as shown by Ansari~~
152 ~~et al. (2015).~~ Additionally, bioaerosols over the Indian sub-continent can ~~have a directly~~ societal
153 impact society ~~where huge set of population may directly get affected by~~ through the spread of
154 diseases and indirectly due to increased risk of loss of ~~covertly due to the loss in~~ agricultural
155 output due to emerging diseases caused by, e.g. fungal attacks on agriculture (Fisher et al.,
156 2012).

157 ~~Thus, s~~Studies involving characterization of bioaerosols using advanced techniques over this
158 region are important to understand and quantify the impact of bioaerosols on regional
159 biodiversity with larger implication towards human and ecosystem health. With this motivation

Formatted: Justified

160 | we have deployed a UV-APS for the detection and measurement of number size distribution of
161 | PBAPs at a high-altitude site of Munnar in Western Ghats of southern tropical India during
162 | Southwest monsoon season for ~3 months. To our knowledge this study presents the first ~~multi-~~
163 | ~~month-~~ambient measurement investigations involving UV-APS for multiple months over the
164 | Indian subcontinent.

165 |

166 | 2 Methods

167 | 2.1 Site Description

168 | Measurements were performed to sample the air masses (see section 2.2) from a high-altitude
169 | site (Munnar; 10.09°N, 77.06°E; 1605 m amsl – above mean sea level – Fig. 1) located in the
170 | Western Ghats region of ~~just 90 km away as the crow flies from Arabian Sea in the~~ Southern,
171 | ~~part of~~ tropical India, just 90 km away from the Arabian Sea. The observational site is located on
172 | a hill with a valley towards the South and a small mountain towards the North surrounded by
173 | dense vegetation including tea gardens and Eucalyptus trees. Climatologically this region is
174 | classified as subtropical highland with dry winters and is listed as the Shola forest-grass
175 | ecosystem as defined in the land-use type terminology (Fig. S1). The Western Ghats, one of the
176 | eight mountain ranges in India and identified as one of the ~~hottest-~~most significant hot spots of
177 | biodiversity (Myers et al., 2000) in the world, originates near the border of Maharashtra and
178 | Gujarat running ~1600 km towards South, parallel to the Western coast through the states of
179 | Gujarat, Maharashtra, Karnataka, Kerala, and Tamilnadu ending at the Southern tip of India near
180 | Kanyakumari. This mountain range separates the coastal plain from the Deccan plateau making
181 | Western coastal plain a narrow land strip with a maximum width of ~ 110 – 120 km, sandwiched
182 | between the Western Ghats and the Arabian Sea. During the SW Monsoon season (June –

Formatted: Justified

183 | September) the Southwesterly, moisture laden winds are intercepted by the Western Ghats
184 | causing persistent and heavy rainfall on the windward side of these mountains. This causes the
185 | wash out and wet deposition of the pollutants in the coastal strip (Kerala) emitted due to
186 | anthropogenic activities, thus bringing clean marine influx with minimum impact of
187 | anthropogenic emissions (Satheesh and Srinivasan, 2002). Therefore, during this particular
188 | season this observational site can be regarded as relatively pristine, as compared to any other
189 | operational high-altitude observatory/site in Indian tropical region (Shika et al., 2016).

190 |

191 | 2.2 General Meteorology

192 | Southern India nominally experiences two Monsoon seasons, the ~~Southwest~~ SW monsoon (~~SW;~~
193 | ~~June – September~~) and the Northeast monsoon (NE; November – January), which are strongly
194 | associated with the movement of Inter-Tropical Convergence Zone, the ITCZ (Kanawade et al.,
195 | 2014). The SW monsoon winds ~~are dominant during June to September bringing almost~~
196 | ~~anthropogenically “clean” (not affected by human activities)~~ relatively clean marine influx over
197 | the continent from Arabian Sea when the ITCZ moves Northwards reaching 30°N during July
198 | (Naja and Lal, 2002). These air masses originate over the Indian Ocean and travel thousands of
199 | kilometers over the ocean ~~oceanic water~~, including the Arabian Sea, before reaching the
200 | observational site. The Southward movement of ITCZ reaching up to the equator is associated
201 | with the NE monsoon, which is also marked as winter season in India occurring during October
202 | to January, when the prevailing winds are predominantly blowing in the NE direction. The
203 | measurement site of Munnar receives more than 85% of its annual rainfall during SW monsoon
204 | season and experiences scattered rainfall events during NE monsoon. ~~season~~. The detailed

Formatted: Justified

meteorological parameters measured during the field measurement campaign carried out during SW Monsoon season at Munnar are discussed below.

207

2.3.2 Real-time fluorescence measurement

Biological aerosol particles at Munnar from a high altitude relatively pristine site were measured using an UV-APS (TSI Inc. Model 3314; Serial Number: 71331023) as per the standard instructions given in the technical manual. The detailed description about the instrument including operating principles, field operation, data analysis protocol, and critical operational parameters are discussed elsewhere (Kanaani, et al., 2007, 2008; Agranovski et al., 2003, 2004, 2005; Brosseau et al., 2000; Huffman et al., 2010, 2012; Hairston et al., 1997).

Briefly, the instrument is capable of measuring the aerosol particles in the aerodynamic diameter (D_a) range of 0.54 – 20.19 μm over 52 channels by means of measuring the time-of-flight between two He-Ne red lasers ($\lambda=633$ nm). Once the particle size is determined, each the same particle is further excited using an third-ultraviolet Nd:YAG laser ($\lambda=355$ nm) and fluorescent emissions are measured in the range of 420 – 575 nm. The spectrally unresolved total fluorescence is recorded for each individual particle in to one of the 64 channels, with increasing order of fluorescence intensity. Huffman et al., (2010) described that the counting efficiency of the instrument drops below 100% at $D_a < 0.7 \mu\text{m}$ (counting efficiency ~ 50% at 0.54 μm), hence, the particle number concentration values reported for particle sizes of $< 0.7 \mu\text{m}$ are lower limit of the actual concentration of the air sample. During analysis presented in this paper the particles detected in the size range of 15 – 20 μm were included and the reported number concentration values should be considered as the lower limit of the actual values present in the air sample, due to limitations in the size calibration for particles of this size. The UV-APS measurement cycle

Formatted: Justified

was initiated with 5 minutes intervals ~~s (including the full diameter range scan for 285 seconds and~~
~~15 seconds of back scanning~~ recording total of 22280 sampling points during entire
measurement campaign) ~~where air sample was drawn with a~~ volumetric flow rate of 5 L~~pm~~ min⁻¹
~~(4pm)~~ at ambient temperature and pressure. All ~~the~~ times reported in this study are local time
pertaining to Indian Standard Time ~~(IST; GMT+5:30)~~.
~~The UV-APS was placed next to the window inside a room in the College of Engineering,~~
~~Munnar, Kerala located on a hill. A stain less steel tubing with 3/4" OD (outer diameter) and TSP~~
~~inlet was used to construct the inlet unit for air sampling, which was 9 m and 2 m above the~~
~~ground and rooftop, respectively. Thus the sampled air masses were expected to have minimal~~
~~influence caused by the dynamics associated with the building structure. Sampling was~~
~~performed at a building of the College of Engineering, Munnar, Kerala. The sampling inlet was~~
~~approximately 2m and 8m above the rooftop of the building and the adjacent ground~~
~~respectively. The sampling inlet was connected to the UV-APS, which was placed next to the~~
~~window inside a room by 3m of 3/4" OD stainless steel tubing.~~ To minimize the particle losses
due to impaction resulting from sharp bends, ~~the~~ electrically conductive silicon rubber tubing
(~1.5 m; 12 mm inner diameter) was attached to the stain-less steel tube just outside the window
(Fig. S1), ~~avoiding the sharp bends. Before the sampled air~~ The air sample was passed ~~through a~~
~~to the instrument,~~ diffusion dryer (~1 m ~~length~~) with silica gel ~~(orange color indicating) was used~~
~~to dry and before entering the UV-APS, thus~~ maintaining the ~~humidity of inlet air to a~~ relative
humidity <40%. ~~Thus combining all the tubing involved in the air sampling the sample flow. The~~
~~residence time of sampled air in the inlet tube~~ was calculated to be ~ 20 seconds, ~~and the flow~~
~~was calculated to be laminar during entire sampling line. The sample flow through all the tubing~~
~~was expected to be laminar during entire sampling period and hence,~~ diffusion losses are

251 expected to be negligible for all the size-ranges of the sampled particles ([average penetration](#)
 252 [efficiency of 99.8% at 290K and 840 hPa; Baron and Willeke, 2005](#)).
 253 For the present study ~~we derived the~~ number size distribution of fluorescence biological aerosol
 254 particles, $(dN_F/d\log D_a)$, for each size bin [was derived](#) by summing up the particle number
 255 concentration from the fluorescence channel numbers 3 – 64 and similarly the total particle
 256 number size distribution, $(-dN_T/d\log D_a)$, was derived from channel numbers 1 – 64. In the
 257 present study we have used 1.0 μm as a cut-off diameter for given $dN_F/d\log D_a$ and $dN_T/d\log D_a$
 258 to calculate the fluorescence biological aerosol number and total aerosol number concentrations,
 259 N_F and N_T , respectively. This is mainly due to the fact that particle counting efficiency of the
 260 UV-APS drops below unity at 0.7 μm ([counting efficiency ~50% at 0.54 \$\mu\text{m}\$](#)) and the
 261 interferences ~~due to fluorescence~~ from non-biological aerosol particles below 1.0 μm can at
 262 times be very high (Huffman et al., 2010). [Few other studies have reported a decrease in UV-](#)
 263 [APS counting efficiency for FBAPs < 2 \$\mu\text{m}\$ based on comparison of ambient FBAPs with](#)
 264 [another LIF instrument \(WIBES and Bio-Scout\) using different fluorescence wavelengths \(Healy](#)
 265 [et al. 2014, Saari et al., 2014 \). In the present study we define 1 \$\mu\text{m}\$ as the cutoff diameter to](#)
 266 [distinguish between the submicron \(<1 \$\mu\text{m}\$ \) and the supermicron \(>1 \$\mu\text{m}\$ \) modes of the particle](#)
 267 [number size distribution. Also note that the cutoff at 1 \$\mu\text{m}\$ moreover represents the border](#)
 268 [between fine \(<1 \$\mu\text{m}\$ \) and coarse \(>1 \$\mu\text{m}\$ \) modes of the particle number size distribution.](#) The
 269 subscripts throughout this manuscript text “F” and “T” refer to fluorescent and total coarse mode
 270 particles, respectively. ~~See~~[Please refer to](#) Table 1 for ~~the~~ abbreviations, notations, and symbols
 271 used in this manuscript. The particle mass size distributions $(dM/d\log D_a)$ for total as well as
 272 fluorescent biological aerosol particles were calculated for each size bin by multiplying
 273 $dN/d\log D_a$ with volume of an aerodynamically equivalent sphere with the geometric midpoint

diameter ($D_{a,g}$) and assuming the unit density (1 g cm^{-3}) and unit shape factor. The integral mass concentrations of coarse fluorescent biological aerosol particles and total coarse particles, M_F and M_T , respectively were calculated by integrating the particle mass distribution for $D_a > 1 \mu\text{m}$, thus particle mass reported here; ~~but~~ should be viewed as first approximation as a result of uncertainty associated with the density and shape of the particles (Huffman et al., 2010). To be consistent with previous UV-APS results no standard temperature and pressure (STP) corrections were applied to the concentrations reported in this study. These number concentrations can be normalized to the volume that the sampled air would occupy under dry standard condition (STP: 273K, 1000 hPa, and 0% RH) by multiplying the concentration values reported here with a factor of 1.29 derived using ideal gas law.

Fluorescence of submicron particles

It has been reported by previous researchers that UV-APS is known to exhibit fluorescence for some fraction of non-biological aerosol particles including soot, PAHs, and cigarette smoke, which could be erroneously counted as FBAP (Huffman et al., 2010; Pan et al., 1999a, 1999b). ~~It has also been emphasized that such interference can mostly occur for particles less than $1 \mu\text{m}$ as the contribution from combustion sources at this size range is expected to be dominant.~~ To investigate the contribution of non-biological aerosol particles that are counted as fluorescence biological aerosol particles, Huffman et al., (2010) ~~performed~~ showed the correlation between the integrated number concentrations of fluorescent particles (N_F) and total particles (N_T) for different diameter ranges (only for the fluorescence channels >3). ~~They found that the correlation for the submicron particles was systematically linear, whereas the correlation for supermicron particles was more random, indicating that a large fraction of submicron particles showing fluorescence might have been originated from anthropogenic sources, which may not be the case~~

297 ~~for the supermicron particles.~~ To ~~investigate~~ examine the influence of anthropogenic emissions
 298 on submicron fluorescent particles, we performed the similar correlation analysis for the entire
 299 campaign. ~~and, however, found the different results.~~ The correlation between integrated number
 300 concentrations of fluorescent particles (N_F) and total particles (N_T) for supermicron ($D_a > 1$) and
 301 submicron ($D_a < 1 \mu m$) diameter range exhibited a very poor scatter ($R^2 = 0.03$ and $R^2 = 0.002$
 302 respectively; $N = 22280$; Figs. S2) indicating extremely small percentage of fluorescence was
 303 contributed by non-biological aerosol particles in both supermicron and submicron particle
 304 ranges. This was in contrast with the observations in Huffman et al (2010).
 305 Since certain component of the mineral dust may exhibit a weak fluorescence (Huffman et al.,
 306 2010; Sivaprakasam et al., 2004; Toprak and Schnaiter, 2013), we performed the separate
 307 correlation analysis for ~~a focus period~~ the dusty period, which was dominated by the transport of
 308 mineral dust from West Asia, North Africa, and Arabian region (discussed below). The
 309 correlation between integrated number concentrations of N_F and N_T for $D_a > 1 \mu m$ was moderately
 310 linear ($R^2 = 0.26$; $N = 3138$; Fig. S3a) compared to submicron size range during the dusty period
 311 ($R^2 = 0.007$; $N = 3138$; Fig. S3b). ~~As a result, correlation between N_F and N_T indicates that the~~
 312 ~~fraction of supermicron particles exhibiting fluorescence may have been contributed by mineral~~
 313 ~~dust, but this being not the case~~ not for submicron particles.
 314 From these analyses we infer that the contribution of non-biological aerosol particles exhibiting
 315 fluorescence was negligible in both submicron and supermicron (except during “dusty period”;
 316 discussed below) size ranges. Thus we hypothesize that due to persistent rainfall the submicron
 317 and supermicron particles resulted from combustion and other similar activities, were either
 318 efficiently removed or were not transported to the observational site. ~~indicating that substantial~~
 319 ~~fraction of the particles in both the size ranges were of biological origin.~~ Thus this observational

Formatted: Font: Italic

Formatted: Font: Italic

320 site could be potentially termed as relatively pristine and free from anthropogenic emissions
321 during the monsoon season making this site scientifically interesting for investigating the
322 characteristic properties of bioaerosols on long-term basis using advanced online and offline
323 techniques as future studies..
324 ~~Please note, however~~However, ~~that to have~~to maintain the consistency and uniformity in the
325 comparison of N_F , N_T , and other similar parameters reported by the previous studies ~~we derived~~
326 all the statistics associated with $dN_F/d\log D_a$ and $dN_T/d\log D_a$ with a cutoff diameter of $\sim 1 \mu m$
327 were derived.

329 **2.4.3 Meteorological parameter measurement**

330 The meteorological parameters in parallel with the UV-APS measurements were recorded during
331 the entire campaign using ~~an ultrasonic~~weather sensor (Lufft WS600-UMB) installed on ~~a~~the
332 rooftop at the same height and a few meters away from the UV-APS inlet (Fig. ~~S11b~~1b). The
333 weather station was capable of recording temperature, dew point temperature, relative humidity,
334 precipitation intensity, wind speed, wind direction, and air pressure and was set to record these
335 meteorological parameters with every 5 minutes interval with time synchronized to UV-APS
336 measurement clock. ~~The data from the weather sensor was stored by using an in-house~~
337 ~~developed external data logger.~~The obtained meteorological data was compared with another
338 ~~ultrasonic~~weather station installed within the close vicinity (Vaisala ~~make~~WXT520). The
339 scatter plots between the data (10 min averaged) obtained from our weather station and the one
340 installed in the close vicinity exhibited very strong agreement for all the meteorological
341 parameters measured/recorded (average $R^2 \geq 0.95$).

Formatted: Justified

343 2.4.5 SEM Analysis

344 The samples for Scanning Electron Microscopy (SEM) analysis were collected on a 25 mm
345 diameter Nucleopore® Polycarbonate filter paper with pore sizes of 5 µm and 0.2 µm using a
346 two stage filtering method as described by Valsan et al., (2015). All samples were collected for
347 approximately a duration of 60 min at an average flow rate of 5 Lpm and were stored in an air-
348 tight container at 4°C until the SEM analysis was carried out. ~~The five samples collected~~ More
349 than 100 individual particles analyzed from samples collected on five occasions during the entire
350 campaign, were ~~analyzed~~ investigated using two different scanning electron microscopes. 1.
351 Quanta FEG 200 located at the Sophisticated Analytical Instrument Facility (SAIF) and 2.
352 Hitachi S 4A00 located at the Chemical Engineering Department of Indian Institute of
353 Technology Madras. Before loading the filter paper on to the studs, they were cut into small
354 squares of ~1 cm² and sputter coated with gold particles. The biological aerosol particles were
355 identified purely based on their morphological features adopting the method suggested by
356 Matthias-Maser and Jaenicke (1991,1994). Detailed description on sample collection and
357 analysis was discussed elsewhere (Valsan et al., 2015).

358

359 3 Results and discussions

360 3.1 Campaign overview

361 Figure 2 shows the temporal evolution and variability of the several meteorological parameters,
362 ~~characteristic for the meteorological conditions~~, FBAP, and TAP properties observed throughout
363 the measurement campaign during SW monsoon season at ~~a high altitude site of~~ Munnar.
364 ~~Overall the meteorological conditions during the campaign at Munnar can be summarized as~~
365 ~~follows:~~ Several observations regarding the meteorological conditions during the campaign at

Formatted: Justified

Formatted: Justified

366 [Munnar can be made.](#) The predominant wind direction was observed to be
 367 Westerly/Southwesterly (Fig. 1), which [is characteristic of](#) the monsoon season [and](#) bringing
 368 ~~almost anthropogenically~~ [nearly](#) clean marine influx ([laden with dust and sea salt particles](#); Vinoj
 369 and Satheesh, 2003; [Vinoj and Satheesh, 2003; Satheesh and Srinivasan, 2002; Vinoj et al.,](#)
 370 [2014; Prospero, 1979](#)) over the continent marked by presence of persistent rainfall, high relative
 371 humidity (RH), higher wind speeds, and lower temperatures. During this period ~~the~~ diurnal
 372 variations in temperature and relative humidity were totally absent and temperatures ~~almost~~
 373 approached the dew point temperature. ~~Further, the Westerly/Southwesterly air masses arriving~~
 374 ~~at the observational site were free from any anthropogenic influence and were laden with dust~~
 375 ~~and sea salt particles (Satheesh and Srinivasan, 2002; Vinoj et al., 2014; Prospero, 1979).~~ [On a](#)
 376 few occasions, however, Northerly winds were ~~also observed~~ [recorded](#), ~~which was associated~~
 377 ~~with calm winds~~ [marked by relatively lower wind speed](#), lower RH levels, higher temperatures,
 378 and reduced rainfall. During Northerly winds the temperature exhibited ~~relatively~~ more
 379 pronounced diurnal variations compared to the relative humidity. The average meteorological
 380 parameters (arithmetic mean \pm standard deviation) recorded during entire measurement period
 381 were: (840 \pm 1.3) hPa absolute pressure, (17.2 \pm 1.4) $^{\circ}$ C ambient temperature, (96.4 \pm 5.7) % relative
 382 humidity, (2.8 \pm 1.3) m s $^{-1}$ local wind speed, (270) $^{\circ}$ local wind direction (vector mean weighted by
 383 wind speed), and (4188) mm of accumulated rainfall.
 384 The total of more than five months of bioaerosol measurements in high time and size resolution
 385 were performed at this site ~~comprising for~~ two contrasting seasons, monsoon (dominated by
 386 Southwesterly winds) and winter (dominated by Northeasterly winds). In this study we present
 387 the results from the field campaign carried out during the SW monsoon season whereas the
 388 detailed results from the winter campaign from the same measurement site will be presented in

the ~~a~~ follow up study. We first discuss the characteristic features of the time series as a broad
 overview of the observed concentration levels, variability, and trends in N_T and N_F . Figure 2
 (f,g,h,i,j) shows the time series of geometric mean diameter (D_g), N_F , N_F/N_T , N_T , FBAP and TAP
 3-D ~~and the~~ size distribution measured with the UV-APS for the entire campaign.
 Throughout the measurement period the hourly averaged D_g time series consistently remained in
 the range of $\sim 2 - 4 \mu\text{m}$ with almost no diurnal variations. During the second half of the
 campaign, the D_g , however, exhibited relatively high variability with average mean diameter of
 $2.6 \pm 0.7 \mu\text{m}$. Unlike the N_T and N_F the variability in D_g ~~was observed~~ did not seem to be ~~not~~
 affected by meteorological parameters except for wind direction (see section 3.6.4.1) ~~on few~~
 occasions. The total coarse particle number concentration, N_T , exhibited high and consistent
 variability during entire measurement period, however, with no distinct diurnal cycle. ~~Averaged~~
 (arithmetic mean \pm standard deviation) over the entire measurement period N_T was observed to be
 $1.8 \pm 1.5 \text{ cm}^{-3}$ with lowest and highest concentrations of 0.01 cm^{-3} and 8.6 cm^{-3} , respectively. ~~The~~
~~average N_T concentration during the months of June, July, and August was $2.7 \pm 1.9 \text{ cm}^{-3}$;~~
 ~~$1.5 \pm 0.96 \text{ cm}^{-3}$, and $0.96 \pm 0.77 \text{ cm}^{-3}$, respectively, with highest and lowest values for individual~~
~~months respectively as follows: June: 8.6 and 0.04 cm^{-3} , July: 5.1 and 0.02 cm^{-3} , and August: 3.6~~
~~and 0.01 cm^{-3} (Fig. S4).—~~ The monthly averaged N_T concentration (Fig. S4) exhibited the
 decreasing trend from June to August as the monsoon progressed (Tab. 2). In contrast to the
 total aerosol particle number concentration, N_F , exhibited less pronounced but episodic peaks in
 the time series during the majority of the measurement period, resulting in ~~modest variability~~
~~and~~ a campaign arithmetic mean value ~~of~~ ~~was~~ $0.02 \pm 0.02 \text{ cm}^{-3}$. The highest N_F concentration of
 $\sim 0.52 \text{ cm}^{-3}$ was observed ~~on 3rd of~~ in June, prior to the onset of monsoon rainfall, ~~(and few more~~
~~occasions)~~ whereas the lowest N_F concentration ($< 0.0002 \text{ cm}^{-3}$) was consistently observed on

412 more than one occasion during the months of July and August. ~~The average N_F concentration~~
413 ~~during June and August was $0.03 \pm 0.03 \text{ cm}^{-3}$ and $0.015 \pm 0.02 \text{ cm}^{-3}$, respectively with lowest N_F~~
414 ~~concentration of $0.007 \pm 0.006 \text{ cm}^{-3}$ in July (Tab. 2).~~ The monthly averaged N_F concentrations are
415 listed in Tab. 2.

416 The time series of relative contribution of FBAP to TAP number, N_F/N_T , ~~most of the time during~~
417 ~~campaign~~ exhibited the similar trend in temporal variability ~~to as N_F for most during the~~
418 campaign. The ~~pronounced~~ extreme values of N_F/N_T observed on few occasions corresponded to
419 low values of N_T implying a negative ~~resulted from strong variability in the concentrations of N_T~~
420 ~~rather than resulting from the variations in the concentrations of N_F , indicating the inverse~~
421 correlation between N_T and N_F/N_T during these measurements. Huffman et al., (2010) ~~have~~ also
422 reported ~~the a~~ similar inverse-negative correlation between N_T and N_F/N_T ~~from the measurements~~
423 ~~carried out~~ at a semi-urban site ~~from in~~ central Europe indicating that variability in N_F/N_T was
424 more associated with changes in N_T concentrations. ~~Temporal evolution of N_F , N_F/N_T , and 3-D~~
425 ~~number size distribution for individual campaign months is shown in Fig. S5. A~~ The campaign
426 overview (including individual months) of FBAP mass concentrations and 3-D size distribution
427 for each five minutes of UV-APS ~~sample averaged over the entire measurement period and~~
428 ~~individual months~~ are shown in Figure S56. ~~During the first month of measurement campaign~~
429 ~~M_F exhibited high concentration with sporadic spikes at irregular intervals with broader size~~
430 ~~distribution ($\sim 2 - 8 \mu\text{m}$) towards the end of the month (with highest concentration $\sim 6.0 \mu\text{g m}^{-3}$).~~
431 ~~As the measurement campaign progressed, with arrival of persistent and heavy rainfall (whole of~~
432 ~~July and first half of August) M_F exhibited a gradual decrease with minimum value reaching as~~
433 ~~low as $6 \times 10^{-4} \mu\text{g m}^{-3}$. After a period of consistent low mass concentration, during the last week~~

434 of measurement campaign, M_F exhibited an increase with highest mass concentration of $\sim 5.8 \mu\text{g}$
435 m^{-3} , which coincided with reduced and scattered rainfall.

437 **3.1.12 Particle number and mass concentrations**

438 **3.2.1 Statistical distribution of number concentrations**

439 ~~Statistical distribution of five minute~~The number and mass concentration measurements carried
440 out at Munnar over the course of the campaign are shown in Fig. 3 and tabulated in Tab. 2. [The](#)
441 [box plots show statistical representation of five minute averaged data of the time series.](#) Over the
442 entire measurement period the monthly mean of N_T varied by a factor ~ 3 from minimum in
443 August (0.96 cm^{-3}) to a maximum in June (2.7 cm^{-3} ; [Fig. 3a](#)). In addition to the highest
444 concentration, the variability of N_T was also found to be highest in the month of June as can be
445 seen from the size of the 5 – 95th percentile, [which also reflected in the high variability of \$N_T\$ for](#)
446 [entire measurement period.](#) ~~bars in Fig. 3a. The relative high variability in N_T for entire~~
447 ~~measurement period was largely contributed by the variability in N_T observed in the month of~~
448 ~~June.~~ During the initial phase of Southwest monsoon season the predominant
449 Westerly/Southwesterly winds are known to transport the mineral dust, which constitute large
450 fraction of coarse mode (also in larger diameter size of fine mode fraction) TAP concentration,
451 over the [Indian](#) continental region (Vinoj et al., 2010, 2014; Li and Ramanathan, 2002; Satheesh
452 and Srinivasan, 2002; Vinoj and Satheesh, 2003). As the monsoon progresses the persistent
453 rainfall can cause the washout of these dust particles along the path of monsoonal rain, thus
454 reducing the coarse mode TAP concentration (Pranisha and Kamra, 1997a,b; Radke et al., 1980;
455 Moorthy et al., 1991). The monthly arithmetic mean and median average of N_T did not exhibit
456 significant differences. The monthly mean values of N_F varied by the factor of ~ 4 with

Formatted: Justified

Formatted: Justified, Space After: 0 pt

457 ~~consistently high~~ moderate variability during ~~all the observational months~~ the entire campaign
 458 (Fig. 3b). Similar to N_T , the monthly mean average value and variability in N_F was highest in the
 459 month of June, with mean of $0.03 \pm 0.03 \text{ cm}^{-3}$ and ~~high size of a~~ 95th percentile ~~(with value of~~
 460 0.086 cm^{-3} ~~), respectively~~. The lowest average concentration in N_F ($0.007 \pm 0.006 \text{ cm}^{-3}$) was
 461 observed in the month of July ~~was associated~~ with relatively lower variability as compared to
 462 other months of field measurement campaign. Unlike N_T , the arithmetic mean and median
 463 average of N_F for individual months exhibited a significant difference as can be seen from the
 464 box plot shown in Fig. 3b. The variability of N_F/N_T showed the similar temporal pattern as that of
 465 N_F , except that the campaign average mean N_F concentration was higher than that of the August,
 466 whereas the campaign averaged mean N_F/N_T was observed to be lower than the mean calculated
 467 for August. ~~As can be seen from Fig. 3c, the mean relative contribution of N_F to N_T was lowest in~~
 468 ~~the month of July (~1%) and highest in the month of June and August (~3%).~~ The median and
 469 mean for N_F/N_T , over the course of campaign were ~1 and 2%, respectively (Fig. 3c). The
 470 average values of N_F/N_T over this part of the globe were ~~found to be lower as compared to~~ than
 471 previously investigated sites (Huffman et al., 2010, 2012; Bowers et al., 2009; Schumacher et al.,
 472 2013; Matthias-Maser and Jaenicke, 1995; Matthias-Maser et al., 2000; Gabey et al., 2010).
 473 Though, the UV-APS measures particle numbers, the average size-resolved particle mass can
 474 also be estimated by assuming the particle density equal to 1 g cm^{-3} (Huffman et al., 2010, 2012).
 475 Based on this, the mass concentrations of FBAP (M_F) and TAP (M_T) are presented in Fig. 3. The
 476 monthly mean values of M_T exhibited the similar trend and temporal variability as that of N_T
 477 with overall decrease in M_T through the course of measurement months as campaign progressed
 478 (Fig. 3d). The campaign mean M_T at Munnar was $\sim 7 \mu\text{g m}^{-3}$, which was comparable to the values
 479 reported from central European city ($M_T \sim 7.3 \mu\text{g m}^{-3}$) and higher than concentration of M_T (~ 2.5

Formatted: Not Highlight

Formatted: Not Highlight

480 $\mu\text{g m}^{-3}$) reported from pristine Amazonian rainforest region measured during wet season
 481 (Huffman et al., 2010; 2012). The monthly mean values of M_F , on the other hand, did not exhibit
 482 a similar pattern to M_T , but followed a temporal pattern similar to N_F (Fig. 3e). The highest mean
 483 mass concentration of M_F ($\sim 0.4 \mu\text{g m}^{-3}$) observed during June was ~ 3 and 2 times lower than the
 484 concentrations observed at a central European city ($\sim 1.26 \mu\text{g m}^{-3}$) and pristine Amazonian
 485 rainforest ($\sim 0.85 \mu\text{g m}^{-3}$), respectively. The higher difference between mean and median values
 486 of the box plots indicates the higher temporal variability. The median and mean for M_F/M_T over
 487 the course of entire measurement period were 6 and 3% respectively, which is relatively low
 488 compared to previously reported studies for various other environments (Huffman et al., 2010;
 489 2012; Artaxo and Hansson, 1995; Schumacher et al., 2013; Fig. 3f). On average the relative
 490 contribution of FBAP to TAP coarse mode particle mass was ~ 3 times higher ($\sim 6\%$) than its
 491 contribution to coarse mode particle number concentration ($\sim 2\%$). This is consistent with the
 492 observations that FBAPs show enhanced prevalence among the larger aerosol particles (Huffman
 493 et al., 2010).

Formatted: Not Highlight

Formatted: Not Highlight

495 **3.1.2 Diurnal patterns** ~~of the number concentration~~

Formatted: Font: Bold, Not Italic

496 The average diurnal trends for three individual months and the entire measurement campaign
 497 were analyzed. Figure 4 shows the ~~median-mean~~ FBAP values for each hour of the day for three
 498 individual months ~~and entire~~ in the campaign, and Fig. S6 ~~7~~ shows the corresponding TAP plots.
 499 Overall N_F exhibited a moderately ~~ly~~ diurnal pattern with consistent early morning (06:00 hr) peak
 500 at $\sim 3 \mu\text{m}$ (Fig. 4a) ~~where in the~~ except for the month of July, where this early morning peak was
 501 absent. A ~~relatively-very~~ weak peak during late evening (20:00 hr) in FBAP concentration at ~ 3
 502 μm was ~~consistently~~ observed in the month of July. In the month of June the average diurnal N_F

Formatted: Justified

503 concentration started increasing early in the evening (~18:00 hr), which gradually increased
 504 through the night ~~and~~ reaching maximum at ~06:00 hr and started decreasing thereafter as day
 505 progressed. ~~The average diurnal N_F pattern in August exhibited more or less qualitatively similar~~
 506 ~~features to that of diurnal pattern observed in June. A similar diurnal pattern was also observed~~
 507 ~~in August but without high FBAP concentrations in the evening hours.~~ In general the weak
 508 diurnal pattern observed in N_F during the month of July was consistent with weak diurnal
 509 patterns in RH and temperature, ~~diurnal patterns~~, and persistent rainfall observed during July.
 510 The early morning peak at ~3 μm on the diurnal scale was also reported from pristine
 511 Amazonian rainforest environment (Huffman et al., 2012). Corresponding average size
 512 distributions for entire measurement period will be discussed in details in Sec. 3.3. The diurnal
 513 variations of N_T (Fig. S6~~7~~), on the other hand were very distinct from those of N_F . The size
 514 resolved $dN_T/d\log D_a$ for each individual months exhibited a consistent and flat concentration
 515 profile at <1 μm , ~~except for the month of August where a pronounced afternoon peak (~12:00)~~
 516 ~~at ~1 μm was observed. Reduced rainfall and substantial changes in meteorological parameters~~
 517 ~~including the change in prevailing wind speed and shift in direction during later half of August~~
 518 ~~might have caused the appearance of afternoon peak due to particles resulting from local sources.~~
 519 ~~As like N_F , N_T showed the strong quantitative variability amongst each individual month (Fig.~~
 520 ~~S7).~~ Previous studies where similar instrument was used have reported that pronounced diurnal
 521 variations in N_T are strongly coupled with diurnal variations in meteorological variables
 522 especially mixing layer depth (Garland et al., 2009; Raatikainen et al., 2014; Du et al., 2013).
 523 The absence of pronounced diurnal variations in N_T at this particular site may be a result of weak
 524 dependence of coarse mode TAP concentrations on meteorological parameters combined with
 525 persistent rainfall causing the washout of these particles (Radke et al., 1980; Raatikainen et al.,

2014; Kanawade et al., 2014; Shika et al., 2016). This also indicates the absence of any strong and localized source of anthropogenic emissions during most of the campaign period. Diurnal patterns of N_F/N_T more or less followed the same pattern as that of N_F during all the measurement months. ~~owing to complete absence of diurnal variability in N_T . Averaged over the entire campaign the N_F/N_T was found to be highest during early morning hour at 06:00 hr (3.2%) consistent with the time of high N_F concentration (Fig. 4).~~ The distinct diurnal pattern in N_F and N_T supports the fact that the sources of TAP and FBAP were different over this region.

The diurnal trends in M_F and M_T for individual months and campaign average were also analyzed and are shown in Fig.S7 and S8. The monthly averaged diurnal trends in M_F for individual months and entire campaign exhibited similar trend corresponding to N_F . However, the prominent peak in $dM_F/d\log D_a$ was observed at higher diameter ($\sim 3 - 4 \mu m$). The concentration peak of $<1 \mu m$ observed in N_T shifted to the higher diameter range of $\sim 3 - 4 \mu m$ as increase in mass is more associated with presence of coarse mode particles. The distribution of M_T (Fig. S8), however, exhibited a distinctly different trend compared to both M_F and N_T . The distinct diurnal patterns of M_F and M_T showed very less relative contribution of FBAP to TAP mass as compared to other observational sites (Huffman et al., 2010, 2012; Matthias-Maser and Jaenicke, 1995).

Formatted: Not Highlight

Formatted: Not Highlight

3.2.2 Statistical distribution of mass concentration

~~Basically UV-APS measures the particle number; the average mass of size resolved particles can be derived as first approximation by assuming the particle density equal to 1 g cm^{-3} (unit density). Accordingly the overview of mass concentration of FBAP over the course of measurement period is presented here. The statistical distribution of five minutes mass concentration derived from number concentration measurements over the course of campaign is shown in Fig. 5 and tabulated in Tab. 2. The monthly mean values of M_T exhibited the similar~~

trend and temporal variability as that of N_T with overall decrease in M_T through the course of
 measurement months as campaign progressed. The highest monthly average concentration of M_T
 ($\sim 10.6 \mu\text{g m}^{-3}$) was observed in the month of June whereas the lowest M_T of $\sim 4.2 \mu\text{g m}^{-3}$ was
 observed in the month of August. Averaged over the entire measurement period the mean M_T at
 Munnar was $\sim 7 \mu\text{g m}^{-3}$, which was comparable to the values reported from central European city
 ($M_T \sim 7.3 \mu\text{g m}^{-3}$) and higher than concentration of M_T ($\sim 2.5 \mu\text{g m}^{-3}$) reported from pristine
 Amazonian rainforest region measured during wet season (Huffman et al., 2010; 2012). The
 monthly mean values of M_F , on the other hand, did not exhibit similar pattern like M_T , but
 followed temporal pattern like N_F . The highest mean mass concentration of M_F ($\sim 0.4 \mu\text{g m}^{-3}$)
 observed during June and was ~ 3 and 2 times lower than the concentrations observed at a central
 European city ($\sim 1.26 \mu\text{g m}^{-3}$) and pristine Amazonian rainforest ($\sim 0.85 \mu\text{g m}^{-3}$), respectively.
 The higher difference between mean and median values of the box plots indicates the higher
 temporal variability. The relative difference between mean and median of N_F was found to be
 higher than that of M_F indicating higher temporal variability of N_F during all measurement
 months. Averaged over the course of entire measurement period this trend was found to be
 consistent. The median and mean for M_F/M_T over the course of entire measurement period were
 6 and 3% respectively, which is relatively low compared to previously reported studies for
 various other environments (Huffman et al., 2010; 2012; Artaxo and Hansson, 1995;
 Schumacher et al., 2013). On average the relative contribution of FBAP to TAP coarse mode
 particle mass was ~ 3 times higher ($\sim 6\%$) than its contribution to coarse mode particle number
 concentration ($\sim 2\%$). This is consistent with the observations that FBAPs show enhanced
 prevalence among the larger aerosol particles (Huffman et al., 2010).

Diurnal patterns of mass concentration

The diurnal trends in M_F for individual months and campaign average were also analyzed and are shown in Fig. 6. The corresponding diurnal trends in M_T are shown in Fig. S8. The monthly averaged diurnal trends in M_F for individual months and entire campaign exhibited similar trend corresponding to N_F . However, the prominent peak in $dM_F/d\log D_a$ was observed at higher diameter ($\sim 3-4 \mu\text{m}$), which is due to the fact that $dM_F/d\log D_a$ has been derived from $dN_F/d\log D_a$ assuming unit density. As observed for N_F during the month of June, the consistent morning peak was present in M_F with only difference of prominent second peak in M_F , which starts late in the evening at $\sim 19:00$ hr and further extends up to morning hours ($\sim 08:00$ hr). Thereafter M_F concentration steadily decreased as the day progressed reaching minimum at around mid-day. The early morning peak in M_F concentration was consistently observed in the size range of $3-4 \mu\text{m}$ for all the measurement months. The characteristic distribution of M_T (Fig. S8), however, exhibited distinct behavior as compared to both M_F and N_T . The concentration peak of $<1 \mu\text{m}$ observed in N_T shifted to the higher diameter range of $\sim 2-3 \mu\text{m}$ as increase in mass is more associated with presence of coarse mode particles. For example in June M_T exhibited similar diurnal feature as that of N_T . The flatter trend observed in average M_T during the month of June disappeared during the month of July and August with appearance of less prominent peak in M_T at around 12:00 hr resulting in relatively pronounced diurnal pattern (Fig. S8). The distinct diurnal patterns of M_F and M_T showed very less relative contribution of FBAP to TAP mass as compared to other observational sites (Huffman et al., 2010, 2012; Matthias Maser and Jaenicke, 1995).

3.1.3 Size distribution of particle number and mass

Figure 57 shows the number and mass size distributions for TAPs and FBAPs averaged over the entire measurement period. The TAP number size distribution, $dN_T/d\log D_a$, was generally broad

Formatted: Justified

595 and dominated by a peak at the lower end of the measured size range of number size distribution
 596 ($D_a \approx 0.9 \mu\text{m}$; Fig. 57a). In $dN_T/d\log D_a$ the concentrations exhibited a significant decrease above
 597 diameter $\sim 3 \mu\text{m}$ with a long tail extending on the right hand side of the distribution. This peak
 598 may be comprised of mineral dust and sea salt particles, as also evident from SEM images
 599 (please refer to section 3.3) and as also reported by the previous studies investigating aerosol
 600 composition over India during monsoon season (Vinoj et al., 2014; Moorthy et al., 1991; Vinoj
 601 and Satheesh, 2003; Satheesh and Srinivasan, 2002; Li and Ramanathan, 2002). A similar peak
 602 in $dN_T/d\log D_a$ at $D_a \approx 0.9 \mu\text{m}$ was observed in pristine Amazonian rainforest during wet season
 603 and was attributed to mineral dust (Huffman et al., 2012; Fig. 5b). The corresponding monthly
 604 plots of $dN_T/d\log D_a$ are shown in Fig. S9 and ~~Overall the individual monthly $dN_T/d\log D_a$~~
 605 exhibited the similar qualitative number size distribution pattern as that of campaign averaged
 606 TAP number size distribution. Averaged over the entire measurement period, the mass size
 607 distribution, $dM_T/d\log D_a$ (Fig. 7e5c), exhibited a broad peak at $\sim 2.6 \mu\text{m}$ with an extended tail to
 608 the left side of the mass size distribution, ~~whereas on the right side a second peak started~~
 609 ~~appearing at $D_a \sim 12 \mu\text{m}$.~~ The corresponding monthly averaged $dM_T/d\log D_a$ are shown in Fig. S10
 610 and appeared similar to the campaign average TAP mass size distribution. ~~As evident from the~~
 611 ~~figure the campaign average TAP mass size distribution appeared generally similar to each of the~~
 612 ~~individual months.~~ For accurate representation of mass size distribution the unit-normalized mass
 613 distribution ~~of D_a~~ plotted in Fig. 57 (c and d) is expected to shift to larger particle size with
 614 increased area under the curve, ~~as D_a is directly proportional to square root of density of the~~
 615 ~~particle under consideration~~ (Huffman et al., 2010; DeCarlo et al., 2004).
 616 The campaign average number size distribution of FBAP (Fig. 57b) exhibited monomodal shape
 617 with much narrower peak than the TAP number size distribution, with a dominant mode at

Formatted: Not Highlight

618 $D_a \approx 2.8 \mu\text{m}$, which was consistent throughout measurement period. The corresponding monthly
 619 mean FBAP number size distributions are shown in Fig. S11. ~~This peak was much prominent~~
 620 ~~and narrow in the month of June with highest FBAP concentration and became less pronounced~~
 621 ~~in July, with the lowest FBAP concentration.~~ As reported by Huffman et al., (2010) multiple and
 622 broader peaks in $dN_F/d\log D_a$ are most likely to originate from different sources and biological
 623 species. In the present study, however, we did not find multiple peaks in investigated FBAP
 624 number size distribution, suggesting that observed FBAPs comprised the particles from similar
 625 or same sources. The overall qualitative appearance of the average FBAP number size
 626 distribution is similar to that has been reported by previous measurements. For a semi-urban site
 627 in Central Europe Huffman et al., (2010) reported an average FBAP peak at $3.2 \mu\text{m}$. Gabey et al.,
 628 (2010) observed a similar peak at $\sim 2.5 \mu\text{m}$ at a tropical rain forest site in Borneo. From a pristine
 629 Amazonian rainforest site during wet season Huffman et al., (2012) reported a similar peak at
 630 $\sim 2.3 \mu\text{m}$. For another pristine observational site in boreal forest in Finland Schumacher et al.,
 631 (2013) reported a peak in FBAP number size distribution at $\sim 3 \mu\text{m}$. A similar peak at $\sim 3 \mu\text{m}$ was
 632 also observed by Healy et al., (2014) at a rural site in Killarney national park, Ireland. This
 633 dominant peak in the range of $2 - 3 \mu\text{m}$ in FBAP number size distribution is strongly attributed
 634 to the fungal spores over the continent as reported by numerous previous researchers (Huffman
 635 et al., 2010, 2012; Schumacher et al., 2013, Li et al., 2011; Artaxo and Hansson, 1995; Healy et
 636 al., 2014; Gabey et al., 2010, 2013; Toprak and Schnaiter, 2013). Recently Valsan et al., (2015)
 637 investigated the morphological characteristics of PBAPs from the same site during non-monsoon
 638 season and found that fungal spores constituted the major fraction of PBAPs and nominally
 639 ranged in the size range of $\sim 3 - 10 \mu\text{m}$, which roughly translates into equivalent aerodynamic
 640 diameter of $2 - 5 \mu\text{m}$ (assuming particles to be a prolate spheroid). The scanning electron

641 microscopy images obtained from the filter samples ~~occasionally~~ collected during this field
 642 campaign showed the strong presence of variety of fungal spore in the size range of ~~3-6~~ 3-6 μm
 643 (aerodynamic diameter ~~2-3~~ 2-3 μm ; discussed below; Fig. 117). As an overview of the
 644 comparison, the FBAP concentration values observed at Munnar are compared to the FBAP
 645 concentration ranges obtained using similar online measurements techniques from diverse
 646 environmental conditions across the globe, and the details are tabulated in Tab. 3. The campaign
 647 averaged FBAP mass size distribution is shown in Fig. 57d, which nominally appeared bimodal
 648 with very sharp primary peak at $D_a \approx 3.2 \mu\text{m}$ and very broad but ~~unappreciable~~ small second mode
 649 at $D_a \approx 4 \mu\text{m}$. ~~The distinct presence of particle mass in the higher diameter range ($>10 \mu\text{m}$) in~~
 650 ~~FBAP mass size distribution was not prominently noticed in Munnar as compared to previously~~
 651 ~~reported studies (Huffman et al., 2010; 2012). In case of TAP mass size distribution the right~~
 652 ~~side tail started showing positive slope at larger diameter whereas FBAP mass size distribution~~
 653 ~~consistently showed the negative slope at larger diameters. Such a distinct shape of mass size~~
 654 ~~distributions for TAP and FBAP reconfirms the fact that the larger particles observed in the TAP~~
 655 ~~mass distribution originated from processes that did not produce particles of the biological origin~~
 656 ~~as likewise reported by Huffman et al., (2010).~~ The corresponding monthly mean FBAP mass
 657 size distributions are shown in Fig. S12. The FBAP mass size distribution for individual months
 658 ~~FBAP mass size distribution~~ exhibited the similar qualitative shape to that of average campaign.
 659 ~~As mentioned above highest FBAP mass concentration was observed in June, which coincided~~
 660 ~~with a very sharp and narrow primary peak in FBAP mass size distribution, while the lowest~~
 661 ~~FBAP mass concentration during July, on the other hand, coincided with a broad primary peak~~
 662 ~~with lower slope.~~

663 ~~Figure 6 shows the size-resolved ratio of overall FBAP to TAP averaged over~~ for the course of
 664 measurement ~~is shown in Fig. 8~~ and corresponding monthly ratios are shown in Fig. S13. The
 665 relative contribution of FBAPs (dN_F) to TAPs (dN_T) in each size bin could be used to derive the
 666 relative contribution of biological particles to total aerosol particles at each size. As reported by
 667 Huffman et al., (2010) the assumption of unit density of each particle implies that the value of
 668 the dN_F/dN_T ratio would invariably is equal to dM_F/dM_T . The integrated N_F/N_T and M_F/M_T ,
 669 however, would have the distinct values. As can be seen from Fig. ~~68~~ and S13 ~~a~~ considerable
 670 quantitative and qualitative difference in mean (red) and median (green) curve was consistently
 671 observed in all individual months, which likely is the result of poor counting statistics and very
 672 high variability in ~~FBAP and~~ TAP number concentrations. Based on the results presented by
 673 Huffman et al., (2010) the mean (red) curve, best represents the N_F/N_T ratios at the upper particle
 674 sizes. ~~hence we will stick our further discussion about N_F/N_T ratios for the present study to the~~
 675 ~~mean curve.~~ The mean N_F/N_T ratio curves for individual months and for entire campaign
 676 exhibited two dominant peaks persistently in the particle size range $\sim 3 - 4 \mu m$ and $\sim 6 - 8 \mu m$.
 677 The first prominent peak in dN_F/dN_T distribution at $3 - 4 \mu m$ comprised $15 - 16\%$ while the
 678 second peak at $6 - 8 \mu m$ represented $\sim 14 - 15\%$ of the FBAP material in TAP over the entire
 679 measurement period (Fig. ~~68~~). ~~As can be observed from Fig. S13, the second peak in N_F/N_T~~
 680 ~~ratios for July was higher ($\sim 12\%$) than the first peak ($\sim 10\%$) unlike other two observational~~
 681 ~~months. The fact that N_F/N_T ratio is approximately zero for the particle sizes $< 1.7 \mu m$ indicated~~
 682 ~~that FBAP mainly comprised of very small fraction of submicron aerosols at Munnar. The~~
 683 ~~statistics for the individual months showed that the first peak in dN_F/dN_T was more or less~~
 684 ~~consistent at $\sim 22\%$ during June and August except for the July when second peak in N_F/N_T ratios~~
 685 ~~contributed more ($\sim 12\%$) than the first peak ($\sim 10\%$).~~

686

687 **3.2.4 Focus periods**

688 ~~As described in Sec. 3.1 based on campaign overview,~~ The characteristics properties of FBAP

689 and specifically TAP number concentration exhibited strong temporal variabilities, which could

690 be attributed to changes in prevailing meteorological conditions ~~especially wind direction~~ during

691 monsoon season at Munnar. ~~To explore the potential impact of air mass origin on number and~~

692 ~~size distribution of FBAP and TAP, we highlight~~ The following three distinct focus periods

693 ~~during the campaign are highlighted as follows:~~

694 1. A ~~focus period of “dusty episode”~~ focus period was identified when prevailing wind was

695 predominantly Westerly/Southwesterly and air masses mainly came from the Arabian Sea. These

696 air masses, although ~~almost~~ relatively anthropogenically clean, ~~are~~ were laden with sea salt and

697 dust particles during the start of the monsoon, which dominate the coarse mode fraction of

698 atmospheric aerosols (Vinoj et al., 2014; Li and Ramanathan, 2002). ~~These dust particles~~

699 ~~observed over this region mainly~~ originating from West Asia, North Africa, and Arabian region

700 (Vinoj et al., 2014). ~~During our measurement~~ In this campaign, such a dusty period ~~from 14-06-~~

701 ~~2014 00:00 hr to 25-06-2014 23:55 hr~~ was observed between June 14-25, 2014, and is which was

702 consistent with the description given above and also based on the SEM images of the dust

703 collected in this period, ~~which showed the presence of mineral dust, obtained during dusty period~~

704 (see Sec. 3.5 below). This period was marked with an accumulated rainfall of ~1015 mm,

705 average relative humidity of 94.4±6.5%, average temperature of 17.7±1.5°C, and average wind

706 speed 2.8±1.3 m s⁻¹ (maximum wind speed of 6.7 m s⁻¹).

707 2. A ~~focus period of “clean period”~~ focus period was observed during latter half of the monsoon

708 season when wind direction was still predominantly Westerly/Southwesterly and air masses

Formatted: Justified

Formatted: Font: Italic

Formatted: Font: Italic

709 originated over Arabian Sea. During this period, which was observed from July 9 – August 7,
710 2014, chosen from 09-07-2014 10:25 hr to 07-08-2014 23:55 hr, FBAP and TAP concentrations
711 were extremely low with very ~~weak~~ low variability. This clean period was associated with
712 persistent rainfall (accumulated rainfall of 2650 mm), average relative humidity of $99.5 \pm 1.4\%$,
713 average temperature of $16.4 \pm 0.5^\circ\text{C}$, and average wind speed $3.7 \pm 1 \text{ m s}^{-1}$ (maximum wind speed
714 of 8.3 m s^{-1}).

Formatted: Font: Italic

715 3. A ~~focus period of “high bio”~~ focus period comprised three discrete events of high FBAP
716 concentration observed between June 1-5, 2014, June 26-30, 2014 and August 18-22, 2014.~~from~~
717 ~~01-06-2014 09:10 hr to 05-06-2014 18:20 hr; 26-06-2014 00:05 hr to 30-06-2014 17:00 hr; and~~
718 ~~18-08-2014 00:00 hr to 22-08-2014 08:30 hr. Interestingly,~~ This period is marked with the very
719 distinct metrological parameters compared to the clean period: accumulated rainfall 194 mm,
720 average relative humidity $93.4 \pm 8.4\%$, average temperature $18.0 \pm 2.4^\circ\text{C}$, and average wind speed
721 $1.2 \pm 0.8 \text{ m s}^{-1}$ (with maximum wind speed of 4.6 m s^{-1}). ~~Briefly, during “high bio” period~~
722 ~~stagnant air masses came from densely vegetated region located north of observational site, and~~
723 ~~relative humidity and temperature exhibited high variability. It is suggested that these high-bio~~
724 periods are due to high variability in relative humidity and temperature, and the movement of air
725 masses with relatively low wind speed, over densely vegetated region located north of
726 observational site.

Formatted: Font: Italic

Formatted: Font: Italic

727 3.2.4.1 Particle number and mass concentrations

728 The statistical distributions of N_T , N_F , M_T , and M_F , and corresponding ratios for three different
729 focus periods (dusty, clean, and high bio) are shown in Fig. 7.9 and tabulated in Tab. 4. Each of
730 the focus periods discussed here did not represent equal duration of the observations. The
731 average total particle number concentration, N_T , showed a decrease of $\sim 70\%$ from dusty period to

Formatted: Justified

Formatted: Font: Italic

Formatted: Font: Italic

Formatted: Font: Italic

Formatted: Font: Italic

732 *clean* period ($\sim 4.2 \text{ cm}^{-3}$ and $\sim 1.3 \text{ cm}^{-3}$ respectively), whereas the N_T concentration during *high*
 733 *bio* period was $\sim 1.8 \text{ cm}^{-3}$. The high N_T concentration during the *dusty* period caused the high
 734 variability between 5th and 95th percentile in N_T when averaged over entire campaign period (Fig.
 735 3a). The fraction of dust in coarse mode aerosol, which is observed to be very high during pre-
 736 monsoon and first few days from the onset of monsoon rainfall, gradually decreased as the
 737 monsoon progressed likely as a result of wash out and wet deposition due to persistent rainfall in
 738 the path of air masses (Hirst 1953; Madden, 1997; Burge and Roger, 2000). The M_T exhibited
 739 similar pattern to that of N_T during three distinct focus periods with average mass concentration
 740 of $\sim 16.3 \mu\text{g m}^{-3}$, $\sim 5.1 \mu\text{g m}^{-3}$, and $\sim 7.7 \mu\text{g m}^{-3}$ for *dusty*, *clean*, and *high bio* periods, respectively
 741 (Fig. 7d).
 742 ~~As expected, the~~ the mean N_F concentration was highest during the *high bio* period (Fig. 79b)
 743 ~~with an average concentration of was~~ $0.05 \pm 0.04 \text{ cm}^{-3}$ ~~and~~ with high variability in higher
 744 concentration range ($0.06 - 0.13 \text{ cm}^{-3}$) as evident from the distance between 75th and 95th
 745 percentile. The N_F was found to be relatively stable during the *dusty* period with an average
 746 concentration of $\sim 0.02 \pm 0.008 \text{ cm}^{-3}$. The ~~average-mean~~ N_F concentration was found to be an order
 747 of magnitude lower during *clean* period ($0.005 \pm 0.004 \text{ cm}^{-3}$) as compared to *high bio* period,
 748 whereas corresponding decrease in N_T from *dusty* to *clean* period (\sim by factor of 3) was not of
 749 similar magnitude. ~~We put forward~~ The following are the hypothesis proposed for such a
 750 concentration difference in N_F and N_T during the three distinct periods: During the *clean* period
 751 the predominant wind direction was Westerly/Southwesterly and air masses came from Arabian
 752 Sea bringing clean marine influx marked by persistent rainfall. As a result, the coarse mode
 753 aerosol fraction (N_F and N_T) emitted locally were efficiently removed, however, the sea salt
 754 particles present in the air masses, which came from Arabian Sea contributed to TAP number

Formatted: Font: Italic

Formatted: Font: Italic

Formatted: Font: Italic

Formatted: Font: Italic

Formatted: Font: Italic

Formatted: Font: Italic

Formatted: Font: Italic

Formatted: Font: Italic

Formatted: Font: Italic

Formatted: Font: Italic

Formatted: Font: Italic

Formatted: Font: Italic

Formatted: Font: Italic

concentration (see section 3.35). In addition to the efficient wet removal of FBAP due to persistent rainfall, the high RH level (average 99.5%), which causes the dew formation that further inhibit the spore release in turn reducing the FBAP concentration (Schumacher et al., 2013; Jones and Harrison, 2004). The mean values of M_F exhibited trends similar temporal trends and qualitative pattern as to those shown by N_F , with highest mass concentration of $0.58 \mu\text{g m}^{-3}$ during high bio period, which reduced by ~86% ($0.08 \mu\text{g m}^{-3}$) during the clean period. As anticipated the relative contribution of FBAP in TAP during dusty and clean periods was almost negligible with N_F/N_T ratio of ~1%. Whereas during the high bio period the relative FBAP number and mass contribution to corresponding TAP was ~5% and 12% respectively.

Formatted: Font: Italic

Formatted: Font: Italic

Formatted: Font: Italic

Formatted: Font: Italic

Formatted: Font: Italic

3.2.4.2 Size distribution of particle number and mass concentration

Figure 8a10 highlights the $dN_F/d\log D_a$ during three distinct focus periods and corresponding $dN_T/d\log D_a$ are shown in Fig. S14. In general Overall $dN_F/d\log D_a$ during each focus period exhibited pattern similar to that of campaign average.

The $dN_F/d\log D_a$ averaged over the dusty high bio period exhibited a very prominent and sharp was dominated by a narrow peak at $\sim 2.5 - 3.1 \mu\text{m}$. The corresponding $dN_F/d\log D_a$ during dusty and clean period also exhibited similar bell shaped distribution with less prominent peaks owing to the relatively lower FBAP concentrations as compared to the high bio period. was overall broader compared to dusty and high bio periods with gradual increase in FBAP number concentration from diameter range of $\sim 1 - 2.3 \mu\text{m}$, with a sharp increase thereafter, whereas downward slope exhibited the consistent pattern. $dN_F/d\log D_a$ during high bio period exhibited relatively narrow peak at $\sim 2.5 \mu\text{m}$. Unlike previously reported studies (Huffman et al., 2010; 2012) the peak in $dN_F/d\log D_a$ ($D_a \approx 3 \mu\text{m}$) was not reflected in $dN_T/d\log D_a$ mostly due to relatively less contribution of FBAP in coarse mode TAP number concentration. As can be seen

Formatted: Font: Italic

Formatted: Font: Italic

Formatted: Font: Italic

778 from Fig. S14a the total aerosol particle number size distribution, $dN_T/d\log D_a$, during all the
 779 three focus periods exhibited almost similar pattern to that of campaign averaged $dN_T/d\log D_a$
 780 with higher concentrations peaking at lower diameter. ~~dusty period exhibited a peak at $\sim 0.9 \mu\text{m}$,~~
 781 ~~with a high negative slope on the left side of the distribution curve. This peak may be comprised~~
 782 ~~of mineral dust and sea salt particles, as also evident from SEM images (please refer to section~~
 783 ~~3.5) and based on the previous studies investigated aerosol composition over India during~~
 784 ~~monsoon season (Vinoj et al., 2014; Moorthy et al., 1991; Vinoj and Satheesh, 2003; Satheesh~~
 785 ~~and Srinivasan, 2002; Li and Ramanathan, 2002). A similar peak in $dN_T/d\log D_a$ at $D_a \sim 0.9 \mu\text{m}$~~
 786 ~~was observed in pristine Amazonian rainforest and particles were mostly dominated by mineral~~
 787 ~~dust during high dust period (Huffman et al., 2012, Fig. 5b). During clean period $dN_T/d\log D_a$~~
 788 ~~resembled the similar shape (peaking at $\sim 0.9 \mu\text{m}$) to that of dusty period, however, with lower~~
 789 ~~concentration. The corresponding $dN_T/d\log D_a$ distribution (Fig. S14c), during high bio period,~~
 790 ~~exhibited multiple peaks and appeared noisy for $D_a < 1 \mu\text{m}$ with increasing trend in TAP number~~
 791 ~~concentration for the lower diameter range of the distribution. The downward slope for $D_a > 1 \mu\text{m}$~~
 792 ~~exhibited consistent shape (mean curve) compared to distributions observed during other two~~
 793 ~~focus periods.~~

794 The FBAP mass size distribution (Fig. ~~8b~~¹⁴) during *dusty* period was dominated by bimodal
 795 peaks with prominent peak at $\sim 3 \mu\text{m}$ and relatively less pronounced peak in the range of $\sim 4 - 6$
 796 μm showing broader tail on the right side of the distribution curve. The $dM_F/d\log D_a$, during
 797 *clean* period, exhibited similar bimodal peaks with extended shoulder in the diameter range from
 798 ~ 4 to $7 \mu\text{m}$. The $dM_F/d\log D_a$ distribution during *high bio* period was distinctly different
 799 compared to two other focus periods discussed above with a prominent monomodal peak at ~ 3
 800 μm . The primary peak observed in $dM_F/d\log D_a$ in the range of ~ 3 to $4 \mu\text{m}$ was consistent during

Formatted: Font: Italic

Formatted: Font: Italic

Formatted: Font: Italic

801 individual months and different focus periods. TAP mass size distribution (Fig. S15) exhibited
 802 similar qualitative pattern to that of campaign averaged $dM_T/d\log D_a$ with peak between ~ 2.5 to
 803 $3.5 \mu\text{m}$ with an extended tail on the right side, which gradually increased for $D_a > 13 \mu\text{m}$. The
 804 statistics representing 5th, 25th, 75th, and 95th percentile for $dN_F/d\log D_a$ and $dM_F/d\log D_a$
 805 during individual focus periods is shown in Fig. S16 and S17, respectively.
 806 The size resolved ratio of FBAP to TAP particles averaged for three distinct focus periods is
 807 shown in Fig. 9.12. As evident from the figure the largest fraction of FBAP particles during *dusty*
 808 period occurred between $\sim 6 - 9 \mu\text{m}$ ($\sim 20\%$) with relatively small ($\sim 7\%$) contribution in the *size*
 809 *diameter* range of $\sim 3 - 4 \mu\text{m}$. ~~($\sim 7\%$). The dN_F/dN_T exhibited the sloping tails on both the sides~~
 810 ~~of the distribution with steep slope on the right side.~~ The fact that N_F/N_T is ~~approximately~~ near to
 811 zero for the particle size ~~range~~ below $\sim 1.5 \mu\text{m}$ is consistent with previous observations reported
 812 from semi urban site in central Europe and during wet season of pristine Amazonian rainforest
 813 (Huffman et al., 2010; 2012). During the *clean* period the maximum contribution of FBAP to
 814 TAP number concentration reduced to $\sim 10.5\%$ in the diameter range of ~ 6 to $9 \mu\text{m}$, but the peak
 815 at $\sim 3 - 4 \mu\text{m}$ remained almost consistent with relative contribution of $\sim 8\%$. ~~with another~~
 816 ~~prominent, but relatively smaller contributing peak, at $\sim 3 - 4 \mu\text{m}$ with relative contribution of~~
 817 ~~$\sim 8\%$.~~ Whereas ~~D~~ during *high bio* period the maximum contribution of FBAP to TAP occurred
 818 between broader size range of $\sim 3 - 8 \mu\text{m}$ with contribution range of $\sim 28 - 19\%$. ~~and relatively~~
 819 ~~broad dN_F/dN_T distribution.~~ Interestingly during *high bio* period the highest contribution of
 820 FBAP to TAP number concentration occurred at $D_a \approx 3.5 \mu\text{m}$, as opposed to other two focus
 821 periods when the highest contribution was observed in the larger diameter ranges of $\sim 6 - 8 \mu\text{m}$.
 822 N_F/N_T was consistently found to be very low, with values approaching zero ~~equal to zero~~ for the
 823 diameter beyond $13 \mu\text{m}$, indicating ~~that~~ FBAP comprised extremely small fraction of total

Formatted: Font: Italic

Formatted: Font: Italic

Formatted: Font: Italic

Formatted: Font: Italic

aerosol particles (Huffman et al., 2010; 2012). The two prominent peaks observed during the focus periods were clearly evident in campaign-averaged dN_F/dN_T (Fig. 68; peaks at ~ 3.5 and $6 \mu\text{m}$).

3.2.4.3 Diurnal patterns

A prominent early morning peak in N_F during *high bio* period in the diameter range of $1.5 - 3 \mu\text{m}$ was observed from 06:00 hr to 08:00 hr, which clearly reflected in campaign averaged

diurnal patterns at the same hour of the day. The diurnal variations in N_F during *dusty* and *clean* periods were not so pronounced (Fig. 1013) as compared to the variations during *high bio* period.

During *dusty* period N_F showed slightly high concentration starting from $\sim 2017:00$ hrs (lowest panel Fig. 10a) and persistently remained high until early morning without any variations, whereas during *clean* period N_F concentration consistently remained flat throughout 24 hrs. The

~~evening peak observed during dusty period, however, was clearly absent during high bio period. A moderately pronounced peak in N_F during evening hours at $\sim 20:00$ hr during dusty periods might indicate that releasing mechanism of bioaerosols was efficient as a result of nocturnal sporulation. This can further imply that the morning and late evening peaks in $dN_F/d\log D_a$ at $D_a \sim 3 \mu\text{m}$ most likely resulted from different type of spores (Hirst, 1953).~~ As listed by Huffman

et al., (2012) the emission and dispersal of bioaerosols is strongly coupled with environmental variables such as solar radiation, temperature, and relative humidity. ~~and e~~ Each of these variables ~~have strong diurnal cycles~~ has exhibited relatively pronounced diurnal variations during *high bio* period (upper panel Fig. 10c). It has been well documented that relative humidity, in particular, plays an important role in active wet discharge of fungal spores (Adhikari et al., 2006; Burch and Levetin, 2002; Elbert et al., 2007; Jones and Harrison, 2004; Quintero et al., 2010; Zhang et al., 2010), which constitutes major fraction of atmospheric bioaerosols (Ansari et al.,

Formatted: Font: Italic

Formatted: Justified

Formatted: Font: Italic

Formatted: Font: Italic

Formatted: Font: Italic

Formatted: Font: Italic

Formatted: Font: Italic

2015; Bauer et al., 2008; Bowers et al., 2013; Fröhlich-Nowoisky et al., 2009; Sesartic and
Dallafior, 2011; Spracklen and Heald, 2014). The meteorological parameters exhibited
~~pronounced~~significant diurnal variations during high bio period, where RH decreased to a level
(~60 – 80%), which is considered to be favorable for release of the fungal spores (Jones and
Harrison, 2004; Santarpia et al., 2013). During dusty and clean periods the persistence of high
RH values in the range of ~90 – 100%, ~~however~~, might have inhibited the active wet discharge
of fungal spore (Schumacher et al., 2013;-) -thus resulting in the weak diurnal variation in N_F .
Unlike N_F , N_T remained nearly flat without any pronounced diurnal variations during three
distinct focus periods (Fig. S18~~6~~). The corresponding diurnal cycle of FBAP mass concentration
and 3D size distributions for three focus periods are shown in Fig. S19~~7~~. M_F exhibited similar
diurnal patterns to that of N_F during three distinct focus periods. M_T ~~as like~~and N_T remained flat
during dusty period, ~~however but~~ exhibited slightly pronounced diurnal pattern during clean and
high bio period between 09:00 hrs and 16:00 hrs (Fig. S18~~8~~S20).

Formatted: Font: Italic

Formatted: Font: Italic

Formatted: Font: Italic

Formatted: Font: Italic

Formatted: Font: Italic

Formatted: Font: Italic

Formatted: Justified, Space After: 0 pt

3.35 SEM images

Figure 11~~4~~ shows the exemplary SEM images of biological particle types often observed during
the SW monsoon season at Munnar. The details about the sampling techniques, instrument used,
etc. for obtaining these bioaerosol images are discussed in details by Valsan et al., (2015). Note
that these images are ~~not~~ being presented here ~~for any quantitative purpose and to draw any~~
~~specific scientific conclusions but mainly~~ to showcase the particle types consistently observed
throughout the measurement period and not for quantitative purposes. The presence of mineral
dust and sea salt particles confirms marine influence of the air mass sampled. Many particles
observed by SEM were mostly likely Basidiospores. ~~As seen from the SEM images majority of~~

870 ~~the particles are mostly likely fungal spores. Based on their distinct morphology the spores in~~
871 ~~Fig. 14a-c most likely appeared to be of Basidiospores.~~ The appearance of small protuberances
872 on their surfaces suggests that the spores ~~(~~in e.g.~~ -Fig. 114a and c)~~ most likely belonged to the
873 *Hydnaceae* family (Grand and Vandyke, 1976; Valsan et al., 2015). The Basidiospores shown in
874 Fig. 114b and c were seen in abundance in all the samples collected during the campaign. Some
875 of the spores observed appeared to be coated with salt particles (Fig 114e) and might have been
876 carried from a distant source by the SW monsoon winds. The spores shown in Fig 114 (d and f)
877 most likely appeared to be spores of Ascomycota division. The particle shown in Fig. 114g was
878 most likely a mineral dust particle sampled during high dusty episode. Similar particles of
879 varying size during ~~dusty episode were consistently observed during SEM analysis. Fig 114h and~~
880 i shows the images of the typical sea salt particles observed during samples collected at Munnar
881 during measurement campaign when wind predominantly came from Westerly/Southwesterly
882 direction travelling over Indian Ocean and Arabian Sea.

Formatted: Font: Italic

883 884 **3.46 Meteorological Correlations**

885 The results obtained with UV-APS data analysis during the campaign at Munnar were plotted
886 with respect to meteorological parameters to investigate factors responsible for bioaerosol
887 release and their variations in the atmosphere.

Formatted: Space After: 0 pt

Formatted: Justified, Space After: 0 pt

888 **3.4.1 Impact of wind direction**

889 The wind rose diagrams scaled by N_F , D_g , and $D_{g,T}$ were also prepared for entire measurement
890 period and three distinct focus periods. These plots are ~~in a way~~ similar to the traditional wind
891 rose diagram (Fig. S2149) except ~~that~~, instead of wind speed, they are scaled by characteristic
892 FBAP and TAP parameters, which indicate the frequency of occurrence of respective parameter

Formatted: Font: Bold, Not Italic

Formatted: Space After: 0 pt

Formatted: Justified, Space After: 0 pt

with respect to wind direction (Sherman et al., 2015). As ~~can be~~ seen from Fig. S2149, predominant wind direction during entire campaign was Westerly/Southwesterly with frequency of occurrence of about ~90%. The wind speed broadly ranged between 2 – 5 m s⁻¹ with no prominent diurnal variations. The overall wind direction and back trajectory analysis (Fig. 1) shows that the sampled air masses may have had their origin over the Indian Ocean thereafter turning eastward after crossing the equator and travelling several hundred kilometers over Arabian Sea before reaching the observational site (Fig. 1). The predominant wind pattern during *dusty* (>95% frequency of occurrence; 2 – 6 m s⁻¹) and *clean* periods (~100 frequency of occurrence; 2 – 6 m s⁻¹) was Westerly/Southwesterly. Whereas during *high bio* period only ~50% of the time winds came from Westerly/Southwesterly direction and rest comprised ~~the stagnant and calm~~ of relatively slower (0 – 2 m s⁻¹) winds from all other directions with highest contribution of northerly winds (Fig. S2149). -

Wind rose diagram scaled by FBAP number concentration is shown in Fig. 125. During the entire campaign the predominant wind showed that ~85% of the time FBAP concentration occurred in the range of 0 – 0.05 cm⁻³ (Fig. 125a) occasionally exceeding 0.05 cm⁻³ and was contributed by Westerly/Southwesterly winds. The occurrence of relatively low FBAP concentration during entire campaign is consistent with low concentration occurrence during *dusty* (0 – 0.05 cm⁻³; >90% frequency of occurrence) and *clean* (<0.01 cm⁻³; ~90% frequency of occurrence) periods. During *high bio* period the FBAP concentration, >0.05 cm⁻³ exhibited ~40% frequency of occurrence of which ~50% was contributed by predominant wind from the North and the Northwest.

Similarly the wind rose diagram scaled by geometric mean diameter (D_g) of $dN_F/d\log D_a$, is shown in Fig. 136. The average size of the FBAP particles associated with

Formatted: Font: Italic

Formatted: Font: Italic

Formatted: Font: Italic

Formatted: Font: Italic

Formatted: Font: Italic

Formatted: Font: Italic

916 Westerly/Southwesterly winds when analyzed for the entire ~~the~~ campaign ranged between 2 – 4
 917 μm of which ~65% of the time D_g was observed to be $\leq 3 \mu\text{m}$. During the three ~~distinct~~ focus
 918 periods the frequency of occurrence of FBAP particles in the higher size range (3 – 4 μm) was
 919 strongly associated with the Westerly/Southwesterly winds (Figs. 13**6**b – d). The corresponding
 920 wind rose diagram scaled by geometric mean diameter of $dN_T/d\log D_a (D_{g,T})$ is shown in Fig.
 921 S22**0**. During entire measurement campaign the frequency of occurrence of $D_{g,T}$ in the size range
 922 of 0.8 – 0.9 μm was ~70% and was mostly associated with Westerly/Southwesterly winds.
 923 During the *dusty* period, particles in the size range of 0.8 – 0.9 μm diameter contributed for
 924 >95% frequency of occurrence for the entire size range, whereas during *clean* period ~20%
 925 occurrence of the particles in the size range other than 0.8 – 0.9 μm were also observed. On the
 926 other hand during *high bio* period total particles in the size range 0.5 – 0.8 μm were observed
 927 with ~50% frequency of occurrence ~~constituted by varying wind patterns~~ mostly dominated by
 928 northerly winds.
 929 The FBAP concentration exhibited strong dependence on the wind direction for this
 930 observational site. During the *high bio* period the increase in frequency of occurrence of FBAP
 931 number concentrations $>0.1 \text{ cm}^{-3}$ coincided with ~~stagnant~~ lower wind speed coming from the
 932 North and Northwest (Fig. 14**7**a). During the *high bio* period, as ~~like in the case of the~~ *dusty* and
 933 *clean* periods, the predominant wind pattern was Westerly/Southwesterly, ~~however~~ but, with
 934 relatively low frequency of occurrence as compared to the other two periods. To have ~~the a~~ better
 935 understanding of the relative contribution of wind direction in high FBAP number concentration
 936 during the *high bio* period, ~~we prepared the~~ separate wind rose diagrams for FBAP concentration
 937 $>0.1 \text{ cm}^{-3}$ and $<0.1 \text{ cm}^{-3}$ as shown in Fig. 14**7**. The FBAP number concentration $>0.1 \text{ cm}^{-3}$ was
 938 associated with ~~calm~~ lower wind speed ($0 - 1 \text{ m s}^{-1}$; ~80% frequency of occurrence) and

Formatted: Font: Italic

Formatted: Font: Italic

Formatted: Font: Italic

Formatted: Font: Italic

Formatted: Font: Italic

Formatted: Font: Italic

Formatted: Font: Italic

Formatted: Font: Italic

939 | predominant Northerly winds (Fig. 147a) as opposed to high wind speed ($2 - 5 \text{ m s}^{-1}$) and
 940 | predominant Westerly/Southwesterly winds for the FBAP number concentration $< 0.1 \text{ cm}^{-3}$ (Fig.
 941 | 147b). The ~~calm~~ Northerly winds with lower wind speed coming over from densely vegetated
 942 | regions in combination with local FBAP sources during *high bio* period could be the strong
 943 | reason for the built up resulting in higher FBAP number concentration during this episode,
 944 | whereas, Westerly/Southwesterly winds were consistently marked by very low FBAP number
 945 | concentration mostly owing to higher wind speeds. Further, it might also due to the fact that the
 946 | air masses arriving at observational site originated over cleaner marine region, which may be
 947 | potential but weak source of bioaerosols combined with possible wash out/wet deposition due to
 948 | persistent rainfall during the transport. Nominally the frequency of occurrence of larger particles
 949 | ($3 - 4 \text{ }\mu\text{m}$) during Westerly/Southwesterly winds was high compared to the Northerly winds,
 950 | where particles were mostly of smaller size ($1 - 3 \text{ }\mu\text{m}$). We hypothesize that during the Northerly
 951 | wind the bioaerosols were mostly comprised of Basidiospores, which is consistent with SEM
 952 | images obtained during measurement period. Frohlich-Nowoisky et al., (2012) reported that,
 953 | region with dominant prevalence of marine air masses have larger proportions of Ascospores and
 954 | in contrast, the continental air masses exhibit higher proportions of Basidiospores. However, due
 955 | to technical difficulties associated with sampling we could not establish the fact that spores
 956 | observed at this observational site during Westerly/Southwesterly winds were dominated by
 957 | Ascospores and these details will be addressed in follow up studies. The corresponding wind
 958 | rose scaled by $D_{g,T}$ obtained from $dN_T/d\log D_a$ is shown in Fig. S23+.
 959 | As shown in Tab. 5 the wind speed was observed to be negatively affecting the N_F during entire
 960 | measurement period and is consistent with previously reported studies (Hameed et al., 2012;
 961 | Almaguer et al., 2013; Lyon et al., 1984; Quintero et al., 2010). The increased N_F concentration

Formatted: Font: Italic

962 | levels during ~~calm and stagnant~~lower wind speed might indicate that observed bioaerosols were
963 | dominated by the local source rather than transported from longer distances (Sadys et al., 2014;
964 | Hara and Zhang, 2012; Bovallius et al., 1978; Maki et al., 2013; Prospero et al., 2005; Creamean
965 | et al., 2013) as lower wind speed may actually increase emission of some specific type of spores
966 | (Huffman et al., 2012; Jones and Harrison, 2004; Troutt and Levetin, 2001; Kurkela, 1997).

967 | 3.4.6.21 Correlation with relative humidity and temperature

968 | Correlation coefficient derived between N_F and relative humidity averaged over the entire
969 | campaign is shown in Fig. 158 and corresponding R^2 values for three distinct focus periods are
970 | shown in Tab. 5. In general an increase in N_F concentration with increasing relative humidity was
971 | observed with moderate correlation coefficient ($R^2=0.58$). Depending upon the type of
972 | bioaerosols, geographical location, and local climate, N_F has shown varied dependence on
973 | relative humidity and the precise response of the spore concentration to relative humidity is
974 | difficult to characterize. For example, a number of studies have shown that spores of genus like
975 | *Cladosporium*, *Alternaria*, and *Epicoccum* are known to exhibit the negative correlation with
976 | relative humidity (Oliveira et al., 2010; Herrero et al., 1996; Kurkela, 1997; Oh et al., 1998;
977 | Healy et al., 2014); while on the other hand, other studies have also found these spores to be
978 | positively correlated with relative humidity (Quintero et al., 2010; Hjelmroos, 1993; Ho et al.,
979 | 2005). Whereas Genus like *Ustilago* and some other Basidiospores may as well exhibit strong
980 | positive correlation with relative humidity (Sabariego et al., 2000; Quintero et al., 2010; Ho et
981 | al., 2005; Calderon et al., 1995). Further, Ascospores concentrations are known to increase
982 | during and after rainfall (Burch and Levetin, 2002; Elbert et al., 2007; Hasnain, 1993; Hirst,
983 | 1953; Toutt and Levetin, 2001; Lyon et al., 1984; Oh et al., 1998) whereas Basidiospores
984 | exhibited a strong resemblance to the diurnal pattern of relative humidity (Li and Kendrick 1994;

Formatted: Space After: 0 pt

Formatted: Justified, Space After: 0 pt

985 Hasnain 1993; Tarlo et al., 1979; Trout and Levetin 2001). Almaguer et al., (2013) have reported
 986 that in tropical region relative humidity has greater influence than temperature on the airborne
 987 spore counts and may be a pre-requisite for release of spores (Hollins et al., 2004). Thus, the
 988 combination of persistent threshold relative humidity (~60 – 95% as reported by Ho et al., 2005)
 989 and rainfall can cause the increase in the spore concentration and the excessive and persistent
 990 rain, however, tends to wash the spore out of the atmosphere further reducing their concentration
 991 levels (Burge 1986; Horner et al., 1992; Trout and Levetin, 2001). Based on these arguments
 992 combined with observed meteorological conditions we expect that the bioaerosols reported here
 993 from Munnar mainly consisted of Basidiospores during the SW monsoon season as also evident
 994 from SEM images (discussed above). This is consistent with results reported by Valsan et al.,
 995 (2015) where they found the dominant presence of dry air spora (*Cladosporium*) during
 996 relatively dry and warm weather from the same observational site. In general, N_F and N_F/N_T
 997 decreased with increasing wind speed ($R^2=0.6$ and $R^2=0.78$, respectively) indicating that wind
 998 speed may be one of the strong factors for observed high N_F concentrations at this site. As
 999 compared to previously reported correlation between N_F and meteorological parameters
 1000 (Santarpia et al., 2013), the relations shown for this observational site appeared to be more robust
 1001 and conclusive. For example since the variability derived in N_T ($N_T - N_{T,min} / N_{T,max} - N_{T,min}$; not
 1002 shown here) was more consistent and high as compared to variability derived in N_F ($N_F - N_{F,min} /$
 1003 $N_{F,max} - N_{F,min}$), which was more episodic and hence one would expect the weak correlation
 1004 between N_T and meteorological parameters (Tab. 5).
 1005 ~~On the other hand,~~ Several studies have reported that in temperate regions, temperature is
 1006 probably the most important meteorological parameter affecting the spore concentration (Levetin
 1007 and Horner, 2002; Adhikari et al., 2006) with highest spore concentration during summer season

(Emberlin et al., 1995; Hasnain, 1993; Herrero et al., 1996; Hjelmroos, 1993; Li et al., 2011; Schumacher et al., 2013). When the relation between temperature and spore concentration was investigated on averaged diurnal basis, however, spore concentration have been observed to decrease with the increasing temperature (Burch and Levetin, 2002; Calderon et al., 1995; Sabariego et al., 2000; Schumacher et al., 2013; Trejo et al., 2013). Consistent with this trend, we have found significant negative correlation between N_F and temperature ($R^2=0.65$) averaged over the entire measurement period at Munnar. The correlation coefficient between N_F and temperature for three distinct focus periods is given in Tab. 5 and are specific to this locality of sampling and may not be extrapolated to represent behavior in other ecosystems in the Indian region. ~~The correlation coefficient between N_F/N_T and meteorological parameters in general yielded higher R^2 values. Note, however, that the interpretation presented here based on the correlation analyses performed between N_F and meteorological parameters were intended not to generalize and extrapolate conclusions to various other ecosystems (including Indian region) and different seasons of the year (including non monsoon in India).~~ These results were, however, but ~~were~~ presented to take an opportunity to formulate preliminary hypothesis about role of meteorological parameters in governing the variabilites of bioaerosls specific to this observational site for the monsoon season only.

4 Summary and Conclusions

~~During these maiden online measurements of biological aerosol particles we operated a~~ A UV- ~~APS was continuously operated during the SW monsoon season (1 June – 21 August~~ June 1 - August 21, 2014) ~~of 2014 at a high altitude site of~~ the Western Ghats in Southern tropical India. The number and mass size distributions and corresponding concentrations of

Formatted: Space After: 0 pt

Formatted: Justified, Space After: 0 pt

1031 biological aerosol were quantified for three distinct focus periods namely ~~dusty-period, high-bio~~
 1032 ~~period, and clean, period~~ identified based on the prominent wind direction. ~~We have analyzed~~
 1033 ~~the three month time-series of integrated coarse particle number and mass concentrations, as well~~
 1034 ~~as particle number and mass size distributions of both, the total and fluorescence biological~~
 1035 ~~aerosol particles.~~ Over the course of the entire measurement period the coarse particle number
 1036 concentration of FBAPs varied in the range of $0.2 \times 10^{-3} \text{ cm}^{-3}$ to 0.63 cm^{-3} with an arithmetic
 1037 mean value of 0.02 cm^{-3} ($\pm 0.02 \text{ cm}^{-3}$). This average concentration accounted for 0.04 – 53%
 1038 (mean value $2.1\% \pm 4.05\%$) of the total coarse particle number concentration. The coarse particle
 1039 mass concentrations of FBAPs varied in the range of $0.5 \times 10^{-3} - 4.93 \mu\text{g m}^{-3}$ with an arithmetic
 1040 mean (\pm standard deviation) value of $0.24 (\pm 0.28) \mu\text{g m}^{-3}$.

1041 The ~~average~~ FBAP concentrations observed at Munnar during SW monsoon season were within
 1042 the range but slightly on the lower side of the concentrations reported by previous researchers
 1043 using various online and offline techniques from varying environments ~~the entire measurement~~
 1044 ~~period was found to be highest in June (0.03 cm^{-3}) and lowest in July (0.007 cm^{-3}). The FBAP~~
 1045 ~~concentrations observed at Munnar during SW monsoon season are within the range but slightly~~
 1046 ~~on the lower side of the bioaerosol concentrations reported by previous researchers using various~~
 1047 ~~online and offline techniques. Numerous other studies from different part of the world have~~
 1048 ~~reported detailed description about observed biological aerosol particle number concentrations~~
 1049 ~~using offline and online techniques from various environments~~ (Despres et al., 2007; Huffman et
 1050 al., 2010, 2012; Adhikari et al., 2004; Bovallius et al., 1978; Bowers, et al., 2009, 2013; Lee et
 1051 al., 2010; Matthias-Maser and Jaenicke, 1995; Matthias-Maser et al., 2000; Shaffer and
 1052 Lighthart, 1997; Tong and Lighthart, 1999; Wang et al., 2007; Li et al., 2011; Hameed et al.,
 1053 2009; Bauer et al., 2008; Schumacher et al., 2013; Gabey et al., 2010, 2011, 2013; Saari et al.,

Formatted: Font: Italic

Formatted: Font: Italic

Formatted: Font: Italic

1054 2015; Toprak and Schnaiter, 2013; Healy et al., 2014). For brevity, here we compare the number
 1055 concentrations observed at Munnar only with number concentrations from varying environments
 1056 ~~reported by previous researchers~~carried out using online measurements. Huffman et al., (2010)
 1057 have reported coarse mode average FBAP number concentration from four months of
 1058 measurement to be 0.03 cm^{-3} , which constituted ~4% of total coarse mode particles from a semi-
 1059 urban site of Mainz in Central Europe. The median FBAP concentration during the wet season of
 1060 pristine tropical Amazonian rainforest region was found be 0.07 cm^{-3} , which constituted ~24% of
 1061 total coarse mode particle number concentration (Huffman et al., 2012). By analyzing the full
 1062 one-year observations from Boreal forest in Hyttiala and pine forest in Colorado, Schumacher et
 1063 al., (2013) reported highest FBAP concentration in summer of 0.046 cm^{-3} (constituting ~13% of
 1064 total coarse mode particles) and 0.03 cm^{-3} (constituting ~8.8% of total coarse mode particles),
 1065 respectively. Healy et al., (2014) reported the average FBAP concentration of $\sim 0.01 \text{ cm}^{-3}$ using
 1066 the UV-APS measurements carried out with in the Killarney national park, Kerry situated in
 1067 Southwest of Ireland. Gabey et al., (2013) by performing the measurements at a high altitude
 1068 ~~es~~site in central France reported averaged FBAP concentration of 0.012 cm^{-3} and 0.095 cm^{-3} using
 1069 two-wavelength (280 nm and 370 nm respectively) single-particle UV-induced fluorescence
 1070 spectrometer. Gabey et al., (2010) from tropical rainforest in Borneo, Malaysia reported that
 1071 mean FBAP number fraction in the size range of $0.8 - 20 \mu\text{m}$ was ~55% and ~28% below and
 1072 above the forest canopy, respectively. It is important to note, however, that the measurement
 1073 results compared here were obtained from different instrumentation operating with different
 1074 wavelength. ~~Nevertheless, the FBAP number concentrations observed under various~~
 1075 ~~environmental conditions are largely comparable to the FBAP number concentration observed at~~

Formatted: Superscript

1076 ~~Munnar during SW monsoon season. Note that the relative contribution of FBAP number~~
1077 ~~concentration to total coarse mode particles may show a strong spatial variability.~~

1078 The average observed $dN_F/d\log D_a$ exhibited a peak at $\sim 3 \mu\text{m}$, which was consistent even during
1079 distinct focus periods with slight quantitative variation in the FBAP number concentration. Such
1080 a consistency in the peak of $dN_F/d\log D_a$ during entire measurement period ~~is an indication of~~
1081 ~~the fact~~ that sources and type of bioaerosols did not exhibit considerable variability and diversity
1082 at Munnar during SW monsoon season. The peak observed in $dN_F/d\log D_a$ in this study is
1083 consistent with range of the peaks published by previous researchers. At a semi-urban site in
1084 Central Europe the peak in $dN_F/d\log D_a$ was observed at $\sim 3 \mu\text{m}$ (Huffman et al., 2010). In
1085 pristine tropical rainforest region of Amazonia a peak in $dN_F/d\log D_a$ was found at $\sim 2.5 \mu\text{m}$
1086 (Huffman et al., 2012). Whereas the peak in $dN_F/d\log D_a$ at a boreal forest in Finland exhibited a
1087 strong seasonal dependence with different modes at $\sim 1.5 \mu\text{m}$, $\sim 3 \mu\text{m}$, and $\sim 5 \mu\text{m}$ indicating
1088 differences in the bioaerosol sources (Schumacher et al., 2013). In the pine forest of Colorado the
1089 distinct peaks were observed at $\sim 1.5 \mu\text{m}$ and $\sim 5 \mu\text{m}$ (Schumacher et al., 2013). The mode at ~ 3
1090 μm [reported for Colorado](#) is likely due to the fungal spore whose release mechanism is strongly
1091 governed by the combination of relative humidity and temperature (Huffman et al., 2010 and
1092 references therein).

1093 On the diurnal scale a pronounced diurnal cycle with $\sim 3 \mu\text{m}$ peak with a maximum concentration
1094 at $\sim 06:00$ hr was observed when averaged over entire measurement period. This general pattern
1095 is consistent with previous studies reporting the early morning peak in FBAP concentration for
1096 various environmental conditions (Healy et al., 2014; Huffman et al., 2012; Schumacher et al.,
1097 2013; Toprak and Schnaiter, 2013). The early morning peak, ~~which in the present case appears to~~
1098 ~~be strongly governed by the diurnal variations in relative humidity, is most likely to be~~ [was](#)

Formatted: Justified

1099 contributed by Basidiospores as their release in the atmosphere is strongly coupled with relative
1100 humidity (Adhikari et al., 2006; Burch and Levetin, 2002; Hasnain, 1993; Healy et al., 2014; Ho
1101 et al., 2005; Huffman et al., 2012). This is also consistent with the SEM images shown and
1102 discussed above.

1103 The meteorological parameters were observed to correlate significantly with FBAP concentration
1104 at Munnar. ~~When investigated on a daily averaged basis (24 hr), however, no significant~~
1105 ~~correlation between N_F and meteorological parameters except moderate negative correlation with~~
1106 ~~precipitation was observed. During the entire measurement campaign, except on few occasions~~
1107 ~~no significant variations in temperature and relative humidity was observed. This in combination~~
1108 ~~with persistent rainfall resulting in the wash-out/wet deposition of biological aerosol particles~~
1109 ~~might have caused such a weak correlation for a daily averaged (24 hr) analysis. On a diurnal~~
1110 ~~scale, however, a significant correlation between N_F and meteorological parameters was~~
1111 ~~observed.~~ We observed that N_F followed the similar diurnal trend to that of relative humidity and
1112 was anti-correlated with temperature. As reported by previous studies from selected locations
1113 (Huffman et al., 2013; Schumacher et al., 2013; Prenni et al., 2013; Hirst 1953) we did not
1114 observe any sharp increase in N_F concentration immediately after or during rainfall. We
1115 hypothesize that the spore built-up and release of certain species can happen only at certain
1116 threshold relative humidity (Jones and Harrison, 2004). Our results indicate that Under the dry
1117 environmental conditions where relative humidity levels rarely attain such threshold required for
1118 fungal spore release can cause the strong built up of fungal spores inside fungal bodies. Under
1119 these conditions precipitation can cause the relative humidity levels to increase up to threshold
1120 required for fungal spore release in combination with mechanical splashing due to raindrops, and
1121 can cause the sudden and sharp increase in spore concentrations. On the contrary, like in present

Formatted: Justified, Space After: 0 pt

1122 | case, the ~~ineessant~~-persistent~~ee-of~~ high humidity conditions can cause the continuous release of
1123 | the spore without an opportunity for built-up of fungal spores in fungal body to be released
1124 | during rainfall. It is also reported that persistent high levels of relative humidity can inhibit the
1125 | sporulation (Schumacher et al., 2013) further considerably reducing the spore release. [More](#)
1126 | [detailed measurements are required from the regions where relative humidity persistently](#)
1127 | [remains low \(<60%\) for extended amount of time and experiences sudden rainfall.](#) The
1128 | correlation between N_F and wind speed was found to be strongly negative. Since majority of the
1129 | spore release was dominated by the local sources, the ~~str~~ong winds coming over from
1130 | West/Southwest direction, which were relatively clean, might have caused the dilution of air
1131 | mass thus reducing the spore concentration.

1132 | Overall, the long-term measurements reported in this manuscript showed the quantitative and
1133 | qualitative agreement with previously reported studies. The emissions and abundance of
1134 | biological aerosol particles in Western Ghats air during monsoon season appeared to be closely
1135 | linked to the variaiblities in the meteorological parameters. ~~As reported by Huffman et al.,~~
1136 | ~~(2012) and corroborated by the observations reported in this study, UV-APS is successfully able~~
1137 | ~~to detect the aerosol particles of biological origin, however, may pose certain limitations in~~
1138 | ~~seientific interpretation from the obtained data.~~ The scatter plot analysis carried out between N_F
1139 | and N_T for submicron and supermicron particles indicated that submicron particles at this
1140 | observational site were also dominated by aerosol particles of biological origin, thus indicating
1141 | the lowest possible interference from particles of anthropogenic origin known to exhibit the
1142 | fluorescence at the prescribed wavelength used in UV-APS. Hence, given observational site can
1143 | be termed as relatively pristine while under the influence of SW monsoon season. [This](#)
1144 | [emphasizes the need to perform similar measurements under different land-use type during same](#)

Formatted: Justified

1145 | [season over Indian region.](#) The contrasting characteristics of this observational site associated
1146 | with pollution and interference of non-biological aerosol particles in fluorescence will be
1147 | discussed in follow up studies. We propose ~~and intend to take forward these~~[more](#) studies by
1148 | means of performing simultaneous online measurements of biological aerosol particle ~~number~~
1149 | ~~concentrations in high time and size resolution~~ under contrasting environments during distinct
1150 | meteorological seasons over Indian region. [These measurements](#) ~~This future work~~ could be
1151 | supplemented with advanced offline measurement techniques including SEM analysis, DNA
1152 | analysis, and fluorescence microscopy of the samples collected in parallel with the
1153 | measurements. We believe that such a comprehensive approach over Indian region would be
1154 | helpful in understanding the possible tight coupling between aerosol and hydrological cycle
1155 | especially during monsoon. This could also help to better understand the implication of
1156 | biological aerosols on crops and human health where agricultural industry has the major share in
1157 | GDP to cater the need of 18% of the world's total population.

1158 **Acknowledgement:**

1159 | SSG acknowledge the combined financial support from Max Planck Society and Department of Science and
1160 | Technology, Government of India under the Max Planck Partner Group Program. Authors are thankful to Akila M,
1161 | Hema P, Shika S, ~~Aljeena~~, Hasitha, Reshma, Sanu, and Tabish U. Ansari for their support in planning, execution,
1162 | and completion of the measurement campaign. Authors thankfully acknowledge the support from Gerhard Lammel,
1163 | Multiphase Chemistry Department, Max Planck Institute for Chemistry for his support during campaign and
1164 | providing the meteorological data for comparison. Authors are grateful to the Sophisticated Analytical Instrument
1165 | Facility (SAIF), IIT Madras for making SEM available for morphological analysis. Authors gratefully acknowledge
1166 | US Geological Survey for the topography data in DEM format and NOAA ARL for providing HYSPLIT air mass
1167 | back trajectory calculations.

1168 **References:**

1169 | Adhikari, A., Sen, M. M., Gupta-Bhattacharya, S., and Chanda, S.: Air-borne viable, non-viable,
1170 | and allergenic fungi in a rural agricultural area of India: a 2-year study at five outdoor sampling
1171 | stations, Science of the Total Environment, 326, 123-141, 10.1016/j.scitotenv.2003.12.007,
1172 | 2004.

1173 Adhikari, A., Reponen, T., Grinshpun, S. A., Martuzevicius, D., and LeMasters, G.: Correlation
 1174 of ambient inhalable bioaerosols with particulate matter and ozone: A two-year study,
 1175 *Environmental Pollution*, 140, 16-28, 10.1016/j.envpol.2005.07.004, 2006.

1176 Agranovski, V., Ristovski, Z., Hargreaves, M., Blackall, P. J., and Morawska, L.: Performance
 1177 evaluation of the UVAPS: influence of physiological age of airborne bacteria and bacterial
 1178 stress, *Journal of Aerosol Science*, 34, 1711-1727, 10.1016/s0021-8502(03)00191-5, 2003.

1179 Agranovski, V., Ristovski, Z. D., Ayoko, G. A., and Morawska, L.: Performance evaluation of
 1180 the UVAPS in measuring biological aerosols: Fluorescence spectra from NAD(P)H coenzymes
 1181 and riboflavin, *Aerosol Sci. Technol.*, 38, 354-364, 10.1080/02786820490437505, 2004.

1182 Agranovski, V., and Ristovski, Z. D.: Real-time monitoring of viable bioaerosols: capability of
 1183 the UVAPS to predict the amount of individual microorganisms in aerosol particles, *Journal of*
 1184 *Aerosol Science*, 36, 665-676, 10.1016/j.jaerosci.2004.12.005, 2005.

1185 Almaguer, M., Aira, M.-J., Rodríguez-Rajo, F. J., and Rojas, T. I.: Temporal dynamics of
 1186 airborne fungi in Havana (Cuba) during dry and rainy seasons: influence of meteorological
 1187 parameters, *International Journal of Biometeorology*, 58, 1459-1470, 10.1007/s00484-013-0748-
 1188 6, 2013.

1189 Andreae, M. O., and Rosenfeld, D.: Aerosol-cloud-precipitation interactions. Part 1. The nature
 1190 and sources of cloud-active aerosols, *Earth Science Reviews*, 89, 13-41, 2008.

1191 Ansari, T. U., Valsan, A. E., Ojha, N., Ravikrishna, R., Narasimhan, B., and Gunthe, S. S.:
 1192 Model simulations of fungal spore distribution over the Indian region, *Atmospheric*
 1193 *Environment*, 122, 552-560, <http://dx.doi.org/10.1016/j.atmosenv.2015.10.020>, 2015.

1194 Artaxo, P., and Hansson, H. C.: Size distribution of biogenic aerosol-particles from the Amazon
 1195 basin, *Atmospheric Environment*, 29, 393-402, 10.1016/1352-2310(94)00178-n, 1995.

1196 [Baron, P. A., and Willeke, K.: Aerosol Measurement – Principles, Techniques and Applications.](#)
 1197 [Second edition, John Wiley & Sons. 2005.](#)

1198

1199 Bauer, H., Schueller, E., Weinke, G., Berger, A., Hitzenberger, R., Marr, I. L., and Puxbaum, H.:
 1200 Significant contributions of fungal spores to the organic carbon and to the aerosol mass balance
 1201 of the urban atmospheric aerosol, *Atmospheric Environment*, 42, 5542-5549,
 1202 10.1016/j.atmosenv.2008.03.019, 2008.

1203 Bhati, H. S., and Gaur, R. D.: Studies on Aerobiology - Atmospheric fungal spores, *New*
 1204 *Phytologist*, 82, 519-527, 10.1111/j.1469-8137.1979.tb02678.x, 1979.

1205 Bovallius, A., Bucht, B., Roffey, R., and Anas, P.: 3-Year investigation of natural airborne
 1206 bacterial-flora at 4 localities in Sweden, *Applied and Environmental Microbiology*, 35, 847-852,
 1207 1978.

- 1208 Bowers, R. M., Lauber, C. L., Wiedinmyer, C., Hamady, M., Hallar, A. G., Fall, R., Knight, R.,
1209 and Fierer, N.: Characterization of Airborne Microbial Communities at a High-Elevation Site
1210 and Their Potential To Act as Atmospheric Ice Nuclei, *Applied and Environmental*
1211 *Microbiology*, 75, 5121-5130, 10.1128/aem.00447-09, 2009.
- 1212 Bowers, R. M., Clements, N., Emerson, J. B., Wiedinmyer, C., Hannigan, M. P., and Fierer, N.:
1213 Seasonal Variability in Bacterial and Fungal Diversity of the Near-Surface Atmosphere,
1214 *Environmental Science & Technology*, 47, 12097-12106, 10.1021/es402970s, 2013.
- 1215 Brosseau, L. M., Vesley, D., Rice, N., Goodell, K., Nellis, M., and Hairston, P.: Differences in
1216 detected fluorescence among several bacterial species measured with a direct-reading particle
1217 sizer and fluorescence detector, *Aerosol Sci. Technol.*, 32, 545-558, 10.1080/027868200303461,
1218 2000.
- 1219 Burch, M., and Levetin, E.: Effects of meteorological conditions on spore plumes, *International*
1220 *Journal of Biometeorology*, 46, 107-117, 10.1007/s00484-002-0127-1, 2002.
- 1221 Burge, H. A.: Some comments on the aerobiology of fungus spores, *Grana*, 25, 143-146, 1986.
- 1222 Burge, H. A., and Rogers, C. A.: Outdoor allergens, *Environmental Health Perspectives*, 108,
1223 653-659, 10.2307/3454401, 2000.
- 1224 Burrows, S. M., Butler, T., Jöckel, P., Tost, H., Kerkweg, A., Pöschl, U., and Lawrence, M. G.:
1225 Bacteria in the global atmosphere - Part 2: Modeling of emissions and transport between
1226 different ecosystems, *Atmos. Chem. Phys.*, 9, 9281-9297, 2009.
- 1227 Calderon, C., Lacey, J., McCartney, H. A., and Rosas, I.: Seasonal and diurnal-variation of
1228 airborne basidiomycete spore concentrations in Mexico-city, *Grana*, 34, 260-268, 1995.
- 1229 Chakraborty, P., Gupta-Bhattacharya, S., Chakraborty, C., Lacey, J., and Chanda, S.: Airborne
1230 allergenic pollen grains on a farm in West Bengal, India, *Grana*, 37, 53-57, 1998.
- 1231 Coz, E., Artinano, B., Clark, L. M., Hernandez, M., Robinson, A. L., Casuccio, G. S., Lersch, T.
1232 L., and Pandis, S. N.: Characterization of fine primary biogenic organic aerosol in an urban area
1233 in the northeastern United States, *Atmospheric Environment*, 44, 3952-3962,
1234 10.1016/j.atmosenv.2010.07.007, 2010.
- 1235 Creamean, J. M., Suski, K. J., Rosenfeld, D., Cazorla, A., DeMott, P. J., Sullivan, R. C., White,
1236 A. B., Ralph, F. M., Minnis, P., Comstock, J. M., Tomlinson, J. M., and Prather, K. A.: Dust and
1237 Biological Aerosols from the Sahara and Asia Influence Precipitation in the Western U.S.,
1238 *Science*, 339, 1572-1578, 10.1126/science.1227279, 2013.
- 1239 DeCarlo, P. F., Slowik, J. G., Worsnop, D. R., Davidovits, P., and Jimenez, J. L.: Particle
1240 morphology and density characterization by combined mobility and aerodynamic diameter
1241 measurements. Part 1: Theory, *Aerosol Sci. Technol.*, 38, 1185-1205, 2004.
- 1242 DeLeon-Rodriguez, N., Lathem, T. L., Rodriguez-R, L. M., Barazesh, J. M., Anderson, B. E.,
1243 Beyersdorf, A. J., Ziemba, L. D., Bergin, M., Nenes, A., and Konstantinidis, K. T.: Microbiome

1244 of the upper troposphere: Species composition and prevalence, effects of tropical storms, and
 1245 atmospheric implications, *Proceedings of the National Academy of Sciences of the United States*
 1246 of America, 110, 2575-2580, 10.1073/pnas.1212089110, 2013.

1247 Despres, V. R., Nowoisky, J. F., Klose, M., Conrad, R., Andreae, M. O., and Pöschl, U.:
 1248 Characterization of primary biogenic aerosol particles in urban, rural, and high-alpine air by
 1249 DNA sequence and restriction fragment analysis of ribosomal RNA genes, *Biogeosciences*, 4,
 1250 1127-1141, 2007.

1251 Despres, V. R., Huffman, J. A., Burrows, S. M., Hoose, C., Safatov, A. S., Buryak, G., Frohlich-
 1252 Nowoisky, J., Elbert, W., Andreae, M. O., Pöschl, U., and Jaenicke, R.: Primary biological
 1253 aerosol particles in the atmosphere: a review, *Tellus Series B-Chemical and Physical*
 1254 *Meteorology*, 64, 10.3402/tellusb.v64i0.15598, 2012.

1255 Du, C., Liu, S., Yu, X., Li, X., Chen, C., Peng, Y., Dong, Y., Dong, Z., and Wang, F.: Urban
 1256 Boundary Layer Height Characteristics and Relationship with Particulate Matter Mass
 1257 Concentrations in Xi'an, Central China, *Aerosol and Air Quality Research*, 13, 1598-1607,
 1258 10.4209/aaqr.2012.10.0274, 2013.

1259 Elbert, W., Taylor, P. E., Andreae, M. O., and Pöschl, U.: Contribution of fungi to primary
 1260 biogenic aerosols in the atmosphere: wet and dry discharged spores, carbohydrates, and
 1261 inorganic ions, *Atmospheric Chemistry and Physics*, 7, 4569-4588, 2007.

1262 Emberlin, J., Newman, T., and Bryant, R.: The incidence of fungal spores in the ambient air and
 1263 inside homes: Evidence from London, *Aerobiologia*, 11, 253-258, 10.1007/bf02447205, 1995

1264 Fisher, M. C., Henk, D. A., Briggs, C. J., Brownstein, J. S., Madoff, L. C., McCraw, S. L., and
 1265 Gurr, S. J.: Emerging fungal threats to animal, plant and ecosystem health, *Nature*, 484, 186-194,
 1266 10.1038/nature10947, 2012.

1267 Fröhlich-Nowoisky, J., Pickersgill, D. A., Després, V. R., and Pöschl, U.: High diversity of fungi
 1268 in air particulate matter, *Proceedings of the National Academy of Sciences*, 106, 12814-12819,
 1269 10.1073/pnas.0811003106, 2009.

1270 Froehlich-Nowoisky, J., Burrows, S. M., Xie, Z., Engling, G., Solomon, P. A., Fraser, M. P.,
 1271 Mayol-Bracero, O. L., Artaxo, P., Begerow, D., Conrad, R., Andreae, M. O., Despres, V. R., and
 1272 Pöschl, U.: Biogeography in the air: fungal diversity over land and oceans, *Biogeosciences*, 9,
 1273 1125-1136, 10.5194/bg-9-1125-2012, 2012.

1274 Fuzzi, S., Mandrioli, P., and Peretto, A.: Fog droplets - An atmospheric source of secondary
 1275 biological aerosol particles, *Atmospheric Environment*, 31, 287-290, 10.1016/1352-
 1276 2310(96)00160-4, 1997.

1277 Gabey, A. M., Gallagher, M. W., Whitehead, J., Dorsey, J. R., Kaye, P. H., and Stanley, W. R.:
 1278 Measurements and comparison of primary biological aerosol above and below a tropical forest
 1279 canopy using a dual channel fluorescence spectrometer, *Atmospheric Chemistry and Physics*, 10,
 1280 4453-4466, 10.5194/acp-10-4453-2010, 2010.

1281 Gabey, A. M., Stanley, W. R., Gallagher, M. W., and Kaye, P. H.: The fluorescence properties of
 1282 aerosol larger than 0.8 μm in urban and tropical rainforest locations, *Atmospheric Chemistry*
 1283 *and Physics*, 11, 5491-5504, 10.5194/acp-11-5491-2011, 2011.

1284 Gabey, A. M., Vaitilingom, M., Freney, E., Boulon, J., Sellegri, K., Gallagher, M. W., Crawford,
 1285 I. P., Robinson, N. H., Stanley, W. R., and Kaye, P. H.: Observations of fluorescent and
 1286 biological aerosol at a high-altitude site in central France, *Atmospheric Chemistry and Physics*,
 1287 13, 7415-7428, 10.5194/acp-13-7415-2013, 2013.

1288 Gangamma, S.: Characteristics of airborne bacteria in Mumbai urban environment, *Science of*
 1289 *the Total Environment*, 488, 70-74, 10.1016/j.scitotenv.2014.04.065, 2014.

1290 Garland, R. M., Schmid, O., Nowak, A., Achtert, P., Wiedensohler, A., Gunthe, S. S., Takegawa,
 1291 N., Kita, K., Kondo, Y., Hu, M., Shao, M., Zeng, L. M., Zhu, T., Andreae, M. O., and Pöschl, U.:
 1292 Aerosol optical properties observed during Campaign of Air Quality Research in Beijing 2006
 1293 (CAREBeijing-2006): Characteristic differences between the inflow and outflow of Beijing city
 1294 air, *Journal of Geophysical Research-Atmospheres*, 114, 2009.

1295 Grand, L. F., and Vandyke, C. G.: Scanning electron microscopy of basidiospores of species of
 1296 *hydnum*, *hydnum*, *phellodon*, and *bankera* (hydaceae), *Journal of the Elisha Mitchell*
 1297 *Scientific Society*, 92, 114-123, 1976.

1298 Hairston, P. P., Ho, J., and Quant, F. R.: Design of an instrument for real-time detection of
 1299 bioaerosols using simultaneous measurement of particle aerodynamic size and intrinsic
 1300 fluorescence, *Journal of Aerosol Science*, 28, 471-482, 10.1016/s0021-8502(96)00448-x, 1997.

1301 Hallar, A. G., Chirokova, G., McCubbin, I., Painter, T. H., Wiedinmyer, C., and Dodson, C.:
 1302 Atmospheric bioaerosols transported via dust storms in the western United States, *Geophysical*
 1303 *Research Letters*, 38, 10.1029/2011gl048166, 2011.

1304 Hameed, A. A. A., Khoder, M. I., Ibrahim, Y. H., Saeed, Y., Osman, M. E., and Ghanem, S.:
 1305 Study on some factors affecting survivability of airborne fungi, *Science of the Total*
 1306 *Environment*, 414, 696-700, 10.1016/j.scitotenv.2011.10.042, 2012.

1307 Hameed, A. A. A., Khoder, M. I., Yuosra, S., Osman, A. M., and Ghanem, S.: Diurnal
 1308 distribution of airborne bacteria and fungi in the atmosphere of Helwan area, Egypt, *Science of*
 1309 *the Total Environment*, 407, 6217-6222, 10.1016/j.scitotenv.2009.08.028, 2009.

1310 Hara, K., and Zhang, D.: Bacterial abundance and viability in long-range transported dust,
 1311 *Atmospheric Environment*, 47, 20-25, 10.1016/j.atmosenv.2011.11.050, 2012.

1312 Hasnain, S. M.: Influence of meteorological factors on the air spora, *Grana*, 32, 184-188, 1993.

1313 Healy, D. A., Huffman, J. A., O'Connor, D. J., Poehlker, C., Pöschl, U., and Sodeau, J. R.:
 1314 Ambient measurements of biological aerosol particles near Killarney, Ireland: a comparison
 1315 between real-time fluorescence and microscopy techniques, *Atmospheric Chemistry and Physics*,
 1316 14, 8055-8069, 10.5194/acp-14-8055-2014, 2014.

1317 Herrero, B., FombellaBlanco, M. A., FernandezGonzalez, D., and ValenciaBarrera, R. M.: The
 1318 role of meteorological factors in determining the annual variation of *Alternaria* and
 1319 *Cladosporium* spores in the atmosphere of Palencia, 1990-1992, *International Journal of*
 1320 *Biometeorology*, 39, 139-142, 10.1007/bf01211226, 1996.

1321 Hirst, J. M.: Changes in atmospheric spore content: Diurnal periodicity and the effects of
 1322 weather, *Transactions of the British Mycological Society*, 36, 375-IN378,
 1323 [http://dx.doi.org/10.1016/S0007-1536\(53\)80034-3](http://dx.doi.org/10.1016/S0007-1536(53)80034-3), 1953.

1324 Hjelmroos, M.: Relationship between airborne fungal spore presence and weather variables -
 1325 *cladosporium and alternaria*, *Grana*, 32, 40-47, 1993.

1326 Ho, H. M., Rao, C. Y., Hsu, H. H., Chiu, Y. H., Liu, C. M., and Chao, H. J.: Characteristics and
 1327 determinants of ambient fungal spores in Hualien, Taiwan, *Atmospheric Environment*, 39, 5839-
 1328 5850, 10.1016/j.atmosenv.2005.06.034, 2005.

1329 Hollins, P. D., Kettlewell, P. S., Atkinson, M. D., Stephenson, D. B., Corden, J. M., Millington,
 1330 W. M., and Mullins, J.: Relationships between airborne fungal spore concentration of
 1331 *Cladosporium* and the summer climate at two sites in Britain, *International Journal of*
 1332 *Biometeorology*, 48, 137-141, 10.1007/s00484-003-0188-9, 2004.

1333 Horner, W. E., Oneil, C. E., and Lehrer, S. B.: Basidiospore aeroallergens, *Clinical Reviews in*
 1334 *Allergy*, 10, 191-211, 1992.

1335 Huffman, J. A., Treutlein, B., and Pöschl, U.: Fluorescent biological aerosol particle
 1336 concentrations and size distributions measured with an Ultraviolet Aerodynamic Particle Sizer
 1337 (UV-APS) in Central Europe, *Atmos. Chem. Phys.*, 10, 3215-3233, 2010.

1338 Huffman, J. A., Sinha, B., Garland, R. M., Snee-Pollmann, A., Gunthe, S. S., Artaxo, P., Martin,
 1339 S. T., Andreae, M. O., and Pöschl, U.: Size distributions and temporal variations of biological
 1340 aerosol particles in the Amazon rainforest characterized by microscopy and real-time UV-APS
 1341 fluorescence techniques during AMAZE-08, *Atmospheric Chemistry and Physics*, 12, 11997-
 1342 12019, 10.5194/acp-12-11997-2012, 2012.

1343 Huffman, J. A., Prenni, A. J., DeMott, P. J., Poehlker, C., Mason, R. H., Robinson, N. H.,
 1344 Froehlich-Nowoisky, J., Tobo, Y., Despres, V. R., Garcia, E., Gochis, D. J., Harris, E., Mueller-
 1345 Germann, I., Ruzene, C., Schmer, B., Sinha, B., Day, D. A., Andreae, M. O., Jimenez, J. L.,
 1346 Gallagher, M., Kreidenweis, S. M., Bertram, A. K., and Pöschl, U.: High concentrations of
 1347 biological aerosol particles and ice nuclei during and after rain, *Atmospheric Chemistry and*
 1348 *Physics*, 13, 6151-6164, 10.5194/acp-13-6151-2013, 2013.

1349 Jones, A. M., and Harrison, R. M.: The effects of meteorological factors on atmospheric
 1350 bioaerosol concentrations - a review, *Science of the Total Environment*, 326, 151-180,
 1351 10.1016/j.scitotenv.2003.11.021, 2004.

1352 Kanaani, H., Hargreaves, M., Ristovski, Z., and Morawska, L.: Performance assessment of
 1353 UVAPS: Influence of fungal spore age and air exposure, *Journal of Aerosol Science*, 38, 83-96,
 1354 10.1016/j.jaerosci.2006.10.003, 2007.

1355 Kanaani, H., Hargreaves, M., Smith, J., Ristovski, Z., Agranovski, V., and Morawska, L.:
 1356 Performance of UVAPS with respect to detection of airborne fungi, *Journal of Aerosol Science*,
 1357 39, 175-189, 10.1016/j.jaerosci.2007.10.007, 2008.

1358 Kanawade, V. P., Shika, S., Poehlker, C., Rose, D., Suman, M. N. S., Gadhavi, H., Kumar, A.,
 1359 Nagendra, S. M. S., Ravikrishna, R., Yu, H., Sahu, L. K., Jayaraman, A., Andreae, M. O.,
 1360 Poeschl, U., and Gunthe, S. S.: Infrequent occurrence of new particle formation at a semi-rural
 1361 location, Gadanki, in tropical Southern India, *Atmospheric Environment*, 94, 264-273,
 1362 10.1016/j.atmosenv.2014.05.046, 2014.

1363 Kurkela, T.: The number of *Cladosporium* conidia in the air in different weather conditions,
 1364 *Grana*, 36, 54-61, 1997.

1365 Lee, S.-H., Lee, H.-J., Kim, S.-J., Lee, H. M., Kang, H., and Kim, Y. P.: Identification of
 1366 airborne bacterial and fungal community structures in an urban area by T-RFLP analysis and
 1367 quantitative real-time PCR, *Science of the Total Environment*, 408, 1349-1357,
 1368 10.1016/j.scitotenv.2009.10.061, 2010.

1369 Levetin, E., and Horner, W. E.: Fungal aerobiology: Exposure and measurement, *Fungal Allergy*
 1370 *and Pathogenicity*, 81, 10-27, 2002.

1371 Li, D. W., and Kendrick, B.: Functional-relationships between airborne fungal spores and
 1372 environmental-factors in Kitchener-Waterloo, Ontario, as detected by canonical correspondence-
 1373 analysis, *Grana*, 33, 166-176, 1994.

1374 Li, F., and Ramanathan, V.: Winter to summer monsoon variation of aerosol optical depth over
 1375 the tropical Indian Ocean, *Journal of Geophysical Research-Atmospheres*, 107,
 1376 10.1029/2001jd000949, 2002.

1377 Li, M., Qi, J., Zhang, H., Huang, S., Li, L., and Gao, D.: Concentration and size distribution of
 1378 bioaerosols in an outdoor environment in the Qingdao coastal region, *Science of the Total*
 1379 *Environment*, 409, 3812-3819, 10.1016/j.scitotenv.2011.06.001, 2011.

1380 Lyon, F. L., Kramer, C. L., and Eversmeyer, M. G.: Variation of airspora in the atmosphere due
 1381 to weather conditions, *Grana*, 23, 177-181, 1984.

1382 Madden, L. V.: Effects of rain on splash dispersal of fungal pathogens, *Canadian Journal of Plant*
 1383 *Pathology*, 19, 225-230, 1997.

1384 Maki, T., Kakikawa, M., Kobayashi, F., Yamada, M., Matsuki, A., Hasegawa, H., and Iwasaka,
 1385 Y.: Assessment of composition and origin of airborne bacteria in the free troposphere over Japan,
 1386 *Atmospheric Environment*, 74, 73-82, 10.1016/j.atmosenv.2013.03.029, 2013.

1387 Matthias-Maser, S., Obolkin, V., Khodzer, T., and Jaenicke, R.: Seasonal variation of primary
 1388 biological aerosol particles in the remote continental region of Lake Baikal/Siberia, *Atmospheric*
 1389 *Environment*, 34, 3805-3811, 10.1016/s1352-2310(00)00139-4, 2000.

1390 Matthiasmaser, S., and Jaenicke, R.: A method to identify biological aerosol-particles with radius
 1391 greater-than 0.3 μm for the determination of their size distribution, *Journal of Aerosol Science*,
 1392 22, S849-S852, 10.1016/s0021-8502(05)80232-0, 1991.

1393 Matthiasmaser, S., and Jaenicke, R.: Examination of atmospheric bioaerosol particles with radii
 1394 greater-than-0.2 μm , *Journal of Aerosol Science*, 25, 1605-1613, 10.1016/0021-8502(94)90228-
 1395 3, 1994.

1396 MatthiasMaser, S., and Jaenicke, R.: The size distribution of primary biological aerosol particles
 1397 with radii $>0.2 \mu\text{m}$ in an urban rural influenced region, *Atmospheric Research*, 39, 279-286,
 1398 10.1016/0169-8095(95)00017-8, 1995.

1399 Moehler, O., DeMott, P. J., Vali, G., and Levin, Z.: Microbiology and atmospheric processes: the
 1400 role of biological particles in cloud physics, *Biogeosciences*, 4, 1059-1071, 2007.

1401 Moorthy, K. K., Nair, P. R., and Murthy, B. V. K.: Size distribution of coastal aerosols - effects
 1402 of local-sources and sinks, *Journal of Applied Meteorology*, 30, 844-852, 10.1175/1520-
 1403 0450(1991)030<0844:sdocae>2.0.co;2, 1991.

1404 Morris, C. E., Georgakopoulos, D. G., and Sands, D. C.: Ice nucleation active bacteria and their
 1405 potential role in precipitation, *Journal De Physique Iv*, 121, 87-103, 10.1051/jp4:2004121004,
 1406 2004.

1407 Morris, C. E., Conen, F., Huffman, J. A., Phillips, V., Poeschl, U., and Sands, D. C.:
 1408 Bioprecipitation: a feedback cycle linking Earth history, ecosystem dynamics and land use
 1409 through biological ice nucleators in the atmosphere, *Global Change Biology*, 20, 341-351,
 1410 10.1111/gcb.12447, 2014.

1411 Myers, N., Mittermeier, R. A., Mittermeier, C. G., da Fonseca, G. A. B., and Kent, J.:
 1412 Biodiversity hotspots for conservation priorities, *Nature*, 403, 853-858, 10.1038/35002501, 2000.

1413 Naja, M., and Lal, S.: Surface ozone and precursor gases at Gadanki (13.5 degrees N, 79.2
 1414 degrees E), a tropical rural site in India, *Journal of Geophysical Research-Atmospheres*, 107,
 1415 10.1029/2001jd000357, 2002.

1416 Oh, J.-W., Lee, H.-B., Lee, H.-R., Pyun, B.-Y., Ahn, Y.-M., Kim, K.-E., Lee, S.-Y., and Lee, S.-
 1417 I.: Aerobiological study of pollen and mold in Seoul, Korea, *Allergology International*, 47, 263-
 1418 270, <http://dx.doi.org/10.2332/allergolint.47.263>, 1998.

1419 Oliveira, M., Amorim, M. I., Ferreira, E., Delgado, L., and Abreu, I.: Main airborne Ascomycota
 1420 spores: characterization by culture, spore morphology, ribosomal DNA sequences and enzymatic
 1421 analysis, *Applied Microbiology and Biotechnology*, 86, 1171-1181, 10.1007/s00253-010-2448-z,
 1422 2010.

1423 Pachauri, T., Singla, V., Satsangi, A., Lakhani, A., and Kumari, K. M.: Characterization of major
 1424 pollution events (dust, haze, and two festival events) at Agra, India, *Environmental Science and
 1425 Pollution Research*, 20, 5737-5752, 10.1007/s11356-013-1584-2, 2013.

1426 Pan, Y. L., Holler, S., Chang, R. K., Hill, S. C., Pinnick, R. G., Niles, S., and Bottiger, J. R.:
 1427 Single-shot fluorescence spectra of individual micrometer-sized bioaerosols illuminated by a
 1428 351- or a 266-nm ultraviolet laser, *Optics Letters*, 24, 116-118, 10.1364/ol.24.000116, 1999a.

1429 Pan, Y. L., Holler, S., Chang, R. K., Hill, S. C., Pinnick, R. G., Niles, S., Bottiger, J. R., and
 1430 Bronk, B. V.: Real-time detection and characterization of individual flowing airborne biological
 1431 particles: fluorescence spectra and elastic scattering measurements, in: *Air Monitoring and
 1432 Detection of Chemical and Biological Agents II*, edited by: Leonelli, J., and Althouse, M. L.,
 1433 *Proceedings of the Society of Photo-Optical Instrumentation Engineers (Spie)*, 117-125, 1999b.

1434 Poehlker, C., Huffman, J. A., and Poeschl, U.: Autofluorescence of atmospheric bioaerosols -
 1435 fluorescent biomolecules and potential interferences, *Atmospheric Measurement Techniques*, 5,
 1436 37-71, 10.5194/amt-5-37-2012, 2012.

1437 Poehlker, C., Huffman, J. A., Foerster, J. D., and Poeschl, U.: Autofluorescence of atmospheric
 1438 bioaerosols: spectral fingerprints and taxonomic trends of pollen, *Atmospheric Measurement
 1439 Techniques*, 6, 3369-3392, 10.5194/amt-6-3369-2013, 2013.

1440 Pöschl, U.: Atmospheric aerosols: Composition, transformation, climate and health effects,
 1441 *Angewandte Chemie-International Edition*, 44, 7520-7540, 10.1002/anie.200501122, 2005.

1442 Pöschl, U., Martin, S. T., Sinha, B., Chen, Q., Gunthe, S. S., Huffman, J. A., Borrmann, S.,
 1443 Farmer, D. K., Garland, R. M., Helas, G., Jimenez, J. L., King, S. M., Manzi, A., Mikhailov, E.,
 1444 Pauliquevis, T., Petters, M. D., Prenni, A. J., Roldin, P., Rose, D., Schneider, J., Su, H., Zorn, S.
 1445 R., Artaxo, P., and Andreae, M. O.: Rainforest Aerosols as Biogenic Nuclei of Clouds and
 1446 Precipitation in the Amazon, *Science*, 329, 1513-1516, 10.1126/science.1191056, 2010.

1447 Pranesha, T. S., and Kamra, A. K.: Scavenging of aerosol particles by large water drops .2. The
 1448 effect of electrical forces, *Journal of Geophysical Research-Atmospheres*, 102, 23937-23946,
 1449 10.1029/97jd01834, 1997a.

1450 Pranesha, T. S., and Kamra, A. K.: Scavenging of aerosol particles by large water drops .3.
 1451 Washout coefficients, half-lives, and rainfall depths, *Journal of Geophysical Research-
 1452 Atmospheres*, 102, 23947-23953, 10.1029/97jd01835, 1997b.

1453 Prenni, A. J., Petters, M. D., Kreidenweis, S. M., Heald, C. L., Martin, S. T., Artaxo, P., Garland,
 1454 R. M., Wollny, A. G., and Pöschl, U.: Relative roles of biogenic emissions and Saharan dust as
 1455 ice nuclei in the Amazon basin, *Nature Geoscience*, 2, 401-404, 2009.

1456 Prenni, A. J., Tobo, Y., Garcia, E., DeMott, P. J., Huffman, J. A., McCluskey, C. S.,
 1457 Kreidenweis, S. M., Prenni, J. E., Poehlker, C., and Pöschl, U.: The impact of rain on ice nuclei
 1458 populations at a forested site in Colorado, *Geophysical Research Letters*, 40, 227-231,
 1459 10.1029/2012gl053953, 2013.

1460 Prospero, J. M.: Mineral and sea salt aerosol concentrations in various ocean regions, *Journal of
 1461 Geophysical Research-Oceans and Atmospheres*, 84, 725-731, 10.1029/JC084iC02p00725,
 1462 1979.

1463 Prospero, J. M., Blades, E., Mathison, G., and Naidu, R.: Interhemispheric transport of viable
 1464 fungi and bacteria from Africa to the Caribbean with soil dust, *Aerobiologia*, 21, 1-19,
 1465 10.1007/s10453-004-5872-7, 2005.

1466 Quintero, E., Rivera-Mariani, F., and Bolanos-Rosero, B.: Analysis of environmental factors and
 1467 their effects on fungal spores in the atmosphere of a tropical urban area (San Juan, Puerto Rico),
 1468 *Aerobiologia*, 26, 113-124, 10.1007/s10453-009-9148-0, 2010.

1469 Raatikainen, T., Hyvarinen, A. P., Hatakka, J., Panwar, T. S., Hooda, R. K., Sharma, V. P., and
 1470 Lihavainen, H.: The effect of boundary layer dynamics on aerosol properties at the Indo-
 1471 Gangetic plains and at the foothills of the Himalayas, *Atmospheric Environment*, 89, 548-555,
 1472 10.1016/j.atmosenv.2014.02.058, 2014.

1473 Radke, L. F., Hobbs, P. V., and Eltgroth, M. W.: Scavenging of aerosol-particles by
 1474 precipitation, *Journal of Applied Meteorology*, 19, 715-722, 10.1175/1520-
 1475 0450(1980)019<0715:soapbp>2.0.co;2, 1980.

1476 Saari, S., Niemi, J. V., Ronkko, T., Kuuluvainen, H., Jarvinen, A., Pirjola, L., Aurela, M.,
 1477 Hillamo, R., and Keskinen, J.: Seasonal and Diurnal Variations of Fluorescent Bioaerosol
 1478 Concentration and Size Distribution in the Urban Environment, *Aerosol and Air Quality*
 1479 *Research*, 15, 572-581, 10.4209/aaqr.2014.10.0258, 2015.

1480 [Saari, S., Reponen, T., and Keskinen, J.: Performance of Two Fluorescence - Based Real-Time](#)
 1481 [Bioaerosol Detectors: Bioscout vs. UVAPS, *Aerosol Sci. Technol.* 48, 371-378,](#)
 1482 [10.1080/02786826.2013.877579, 2014.](#)

1483

1484 Sabariego, S., de la Guardia, C. D., and Alba, F.: The effect of meteorological factors on the
 1485 daily variation of airborne fungal spores in Granada (southern Spain), *International Journal of*
 1486 *Biometeorology*, 44, 1-5, 10.1007/s004840050131, 2000.

1487 Sadys, M., Skjoth, C. A., and Kennedy, R.: Back-trajectories show export of airborne fungal
 1488 spores (*Ganoderma* sp.) from forests to agricultural and urban areas in England, *Atmospheric*
 1489 *Environment*, 84, 88-99, 10.1016/j.atmosenv.2013.11.015, 2014.

1490 Santarpia, J. L., Ratnesar-Shumate, S., Gilberry, J. U., and Quizon, J. J.: Relationship Between
 1491 Biologically Fluorescent Aerosol and Local Meteorological Conditions, *Aerosol Sci. Technol.*,
 1492 47, 655-661, 10.1080/02786826.2013.781263, 2013.

1493 Satheesh, S. K., and Srinivasan, J.: Enhanced aerosol loading over Arabian Sea during the pre-
 1494 monsoon season: Natural or anthropogenic?, *Geophysical Research Letters*, 29,
 1495 10.1029/2002gl015687, 2002.

1496 Schumacher, C. J., Poehlker, C., Aalto, P., Hiltunen, V., Petaja, T., Kulmala, M., Poeschl, U.,
 1497 and Huffman, J. A.: Seasonal cycles of fluorescent biological aerosol particles in boreal and
 1498 semi-arid forests of Finland and Colorado, *Atmospheric Chemistry and Physics*, 13, 11987-
 1499 12001, 10.5194/acp-13-11987-2013, 2013.

1500 Sesartic, A., and Dallafior, T. N.: Global fungal spore emissions, review and synthesis of
 1501 literature data, *Biogeosciences*, 8, 1181-1192, 10.5194/bg-8-1181-2011, 2011.

1502 Shaffer, B. T., and Lighthart, B.: Survey of culturable airborne bacteria at four diverse locations
 1503 in Oregon: Urban, rural, forest, and coastal, *Microbial Ecology*, 34, 167-177,
 1504 10.1007/s002489900046, 1997.

1505 Sharma, N. K., and Rai, A. K.: Allergenicity of airborne cyanobacteria *Phormidium fragile* and
 1506 *Nostoc muscorum*, *Ecotoxicology and Environmental Safety*, 69, 158-162,
 1507 10.1016/j.ecoenv.2006.08.006, 2008.

1508 Sherman, J. P., Sheridan, P. J., Ogren, J. A., Andrews, E., Hageman, D., Schmeisser, L.,
 1509 Jefferson, A., and Sharma, S.: A multi-year study of lower tropospheric aerosol variability and
 1510 systematic relationships from four North American regions, *Atmospheric Chemistry and Physics*,
 1511 15, 12487-12517, 10.5194/acp-15-12487-2015, 2015.

1512 Shika, S., et al.: Atmospheric aerosol properties at a semi-rural location in South India: particle
 1513 size distributions and implications for cloud formation, to be submitted.

1514 Sivaprakasam, V., Huston, A. L., Scotto, C., and Eversole, J. D.: Multiple UV wavelength
 1515 excitation and fluorescence of bioaerosols, *Optics Express*, 12, 4457-4466,
 1516 10.1364/opex.12.004457, 2004.

1517 Spracklen, D. V., and Heald, C. L.: The contribution of fungal spores and bacteria to regional
 1518 and global aerosol number and ice nucleation immersion freezing rates, *Atmospheric Chemistry
 1519 and Physics*, 14, 9051-9059, 10.5194/acp-14-9051-2014, 2014.

1520 Srivastava, A., Singh, M., and Jain, V. K.: Identification and characterization of size-segregated
 1521 bioaerosols at Jawaharlal Nehru University, New Delhi, *Natural Hazards*, 60, 485-499,
 1522 10.1007/s11069-011-0022-3, 2012.

1523 Tarlo, S. M., Bell, B., Srinivasan, J., Dolovich, J., and Hargreave, F. E.: Human sensitization to
 1524 ganoderma antigen, *Journal of Allergy and Clinical Immunology*, 64, 43-49, 10.1016/0091-
 1525 6749(79)90082-4, 1979.

1526 Tong, Y and Lighthart, B.: Diurnal Distribution of Total and Culturable Atmospheric Bacteria at
 1527 a Rural Site, *Aerosol Sci. Technol.*, 30, 246-254, 10.1080/027868299304822, 1999.

1528 Toprak, E., and Schnaiter, M.: Fluorescent biological aerosol particles measured with the
 1529 Waveband Integrated Bioaerosol Sensor WIBS-4: laboratory tests combined with a one year
 1530 field study, *Atmospheric Chemistry and Physics*, 13, 225-243, 10.5194/acp-13-225-2013, 2013.

1531 Trejo, M., Douarche, C., Bailleux, V., Poulard, C., Mariot, S., Regeard, C., and Raspaud, E.:
 1532 Elasticity and wrinkled morphology of *Bacillus subtilis* pellicles, *Proceedings of the National
 1533 Academy of Sciences of the United States of America*, 110, 2011-2016,
 1534 10.1073/pnas.1217178110, 2013.

1535 Troutt, C., and Levetin, E.: Correlation of spring spore concentrations and meteorological
1536 conditions in Tulsa, Oklahoma, *International Journal of Biometeorology*, 45, 64-74,
1537 10.1007/s004840100087, 2001.

1538 Valsan, A. E., Priyamvada, H., Ravikrishna, R., Després, V. R., Biju, C. V., Sahu, L. K., Kumar,
1539 A., Verma, R. S., Philip, L., and Gunthe, S. S.: Morphological characteristics of bioaerosols from
1540 contrasting locations in southern tropical India – A case study, *Atmospheric Environment*, 122,
1541 321-331, <http://dx.doi.org/10.1016/j.atmosenv.2015.09.071>, 2015.

1542 Vinoj, V., and Satheesh, S. K.: Measurements of aerosol optical depth over Arabian Sea during
1543 summer monsoon season, *Geophysical Research Letters*, 30, 10.1029/2002gl016664, 2003.

1544 Vinoj, V., Satheesh, S. K., and Moorthy, K. K.: Optical, radiative, and source characteristics of
1545 aerosols at Minicoy, a remote island in the southern Arabian Sea, *Journal of Geophysical*
1546 *Research-Atmospheres*, 115, 10.1029/2009jd011810, 2010.

1547 Vinoj, V., Rasch, P. J., Wang, H., Yoon, J.-H., Ma, P.-L., Landu, K., and Singh, B.: Short-term
1548 modulation of Indian summer monsoon rainfall by West Asian dust, *Nature Geoscience*, 7, 308-
1549 313, 10.1038/ngeo2107, 2014.

1550 Wang, C.-C., Fang, G.-C., and Lee, L.: Bioaerosols study in central Taiwan during summer
1551 season, *Toxicology and Industrial Health*, 23, 133-139, 10.1177/0748233707078741, 2007.

1552 Yu, X., Wang, Z., Zhang, M., Kuhn, U., Xie, Z., Cheng, Y., Pöschl, U., and Su, H.: Ambient
1553 measurement of fluorescent aerosol particles with a WIBS in the Yangtze River Delta of China:
1554 potential impacts of combustion-generated aerosol particles, *Atmos. Chem. Phys. Discuss.*,
1555 doi:10.5194/acp-2016-228, in review, 2016.

1556 Zhang, T., Engling, G., Chan, C.-Y., Zhang, Y.-N., Zhang, Z.-S., Lin, M., Sang, X.-F., Li, Y. D.,
1557 and Li, Y.-S.: Contribution of fungal spores to particulate matter in a tropical rainforest,
1558 *Environmental Research Letters*, 5, 10.1088/1748-9326/5/2/024010, 2010.

1559

1560

1561 Table 1: List of frequently used acronyms and symbols with units.

1562

1563

Symbol	Quantity, Unit	
D_a	Aerodynamic diameter, μm	1564
D_g	Geometric midpoint diameter of fluorescent particles	1565
$D_{g,T}$	Geometric midpoint diameter of total particles	1566
DNA	Deoxyribonucleic acid	
FBAP	Fluorescent biological aerosol particle	1567
He-Ne	Helium-Neon	1568
ITCZ	Inter Tropical Convergence Zone	
Lpm	Liters per minute	1569
M_F	Integrated mass concentration of fluorescent particles, $\mu\text{g m}^{-3}$	
M_T	Integrated mass concentration of total particles, $\mu\text{g m}^{-3}$	1570
Nd:YAG	Neodymium-doped yttrium Aluminum garnet	1571
NE	Northeast	
N_F	Integrated number concentration of fluorescent particles, cm^{-3}	1572
N_T	Integrated number concentration of total particles, cm^{-3}	1573
PAH	Polycyclic aromatic hydrocarbon	
PBAPs	Primary Biological Aerosol Particles	1574
RH	Relative Humidity	1575
SEM	Scanning Electron Microscopy	
SW	Southwest	1576
TAP	Total Aerosol Particle	
TSP	Total Suspended Particle	1577
UV-APS	Ultraviolet Aerodynamic Particle Sizer	1578
λ	Wavelength, nm	

1579

Formatted: Font: Not Italic

1580

1581

1582

1583

1584

1585

1586

1587

1588

Number		June	July	August	Campaign
N_T (cm ⁻³)	Mean	2.66	1.54	0.96	1.77
	Median	2.45	1.48	0.73	1.44
N_F (cm ⁻³)	Mean	0.03	0.007	0.015	0.017
	Median	0.02	0.006	0.007	0.01
N_F/N_T (%)	Mean	0.03	0.01	0.03	0.02
	Median	0.01		0.01	0.01
Mass		June	July	August	Campaign
M_T (μg m ⁻³)	Mean	10.61	6.15	4.15	7.17
	Median	9.58	5.55	2.8	5.57
M_F (μg m ⁻³)	Mean	0.42	0.11	0.18	0.24
	Median	0.33	0.09	0.1	0.15
M_F/M_T (%)	Mean	0.09	0.03	0.08	0.06
	Median	0.04	0.02	0.03	0.03

1589

1590 Table 2: Integrated number concentrations and mass concentrations of coarse TAP and FBAP (~1–20 μm):
 1591 arithmetic mean and median for each month and for the entire measurement campaign
 1592

1593

1594

1595

1596

1597

1598

1599

1600

1601

Sl No:	Location	Land Use	Meaurement Period	Season	Instrument	FBAP Number Concentration	Total Number Concentration	Number Ratio (%)	Reference
1	Mainz, Central Europe	Semi-urban	Aug-Dec, 2006		UVAPS	$3 \times 10^{-2} \text{ cm}^{-3}$	1.05 cm^{-3}	4	Huffman et al., 2010
2	Central Amazonia rainforest	Tropical rainforest	Feb-Mar, 2008		UVAPS	$7.3 \times 10^{-2} \text{ cm}^{-3}$	0.33 cm^{-3}	24	Huffman et al., 2012
3	Manchester, UK	Urban	December, 2009		WIBS-3	$2.9 \times 10^{-4} \text{ cm}^{-3}$ (FL1)	$1.38 \times 10^{-2} \text{ cm}^{-3}$	2.1	Gabey et al., 2011
						$5.2 \times 10^{-4} \text{ cm}^{-3}$ (FL2)		3.7	
						$1.1 \times 10^{-5} \text{ cm}^{-3}$ (FL3)		7.8	
4	Central France	Rural	22 Jun-3 July, 2010		WIBS-3	$1.2 \times 10^{-2} \text{ cm}^{-3}$ (280 nm)			Gabey et al., 2013
						$9.5 \times 10^{-2} \text{ cm}^{-3}$ (370 nm)			
5	Helinski, Finland	Urban	Feb, 2012 (Winter)	Winter	BioScout	$1 \times 10^{-2} \text{ cm}^{-3}$		23	Saari et al., 2015
			June-Aug, 2012 (Summer)	Summer		$2.8 \times 10^{-2} \text{ cm}^{-3}$		6	
				Summer	UVAPS	$1.3 \times 10^{-2} \text{ cm}^{-3}$		8	
6	Colarado, USA	Pine forest	June-July, 2011	Dry period	WIBS-3			5.8	Crawford et al., 2014
				Wet Period	WIBS-4			15.2	
7	Finland	Rural forest	August, 2009 - April, 2011	Spring	UVAPS	$1.5 \times 10^{-2} \text{ cm}^{-3}$	0.43 cm^{-3}	4.4	Schumacher et al., 2013
				Summer		$4.6 \times 10^{-2} \text{ cm}^{-3}$	0.45 cm^{-3}	13	
				Fall		$2.7 \times 10^{-2} \text{ cm}^{-3}$	0.41 cm^{-3}	9.8	
				Winter		$0.4 \times 10^{-2} \text{ cm}^{-3}$	0.47 cm^{-3}	1.1	

	Colorado , USA	Rural, semi-arid	2011-2012	Spring	UVAPS	$1.5 \times 10^{-2} \text{ cm}^{-3}$	0.73 cm^{-3}	2.5	
				Summer		$3 \times 10^{-2} \text{ cm}^{-3}$	0.44 cm^{-3}	8.8	
				Fall		$1.7 \times 10^{-2} \text{ cm}^{-3}$	0.28 cm^{-3}	5.7	
				Winter		$0.53 \times 10^{-2} \text{ cm}^{-3}$	0.2 cm^{-3}	3	
8	Karlsruhe, Germany	Semi-rural	April 2010 - April 2011		WIBS - 4	$3.1 \times 10^{-2} \text{ cm}^{-3}$	0.583 cm^{-3}	7.34	Toprak and Schnaiter., 2013
9	Nanjing, China	Sub-urban	Oct-Nov, 2013	Autumn	WIBS-4		13.1 cm^{-3}		Yu et al., 2016
						0.6 cm^{-3} (FL1)		4.6	
						3.4 cm^{-3} (FL2)		25.3	
						2.1 cm^{-3} (FL3)		15.6	

1602

1603 Table 3: Comparison with other online measurements carried out under various environmental conditions across the globe.

Number		Dusty	Clean	HighBio
N_T (cm ⁻³)	Mean	4.2	1.27	1.78
	Median	4.36	1.15	1.4
N_F (cm ⁻³)	Mean	0.02	0.005	0.05
	Median	0.019	0.004	0.038
N_F/N_T	Mean	0.01	0.01	0.05
	Median			0.03
Mass		Dusty	Clean	HighBio
M_T (μg m ⁻³)	Mean	16.34	5.12	7.7
	Median	16.84	4.28	5.85
M_F (μg m ⁻³)	Mean	0.36	0.08	0.58
	Median	0.33	0.05	0.47
M_F/M_T	Mean	0.02	0.03	0.12
	Median	0.02	0.01	0.08

Table 4: Integrated number concentrations and mass concentrations of coarse TAP and FBAP (~1–20 μm): arithmetic mean and median for each focus period (Dusty, Clean and HighBio).

	Campaign			Dusty			Clean			High Bio		
	N_T	N_F	N_F/N_T	N_T	N_F	N_F/N_T	N_T	N_F	N_F/N_T	N_T	N_F	N_F/N_T
RH	-0.64	0.58	0.85	-0.25		0.18	-0.66	-0.01	0.13	-0.64	0.5	0.68
Temperature	0.45	-0.65	-0.82	0.34	-0.04	-0.25	0.78	0.02	-0.2	0.43	-0.68	-0.83
Wind Speed	0.4	-0.6	-0.78	0.09	-0.18	-0.31	-0.18	-0.27	0	0.3	-0.61	-0.74

Table 5: R^2 values for correlation between meteorological parameters (RH, Temperature and Wind Speed) and N_T , N_F and N_F/N_T during the entire campaign and each focus periods.

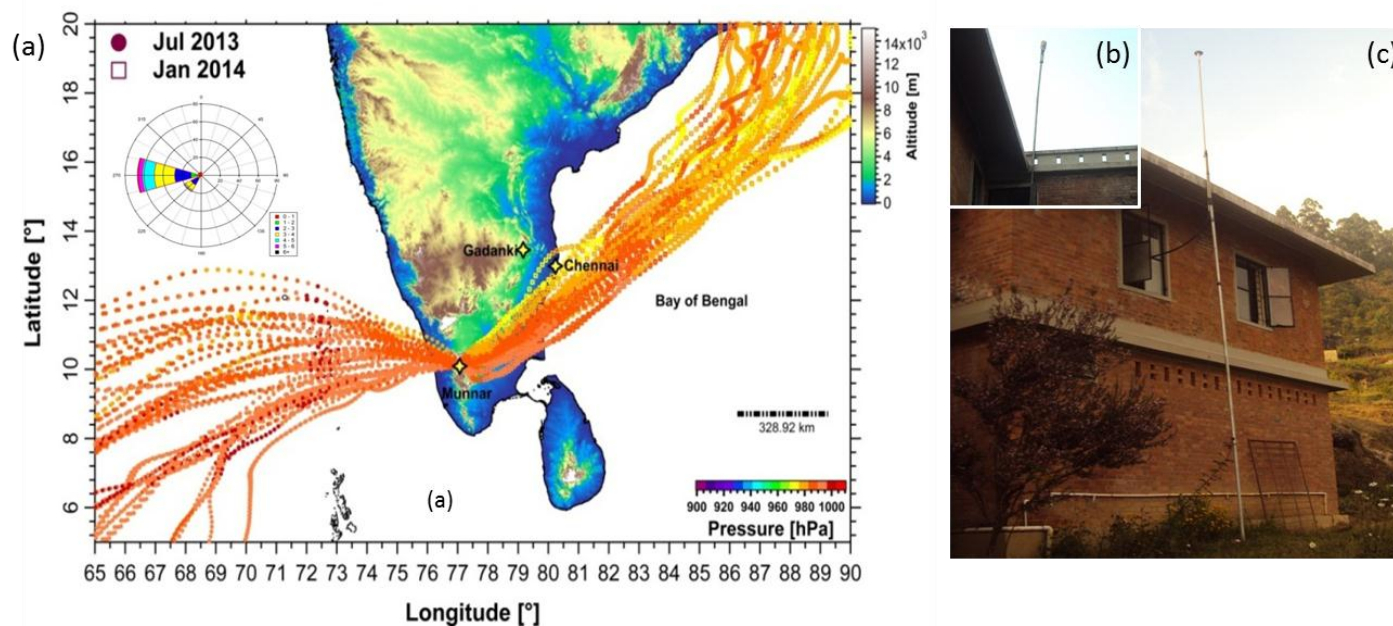
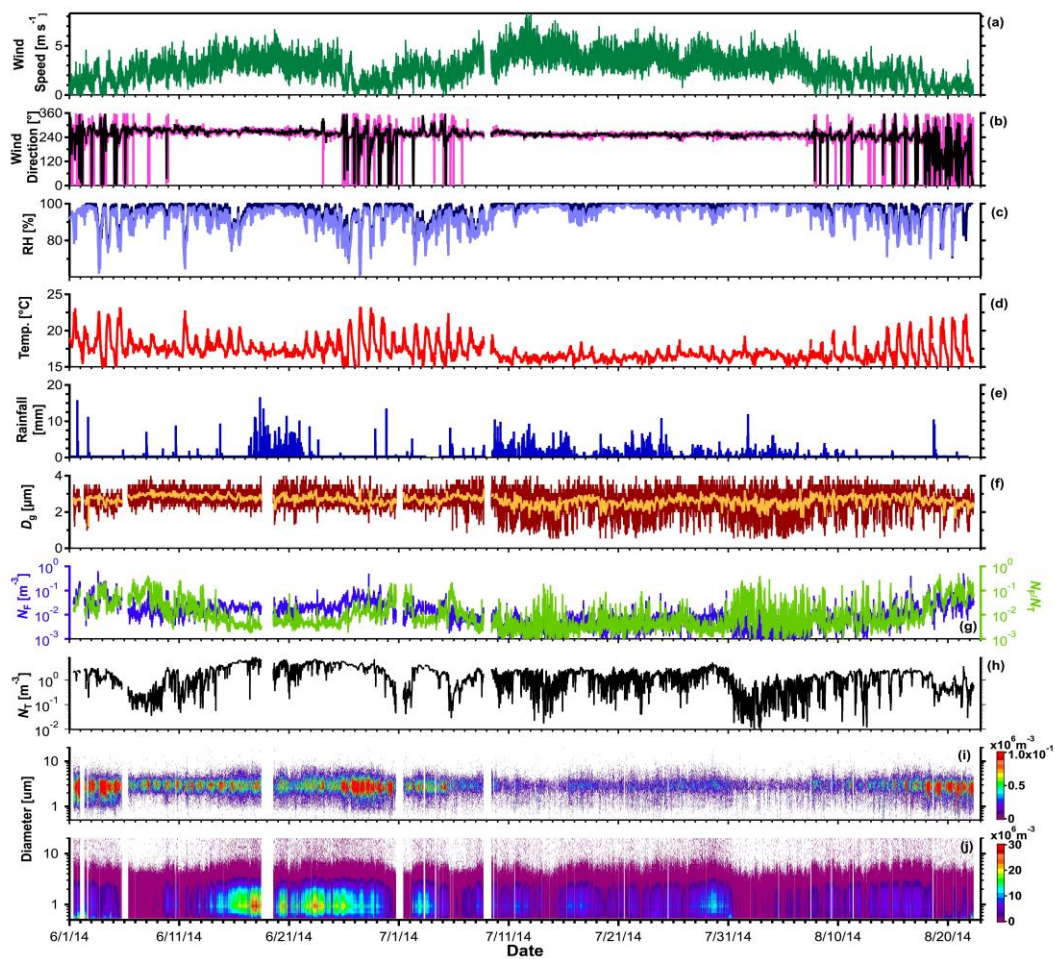


Figure 1: Location of measurement site Munnar (10.09°N, 77.06°E; 1605 m amsl – above mean sea level) located in the Western Ghat mountain range in Southern tropical India with 10 days back trajectories (HYSPLIT, NOAA-ARL GDAS1 model; start height 50 m above ground level; starting time 23:30 local time) illustrating the distinct and contrasting wind patterns during two contrasting seasons; Southwest monsoon season (representative month Jul) and [Winter Northeast monsoon](#)-season (representative month Jan) when field measurement campaigns ~~were~~ [were](#) carried out. It is evident that predominant wind pattern during Southwest monsoon season was Westerly/Southwesterly bringing the clean marine influx [as also evident from the windrose diagram shown in inset\(a\).](#) [The meteorological parameters were recorded using the weather station installed close to the inlet system \(b\).](#) ~~Also shown in inset is wind rose diagram prepared using the data obtained using the ultrasonic weather station (a).~~ The inlet system prepared for sampling the air using Ultraviolet Aerodynamic Particle Sizer (UV-APS) for bioaerosol number size distribution measurement [\(c\).](#) ~~Inset shows the arrangement made for installing the ultrasonic weather station (b).~~ The map shown is color-coded by topography (meters) [and trajectories are color-coded by atmospheric pressure level \(hPa\).](#)



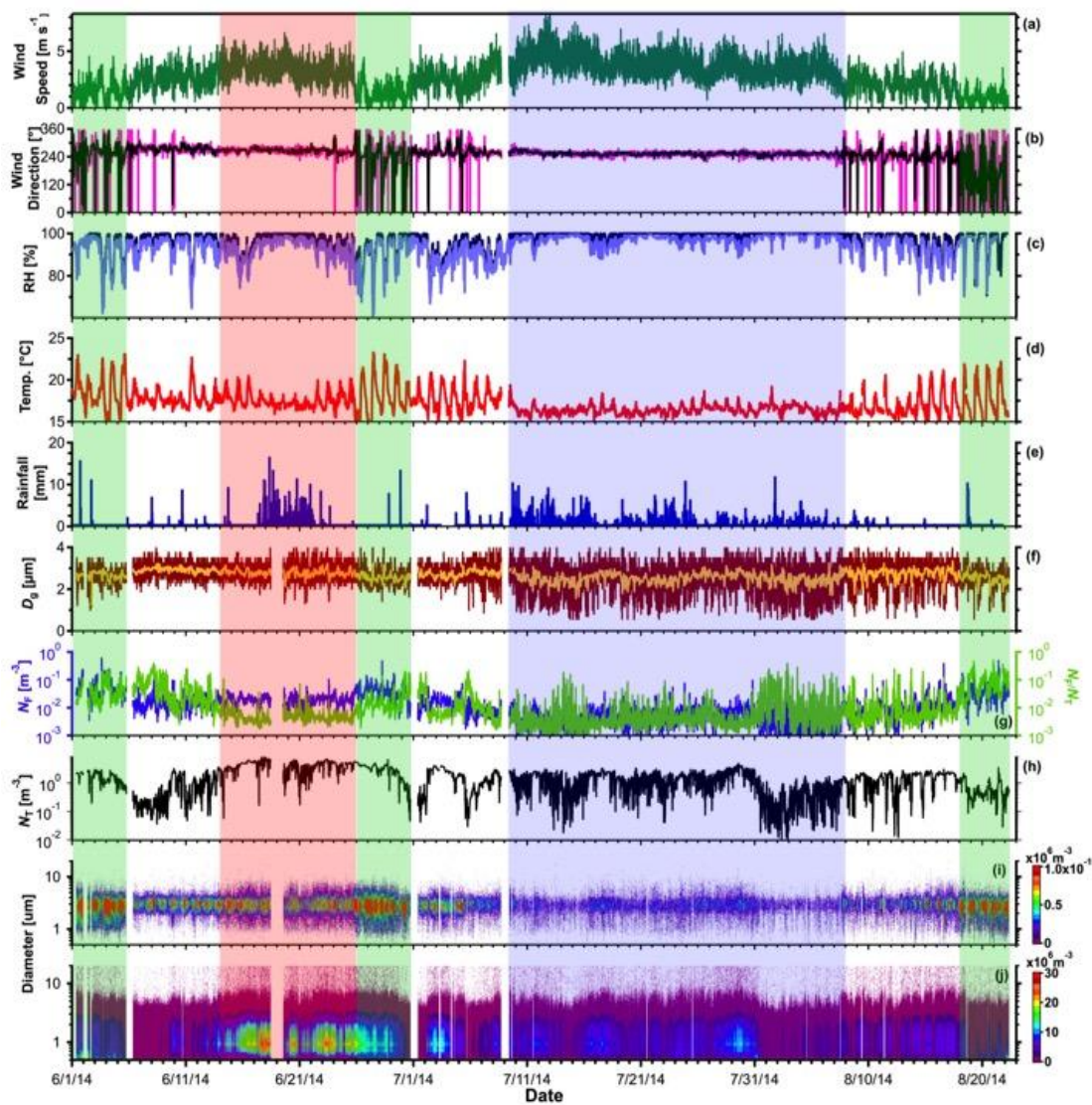


Figure 2: Time series of measured meteorological parameters, parameters derived from FBAP and total particle number size distribution measurements using UV-APS: (a) wind speed, (b) wind direction: five minutes average (magenta) and one hour average (black), (c) relative humidity, (d) temperature, (e) rainfall, (f) geometric mean diameter (D_g) five minutes average (dark red) and one hour average (yellow), (g) FBAP number concentration (N_F ; blue) and relative contribution of FBAP to TAP (N_F/N_T ; green), (h) TAP number concentration (N_T), (i) a contour plot of FBAP number size distribution ($dN/d\log D_F$), and (j) a contour plot of TAP number size distribution ($dN/d\log D_T$). The shadowed block represents the different focus periods (red for dusty; green for high bio; blue for clean; please refer to text for more details).

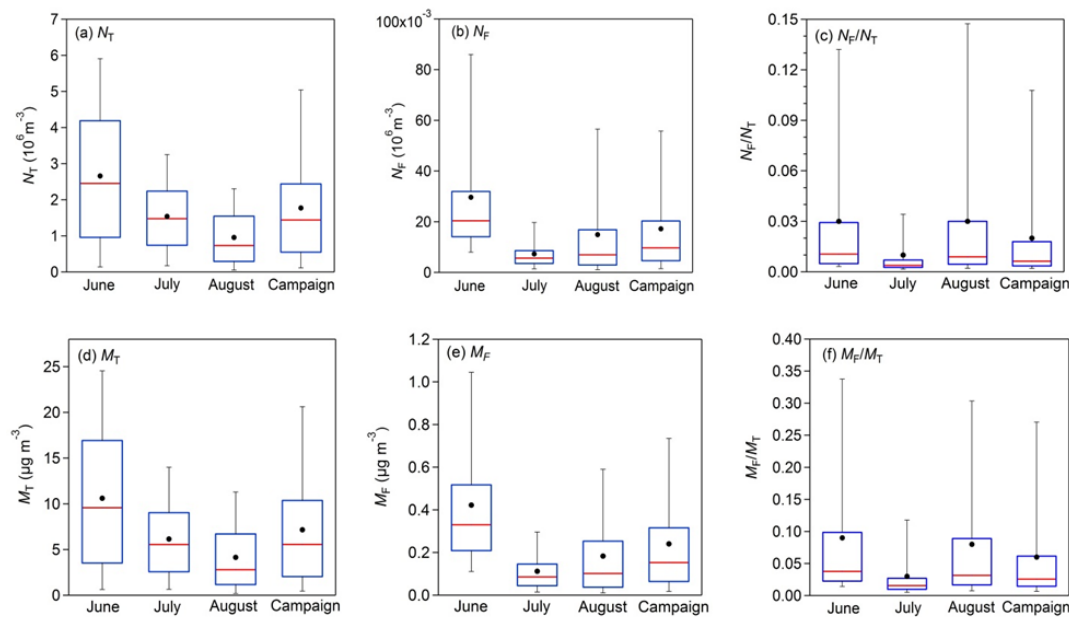


Figure 3: Statistical distribution of integrated ($\sim 1 - 20 \mu\text{m}$) FBAP and TAP number and mass and their ratios measured during each month (Jun – Aug) of SW monsoon season and averaged over the entire measurement campaign carried out at Munnar as box whisker plots: (a) TAP number concentration (N_T), (b) FBAP number concentration (N_F), (c) contribution of FBAP number concentration to TAP number concentration (N_F/N_T), (d) TAP mass concentration (M_T), (e) FBAP mass concentration (M_F) and (f) contribution of FBAP to TAP mass concentration (M_F/M_T).

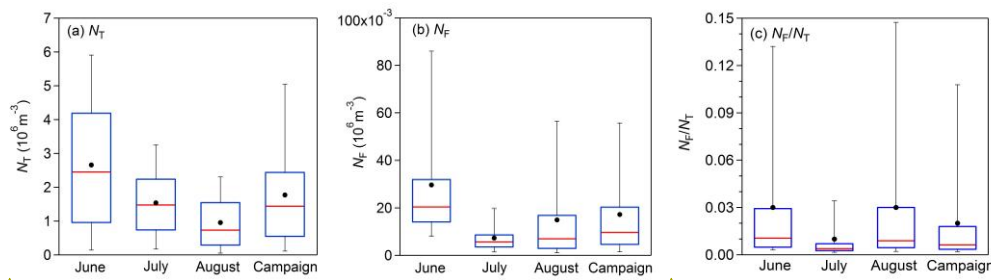
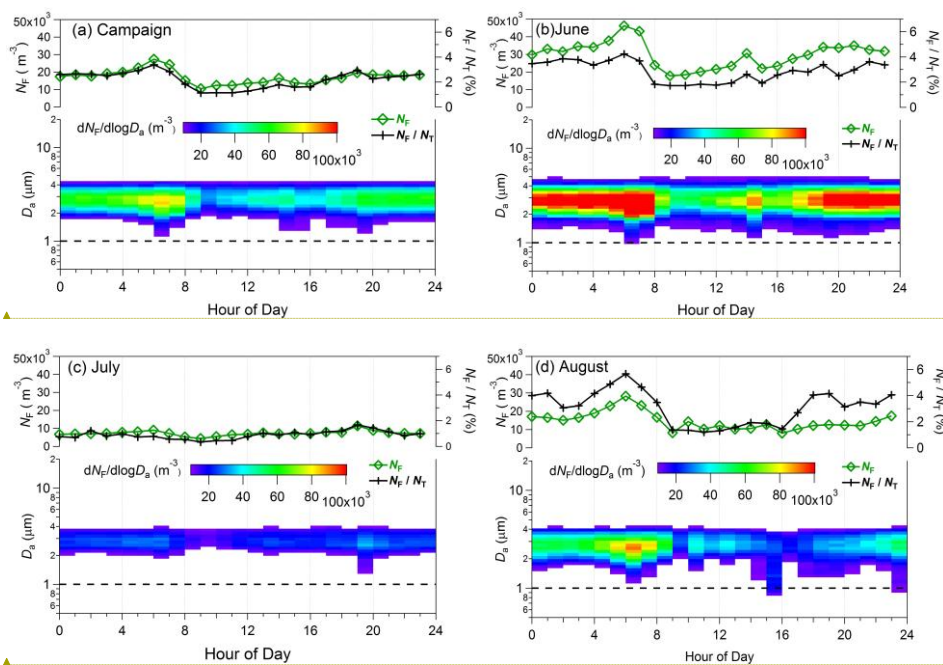


Figure 3: Statistical distribution of integrated ($< 1 - 20 \mu\text{m}$) FBAP and TAP number and contribution of N_F to N_T measured during each month (Jun—Aug) of SW monsoon season and averaged over the entire measurement campaign carried out at Munnar as box whisker plots: (a) TAP number concentration (N_T), (b) FBAP number concentration (N_F), and (c) contribution of FBAP number concentration to TAP number concentration (N_F/N_T).

Formatted: Font: (Default) Times New Roman, 0 pt, Font color: Black, Character scale: 0%, Border: : (No border), Pattern: Clear (Black)

Formatted: Font: (Default) Times New Roman, 0 pt, Font color: Black, Character scale: 0%, Border: : (No border), Pattern: Clear (Black)



Formatted: Font: 10 pt, Bold

Formatted: Font: 10 pt, Bold

Figure 4: Diurnal cycles of FBAP number concentrations (N_T) and size distributions averaged over individual month of measurement and entire campaign (hourly median values plotted against the local time of the day). Upper portion of each panel shows integrated FBAP number concentration (N_T) on the left axis (green color) and FBAP fraction of TAP number (N_T/N_T) on the right axis (black color). Lower portion of each panel FBAP number size distribution (3-D plot) plotted against hour of the day on x axis, aerodynamic diameter on y axis and color is scaled for $dN_T/d\log D_a$ indicates the concentration. Dashed black lines in lower portion of the each panel at $1.0 \mu\text{m}$ shows the particle size cut-off diameter below which fluorescent particles were not considered as FBAP due to potential interference with non-biological aerosol particles. (a) averaged over entire campaign, (b) Jun, (c) Jul, and (d) Aug. Please refer to supplementary Figs. for corresponding TAP plots.

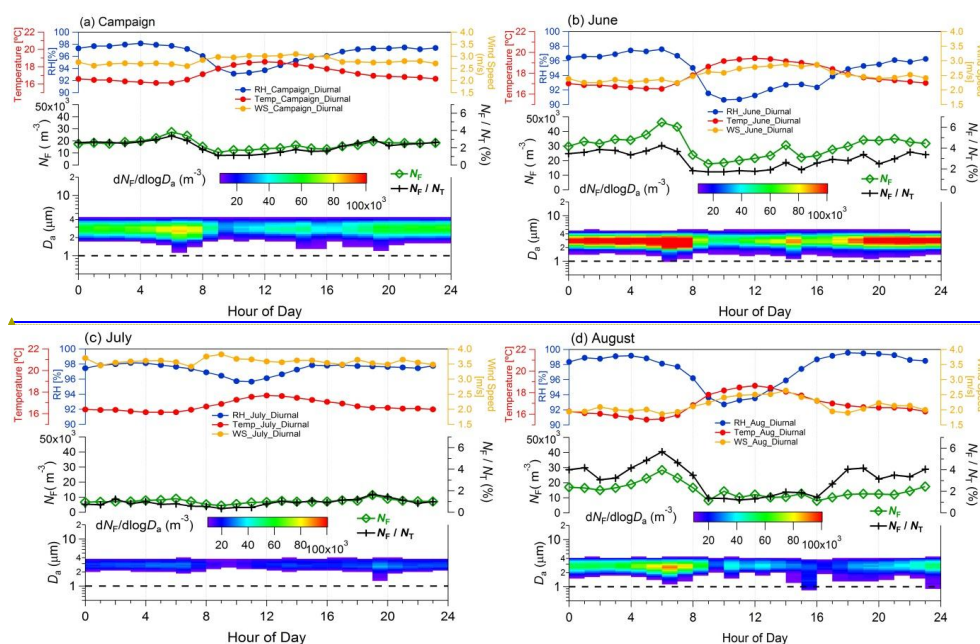


Figure 4: Diurnal cycles of observed meteorological parameters, FBAP number concentrations (N_F) and size distributions averaged over individual month of measurement and entire campaign (hourly mean values plotted against the local time of the day). Upper portion of each panel shows the observed meteorological parameters: relative humidity (%; blue), temperature ($^{\circ}C$; red), and wind speed ($m s^{-1}$; orange on right axis). Middle panel shows integrated FBAP number concentration ($\sim 1 - 20 \mu m$; N_F) on the left axis (green color) and FBAP fraction of TAP number (N_F/N_T) on the right axis (black color). Lower portion of each panel FBAP number size distribution (3-D plot) plotted against hour of the day on x-axis, aerodynamic diameter on y-axis and color is scaled for $dN_F/d\log D_a$. Dashed black lines in lower portion of the each panel at $1.0 \mu m$ shows the particle size cut-off diameter below which fluorescent particles were not considered as FBAP due to potential interference with non-biological aerosol particles. (a) averaged over entire campaign, (b) Jun, (c) Jul, and (d) Aug. Please refer to supplementary Figs. for corresponding TAP plots.

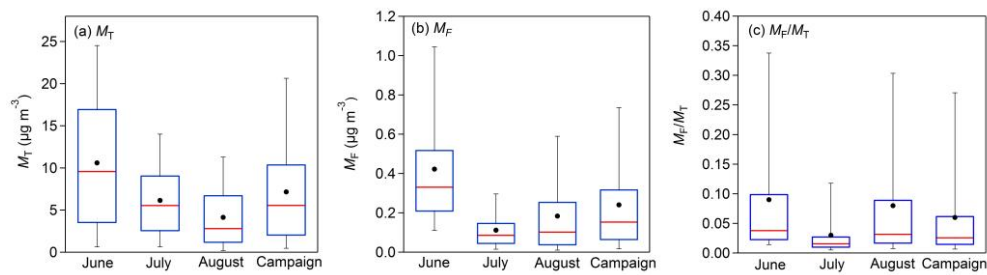
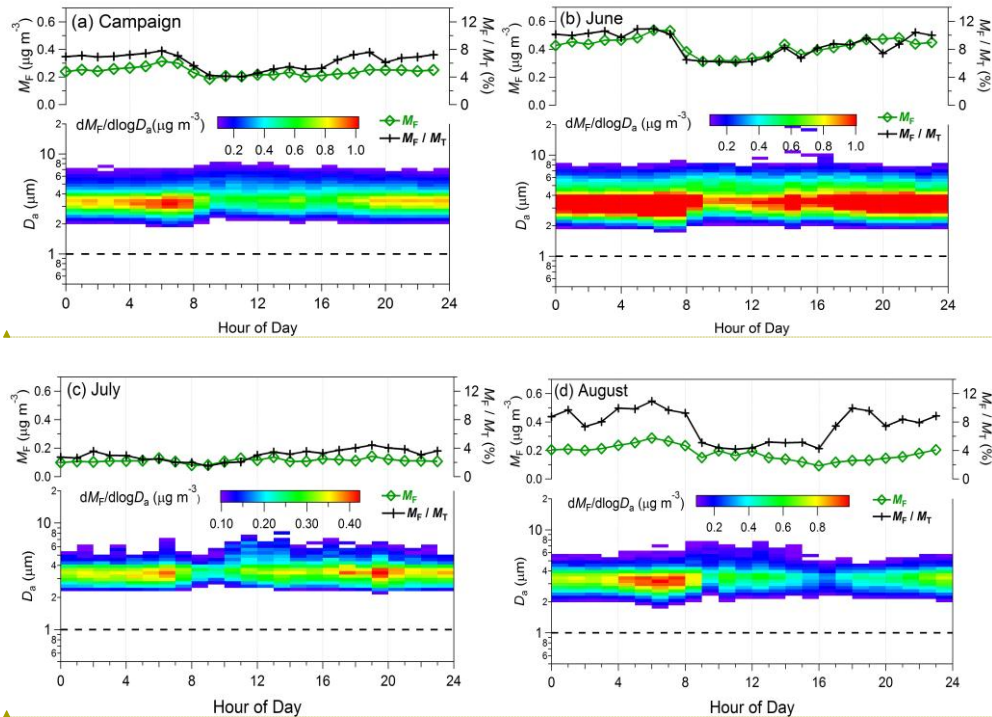


Figure 5: Same as Fig. 3 but for integrated ($< 1 - 20 \mu\text{m}$) FBAP (M_T) and TAP (M_F) mass concentrations derived from number measurements by assuming unit density and shape factor.

Formatted: Font: (Default) Times New Roman, 0 pt, Font color: Black, Character scale: 0%, Border: : (No border), Pattern: Clear (Black)

Formatted: Font: (Default) Times New Roman, 0 pt, Font color: Black, Character scale: 0%, Border: : (No border), Pattern: Clear (Black)

Formatted: Font: (Default) Times New Roman, 0 pt, Font color: Black, Character scale: 0%, Border: : (No border), Pattern: Clear (Black)



Formatted: Font: 10 pt, Bold

Formatted: Font: 10 pt, Bold

Figure 6: Same as Fig. 4 but representing the FBAP (M_F) mass concentrations.

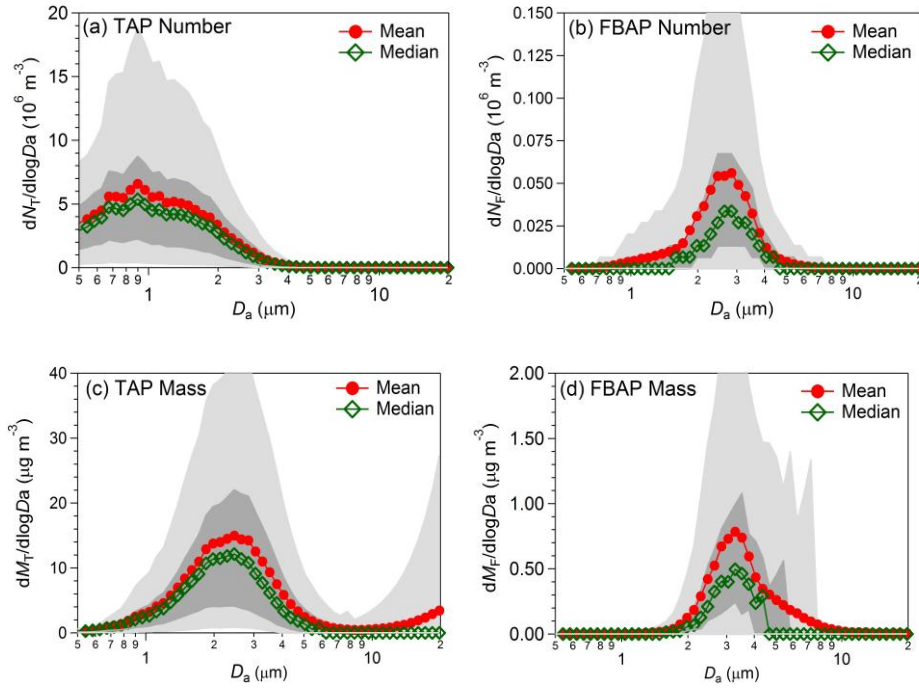


Figure 57: Particle number size and unit-normalized number size and mass size distributions averaged over the entire measurement campaign carried out at Munnar. Lower and upper parts of dark and light shaded area represents the 5th, 25th, 75th, and 95th percentile respectively. (a) TAP number ($dN_T/d\log D_a$), (b) FBAP number ($dN_F/d\log D_a$), (c) total mass ($dM_T/d\log D_a$), and (d) FBAP mass ($dM_F/d\log D_a$).

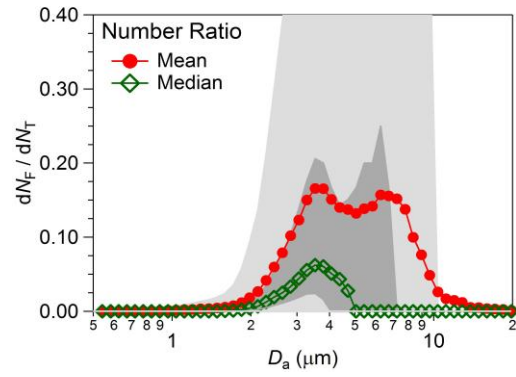


Figure 68: Size distribution of FBAP to TAP ratio averaged over the entire measurement period carried out at Munnar ($dN_F/d\log D_a = dM_F/d\log D_a$). Lower and upper parts of dark and light shaded area represents the 5th, 25th, 75th, and 95th percentile respectively.

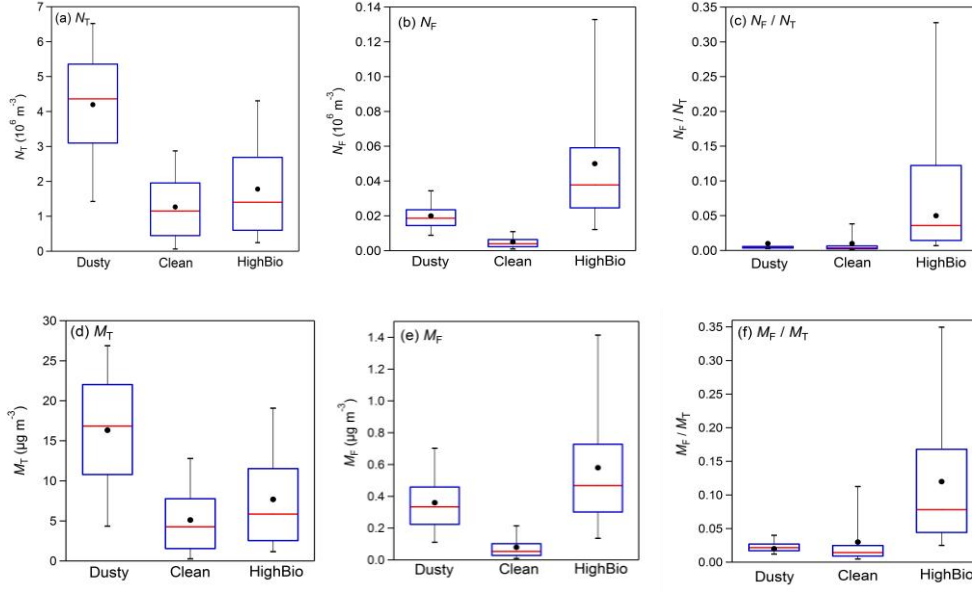
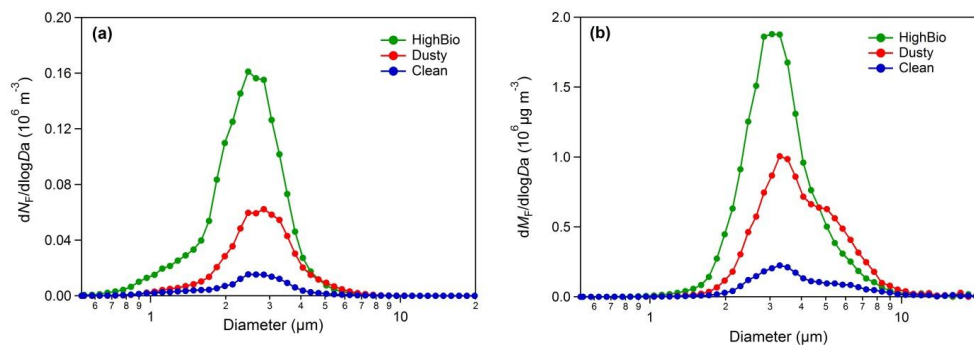
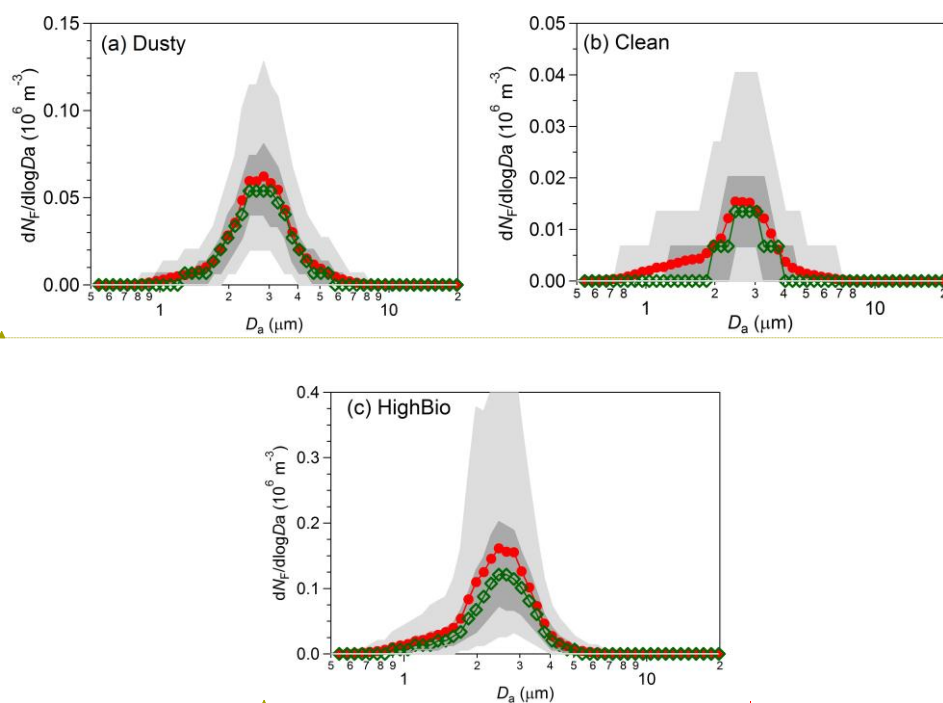


Figure 79: Statistical distribution of integrated ($\sim 1 - 20 \mu\text{m}$) FBAP and TAP number and mass contribution of N_F to N_T , and M_F to M_T averaged over each distinct focus periods (dusty, clean, and high bio; please refer to the text for definitions related to each focus period) measurements carried out at Munnar as box whisker plots: (a) TAP number concentration (N_T), (b) FBAP number concentration (N_F), (c) contribution of FBAP number concentration to TAP number concentration (N_F/N_T), (d) TAP mass concentration (M_T), (e) FBAP mass concentration (M_F), and (f) contribution of FBAP mass concentration to TAP mass concentration (M_T/M_F).



Formatted: Font: 10 pt, Bold

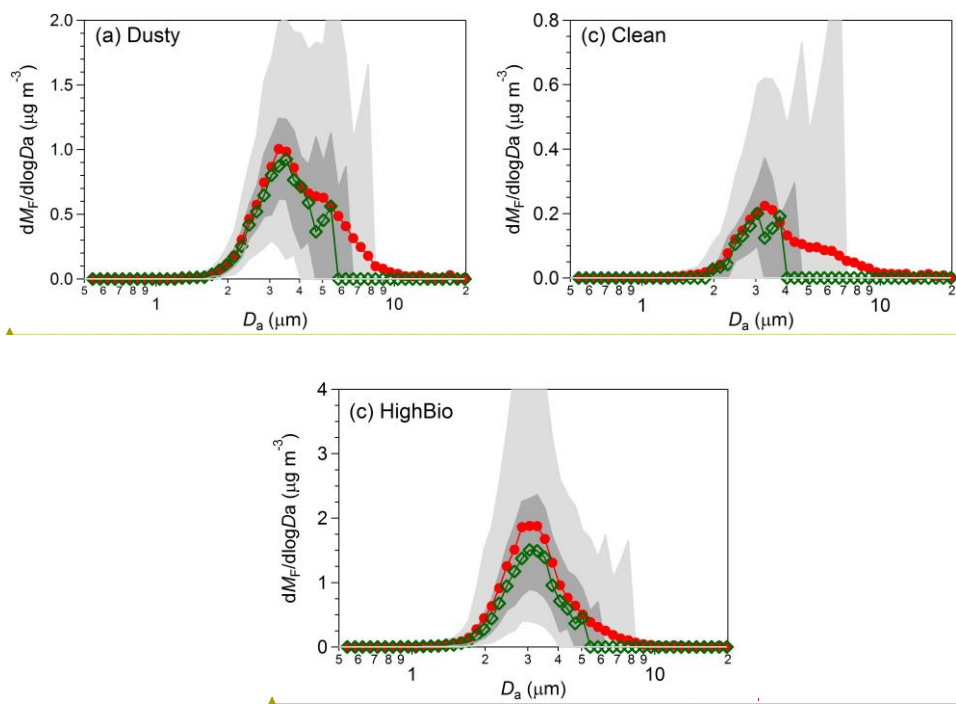
Figure 8: FBAP number size distributions ($dN_F/d\log D_a$) and mass size distribution ($dM_F/d\log D_a$) averaged over each distinct focus periods during the measurement campaign carried out at Munnar.



Formatted: Font: 10 pt, Bold

Formatted: Font: 10 pt, Bold

Figure 10: FBAP number size distributions ($dN_F/d\log D_a$) averaged over each distinct focus periods during the measurement campaign carried out at Munnar. Lower and upper parts of dark and light shaded area represents the 5th, 25th, 75th, and 95th percentile respectively. (a) dusty period, (b) clean period, and (c) high bio period.



Formatted: Font: 10 pt, Bold

Formatted: Font: 10 pt, Bold

Figure 11: Same as Fig. 10 but representing PBAP mass size distribution ($dM_F/d\log D_a$).

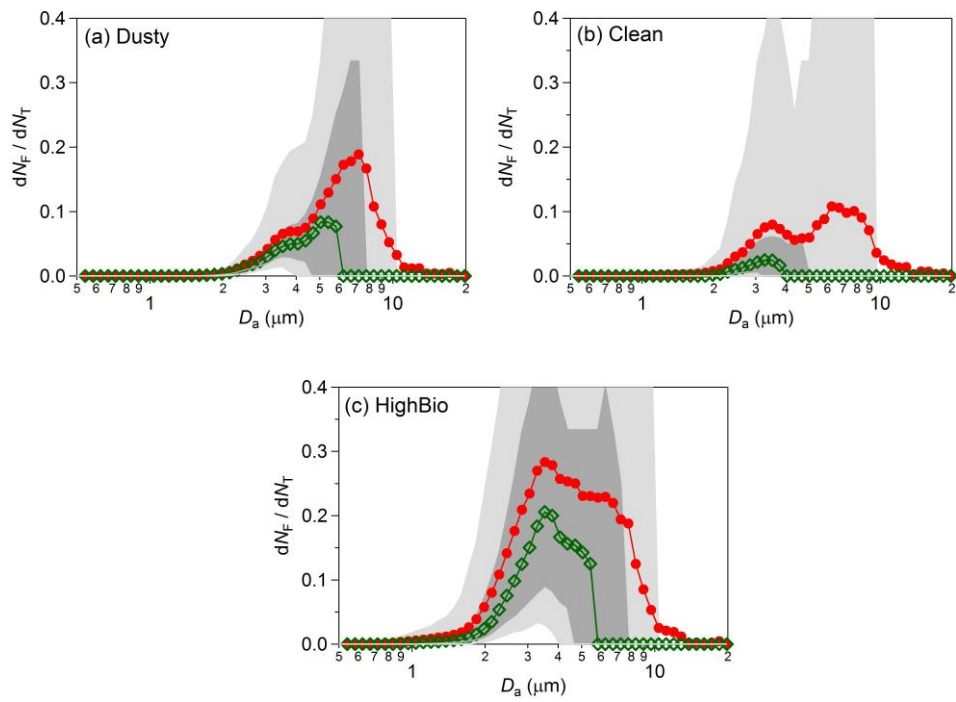
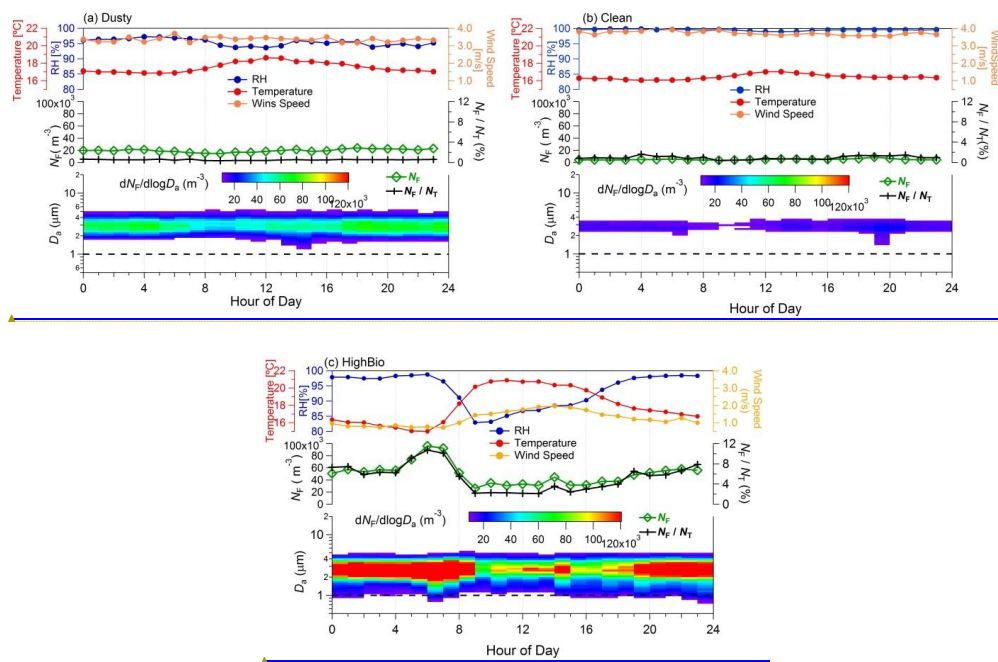


Figure 2+2: Size distribution of FBAP to TAP ratio averaged over the each distinct focus periods during the measurements carried out at Munnar ($dN_F/d\log D_a = dM_F/d\log D_a$). Lower and upper parts of dark and light shaded area represents the 5th, 25th, 75th, and 95th percentile respectively: (a) dusty, (b) clean, and (c) high bio.

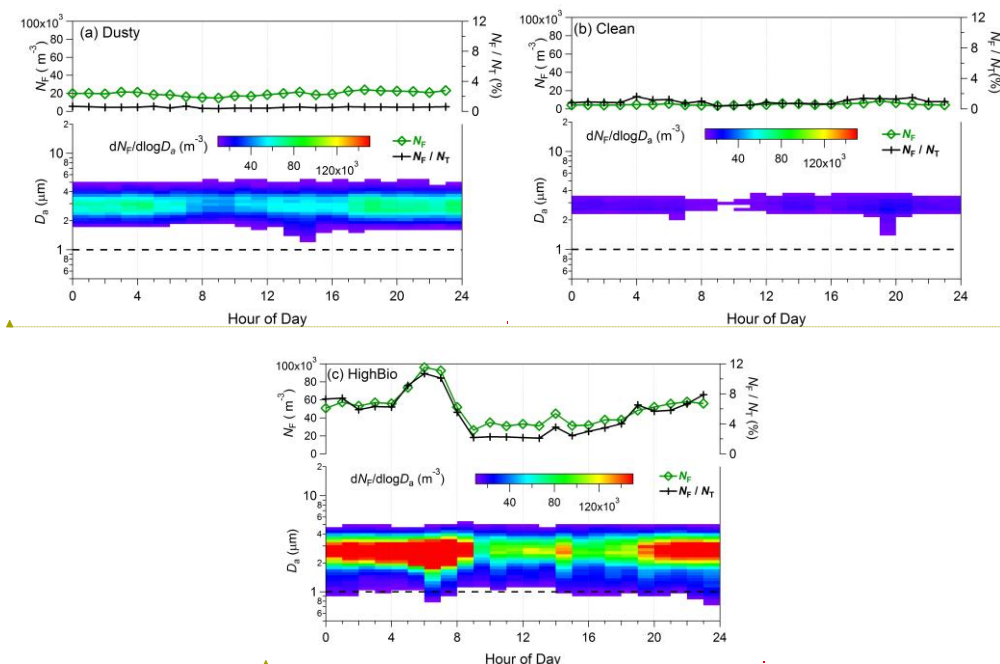


Formatted: Font: 10 pt, Bold

Formatted: Font: 10 pt

Formatted: Centered

Figure 10: Diurnal cycles of observed meteorological parameters, FBAP number concentrations (N_F) and size distributions averaged over each distinct focus period identified during measurements carried out at Munnar (hourly mean values plotted against the local time of the day). Upper portion of each panel shows the observed meteorological parameters: relative humidity (%; blue), temperature ($^{\circ}\text{C}$; red), and wind speed (m s^{-1} ; orange on right axis). Middle panel shows integrated FBAP number concentration ($\sim 1 - 20 \mu\text{m}$; N_F) on the left axis (green color) and FBAP fraction of TAP number (N_F/N_T) on the right axis (black color). Lower portion of each panel FBAP number size distribution (3-D plot) plotted against hour of the day on x-axis, aerodynamic diameter on y-axis and color is scaled for $dN_F/d\log D_a$ indicates the concentration. Dashed black lines in lower portion of the each panel at $1.0 \mu\text{m}$ shows the particle size cut-off diameter below which fluorescent particles were not considered as FBAP due to potential interference with non-biological aerosol particles. (a) dusty (b) clean, and (c) high bio. Please refer to supplementary Figs. for corresponding TAP plots.



Formatted: Font: 10 pt, Bold

Formatted: Font: 10 pt

Figure 13: Diurnal cycles of FBAP number concentrations (N_f) and size distributions averaged over each distinct focus period identified during measurements carried out at Munnar (hourly median values plotted against the local time of the day). Upper portion of each panel shows integrated FBAP number concentration ($\sim 1-20 \mu\text{m}$; N_f) on the left axis (green color) and FBAP fraction of TAP number (N_f/N_t) on the right axis (black color). Lower portion of each panel FBAP number size distribution (3-D plot) plotted against hour of the day on x axis, aerodynamic diameter on y axis and color is scaled for $dN_f/d\log D_a$ indicates the concentration. Dashed black lines in lower portion of the each panel at $1.0 \mu\text{m}$ shows the particle size cut-off diameter below which fluorescent particles were not considered as FBAP due to potential interference with non-biological aerosol particles. (a) dusty (b) clean, and (c) high bio. Please refer to supplementary Figs. for corresponding TAP plots.

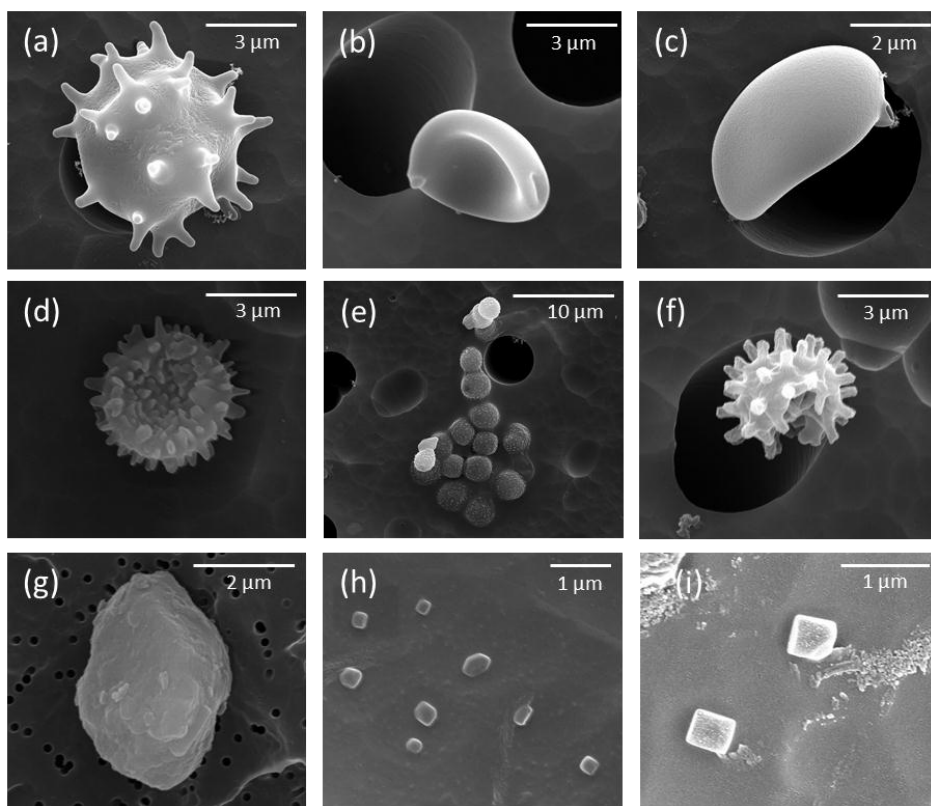
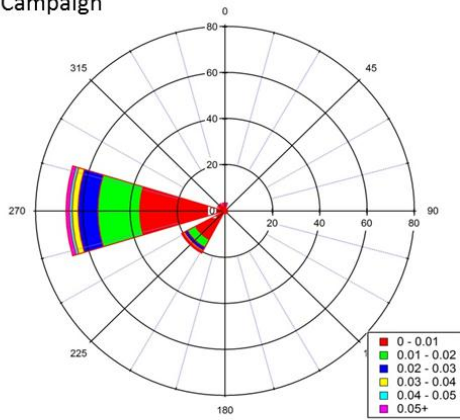
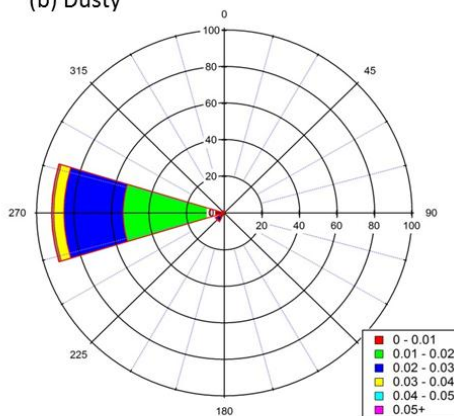


Figure 114: Scanning electron microscope images of the exemplary aerosol particles (FBAP and TAP) observed during the campaign at Munnar. The scale bar is shown at the top right corner of each image.

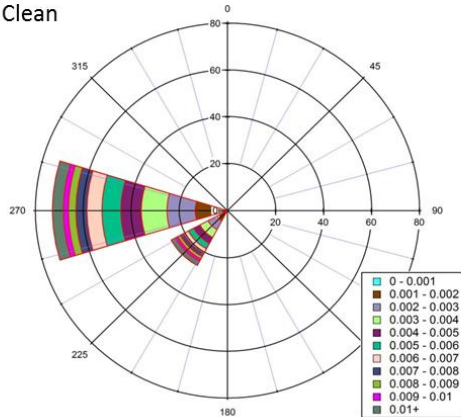
(a) Campaign



(b) Dusty



(c) Clean



(d) High Bio

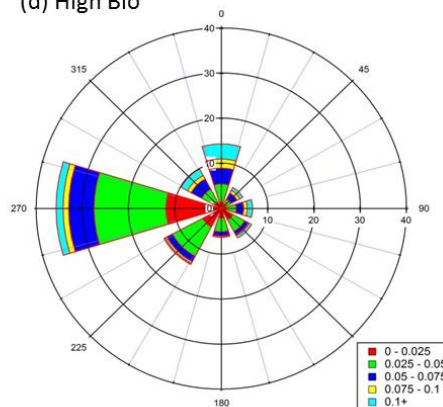
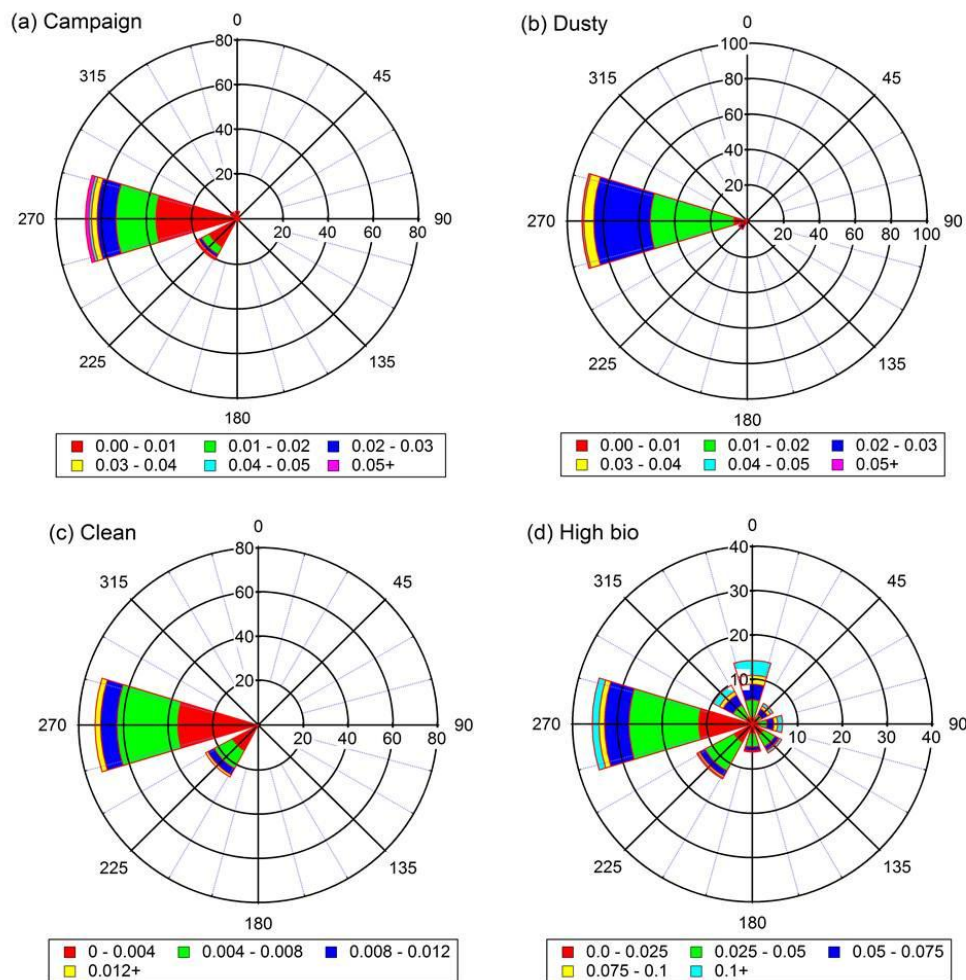


Figure 15: Wind rose diagram scaled over FBAP number concentration (N_p). These diagrams in a way are similar to the traditional wind rose diagram except representing the N_p in this case instead of wind speed. These diagram can be nominally interpreted as followed: For example (a) shows that ~52% of frequency of occurrence of N_p concentration in the range of 0—0.001 cm^{-3} was associated with Westerly/Southwesterly winds and on the contrary (d) indicates that out ~18% of frequency of occurrence of high concentration ($N_p > 0.1 \text{ cm}^{-3}$) ~16% was associated with Northerly/Northwesterly winds. (a) entire campaign, (b) dusty period, (c) clean period, and (d) high bio period.



Formatted: Font: (Default) Times New Roman, 10 pt

Figure 12: Wind rose diagram scaled over FBAP number concentration (N_F). These diagrams in a way are similar to the traditional wind rose diagram except representing the N_F in this case instead of wind speed. These diagram can be nominally interpreted as followed: For example (a) shows that ~52% of frequency of occurrence of N_F concentration in the range of $0 - 0.01 \text{ cm}^{-3}$ was associated with Westerly/Southwesterly winds and on the contrary (d) indicates that out ~18% of frequency of occurrence of high concentration ($N_F > 0.1 \text{ cm}^{-3}$) ~16% was associated with Northerly/Northwesterly winds. (a) entire campaign, (b) dusty period, (c) clean period, and (d) high bio period. Note that non-uniform scale of each panel has unit of cm^{-3} .

Formatted: Font: (Default) Times New Roman, 10 pt

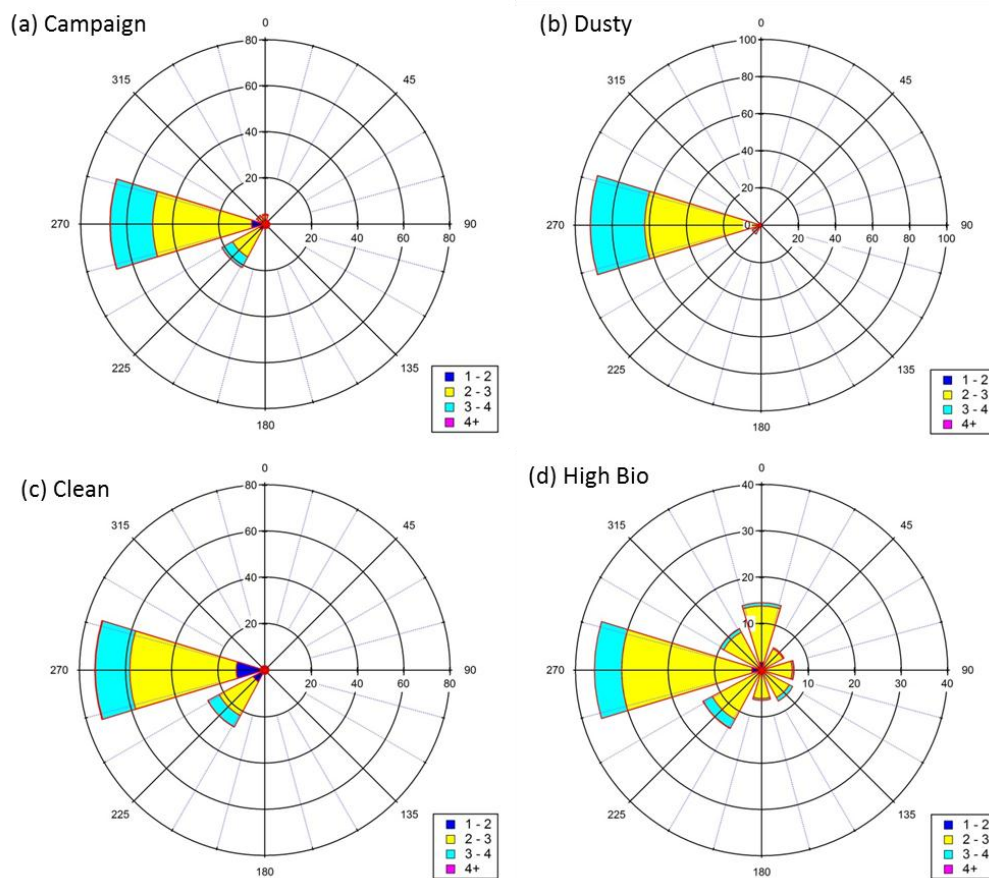
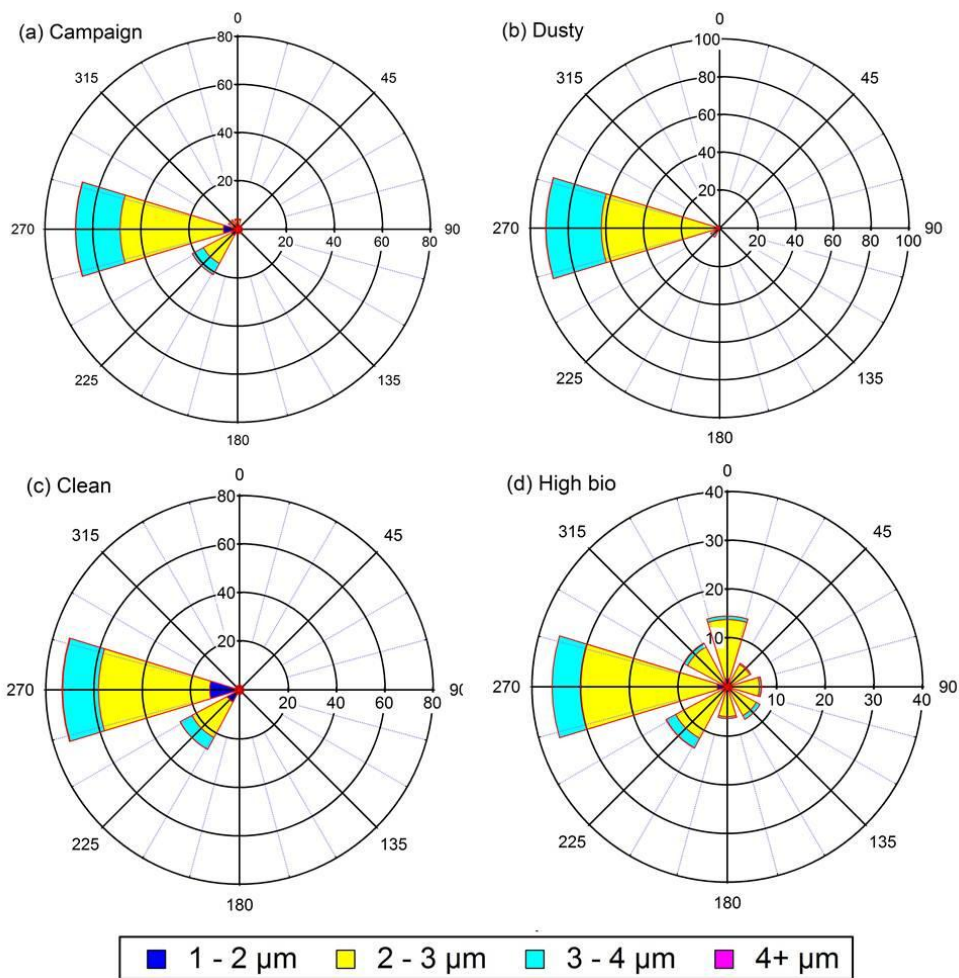


Figure 16: Same as Fig. 18 but scaled by geometric mean diameter (D_g) of $dN_p/d\log D_p$. (a) entire campaign, (b) dusty period, (c) clean period, and (d) high bio period.



Formatted: Font: (Default) Times New Roman, 10 pt

Figure 13: Same as Fig. 13 but scaled by geometric mean diameter (D_g) of $dN_g/d\log D_g$. (a) entire campaign, (b) dusty period, (c) clean period, and (d) high bio period.

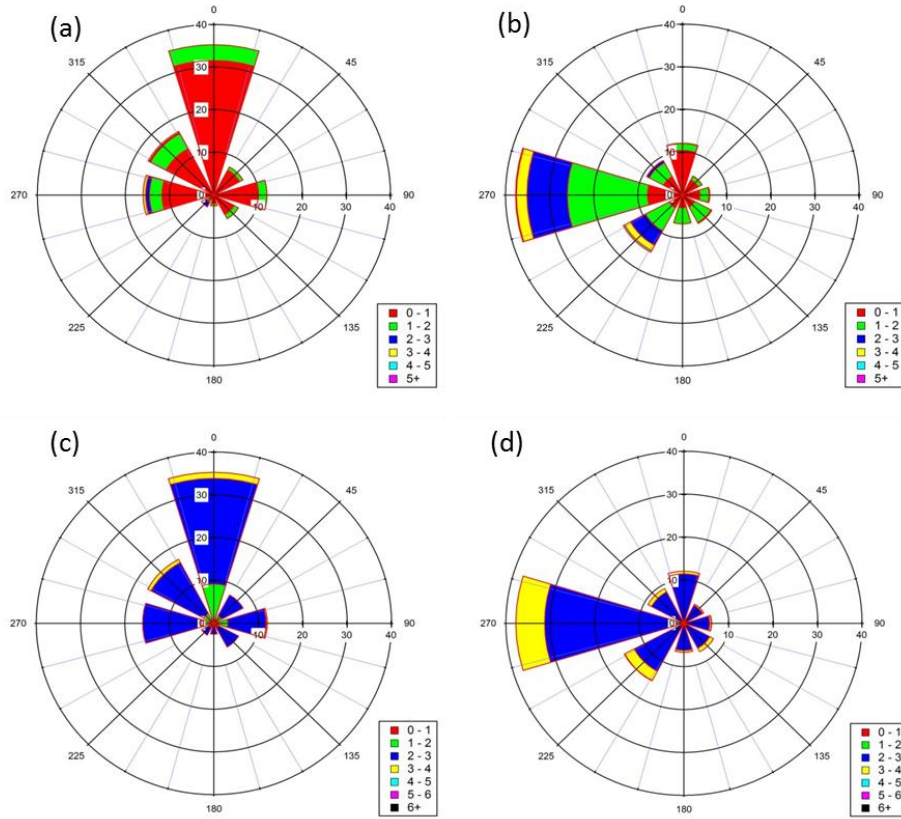


Figure 17: Wind rose diagram scaled by wind speed and geometric mean diameter (D_g) of $dN_t/d\log D_g$. The figures have been separated for FBAP number concentration (N_t) range, $N_t > 0.1 \text{ cm}^{-3}$ and $N_t < 0.1 \text{ cm}^{-3}$ observed during high bio-period. For example: when, $N_t > 0.1 \text{ cm}^{-3}$ —60% of the time wind was observed to be in the range of 0—1 m s^{-1} (a) and ~94% of the time the geometric mean diameter (D_g) of $dN_t/d\log D_g$ was in the range of 2—3 μm (c). On the other hand for $N_t < 0.1 \text{ cm}^{-3}$ —60% of the time wind was greater than 1 m s^{-1} (b), and ~80% of the time geometric mean diameter (D_g) of $dN_t/d\log D_g$ was in the range of 2—3 μm (d).

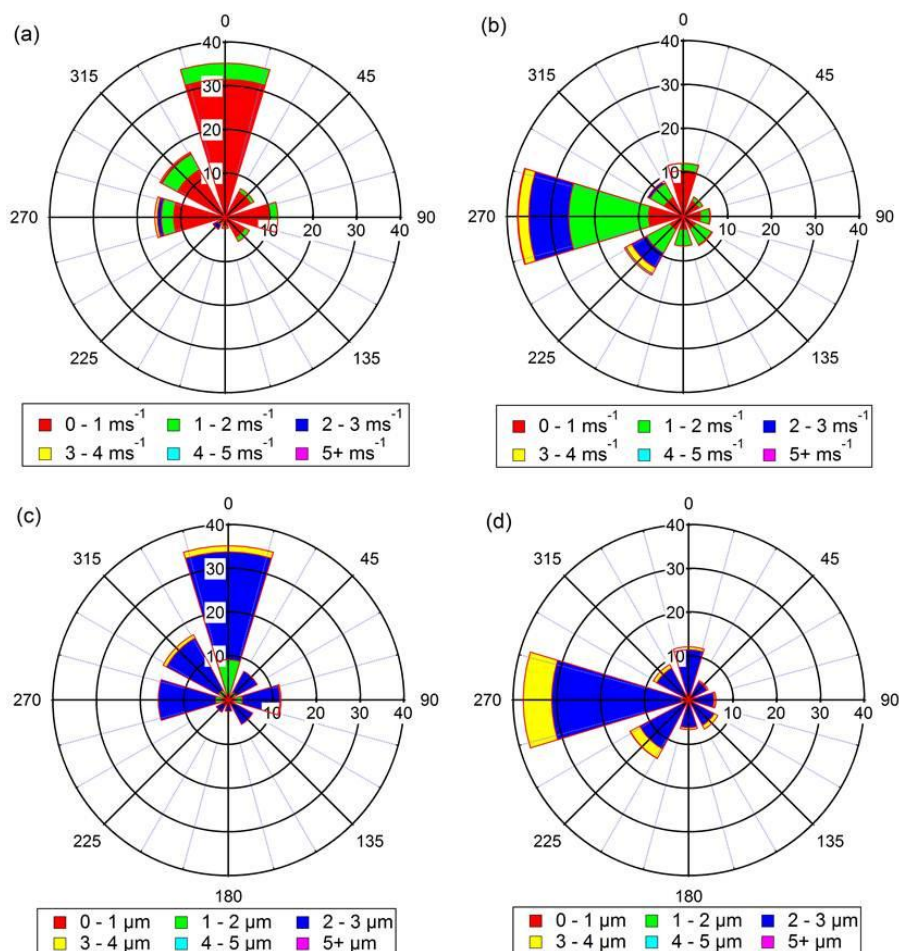


Figure 14: Wind rose diagram scaled by wind speed and geometric mean diameter (D_g) of $dN_F/d\log D_g$. The figures have been separated for FBAP number concentration (N_F) range, $N_F > 0.1 \text{ cm}^{-3}$ and $N_F < 0.1 \text{ cm}^{-3}$ observed during high bio period. For example: when, $N_F > 0.1 \text{ cm}^{-3}$ ~60% of the time wind was observed to be in the range of 0 – 1 m s^{-1} (a) and ~94% of the time the geometric mean diameter (D_g) of $dN_F/d\log D_g$ was in the range of 2 – 3 μm (c). On the other hand for $N_F < 0.1 \text{ cm}^{-3}$ ~60% of the time wind was greater than 1 m s^{-1} (b), and ~80% of the time geometric mean diameter (D_g) of $dN_F/d\log D_g$ was in the range of 2 – 3 μm (d).

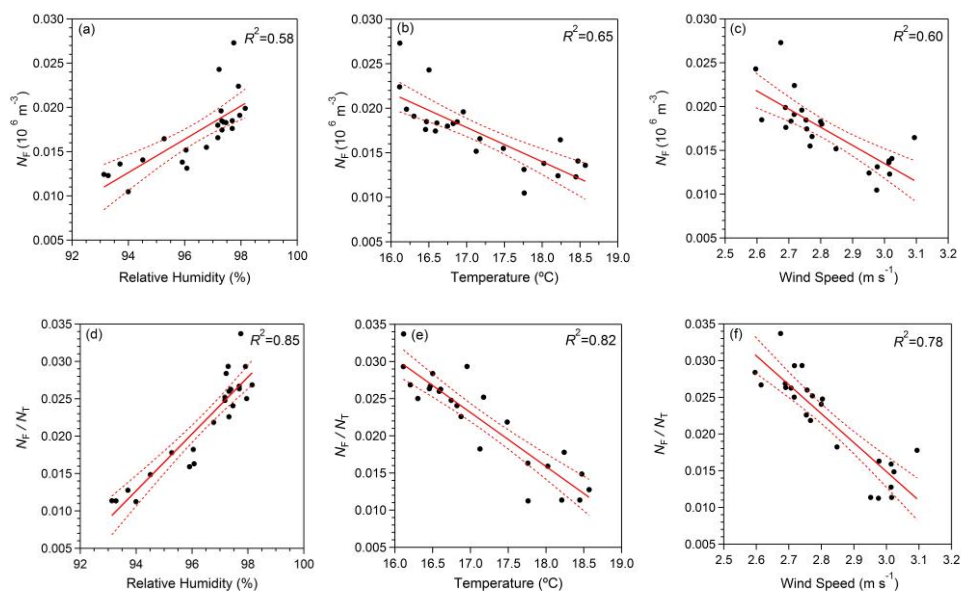


Figure 15-18: Correlation between aerosol particle number concentrations (N_F , N_T , and N_F/N_T) and meteorological parameters (relative humidity, temperature, and wind speed). Red line indicates the best fit to the scattered points and dashed black line indicates the 95% confidence level obtained for the best fit.